Preliminary Methanol Conversion Process Study

It was found that ZSM-48 has a high intrinsic selectivity at high conversion for the production of aliphatics (mostly olefins) from methanol. Moreover, the olefins produced from the conversion over ZSM-48 can be converted to a higher boiling distillate by passing the olefins over a ZSM-5-type zeolite catalyst. The product from this process consisted of about 55 wt. percent hydrocarbons boiling between 422 - 616 K (300 - 650°F) which is in the jet fuel boiling range.[19]

Olefins are intermediates in the conversion of methanol to aromatic hydrocarbons over shape selective zeolites such as ZSM-5. The problem at hand is to suppress or minimize the final aromatization step to single ring aromatics in the first stage of the dual-stage process. The simplest strategy is to use a ZSM-48 catalyst for producing olefins in the first step followed by conversion of the olefins to jet fuel boiling range aromatics over a suitable catalyst. As indicated, aromatic selectivity could be greatly enhanced (see Figure 55) by conversion of the olefins over ZSM-5. The carbon product distribution from these reactions is, of course, related to zeolite pore/channel geometry.

A fixed-bed continuous flow reactor system that could operate in either a single or dual reactor mode was used to study the conversion of methanol to methyl-substituted aromatics in the jet fuel boiling range. Methanol was charged to the system with a positive displacement pump. A J-type thermal couple was inserted in the center of a five cm^3 zeolite catalyst bed for both measuring and controlling temperature.

Methanol Conversion over ZSM-5 and ZSM-48

The typical product distribution from the methanol reaction over ZSM-5 after 24 hours on stream is shown in Figure 56. The reaction was carried out at 643 K, 1 hr^{-1} LHSV, and atmospheric pressure. At this stage of reaction, the conversion of methanol is essentially complete up to 64 hours on stream. The hydrocarbons span a relatively narrow range of molecular weights, terminating at about C_{10} as expected. The catalyst gave high selectivity to methyl-substituted aromatic hydrocarbons that is consistent with reported data.[16] The shape selectivity is generally similar to that observed in the microreactor at relatively low space velocity.

The results obtained for the conversion of methanol in the presence of ZSM-48 at 643 K, 1 LHSV, and atmospheric pressure are shown in Figure 57. The high selectivity of ZSM-48 toward olefins at the moderate operating conditions can be readily seen and it is worth noting the absence of aromatic hydrocarbons in the product slate.

It was reported that the olefins produced from the conversion of methanol over ZSM-48 can be converted to higher aromatics by passing the olefins produced over a ZSM-5 zeolite catalyst in a second reactor.[19] In the investigation of the aromatization of olefins, the first experiment involved the reaction of methanol over ZSM-48 in the upper bed followed by conversion of the olefinic product in a second bed containing ZSM-5 in a lower zone of the reactor. The reaction was conducted at 643 K, 1 atm, and 1 LHSV. The results of this experiment (see Figure 58) indicated that the product distribution does not shift to higher hydrocarbons. The reverse loading sequence (ZSM-5 followed by ZSM-48) was also investigated. The product distribution of this process is shown in Figure 59. It should be noted that the results are similar to those of methanol conversion over ZSM-5 (Figure 56).

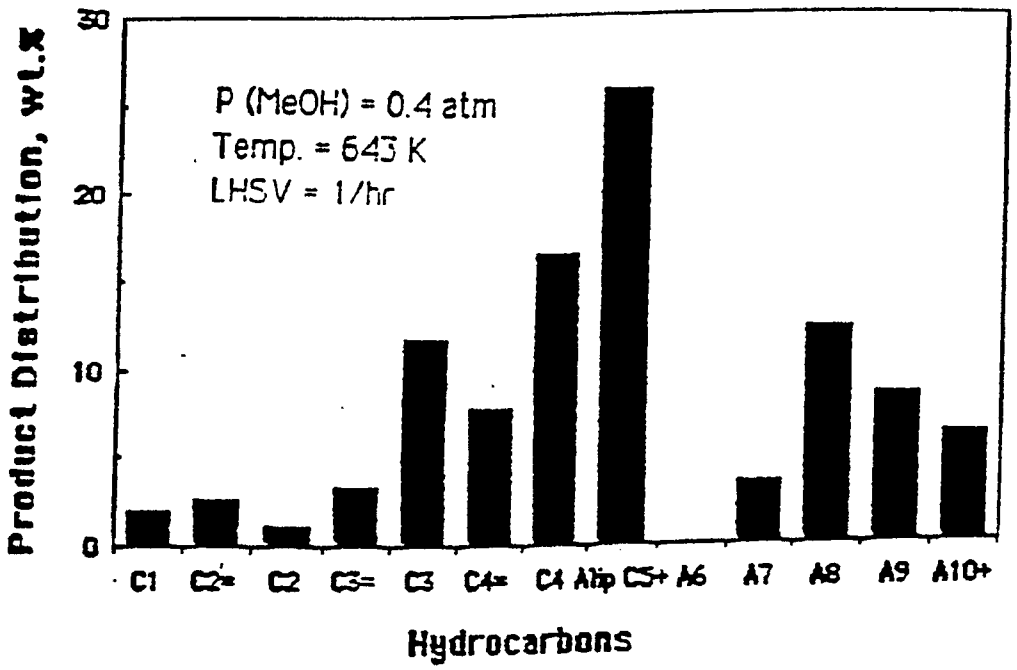

Figure 56. Product Distribution from Methanol Conversion Zeolite ZSM-5

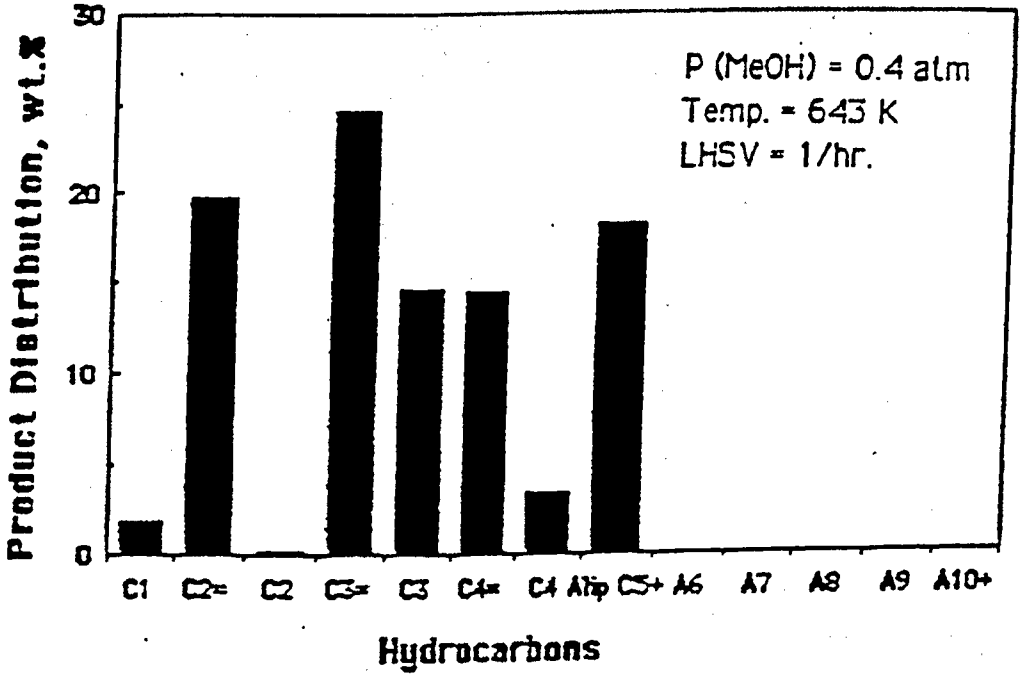

Figure 57. Product Distribution from Methanol Conversion Zeolite ZSM-48

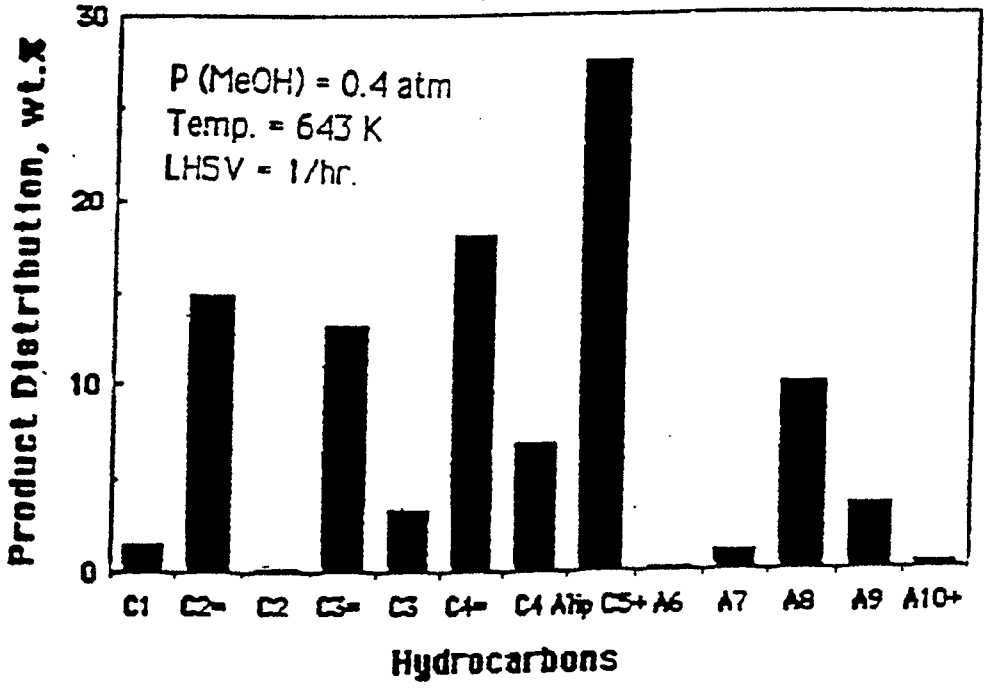

Figure 58. Product Distribution from Methanol Conversion
Zeolites ZSM-48/ZSM-5
Single Reactor Mode

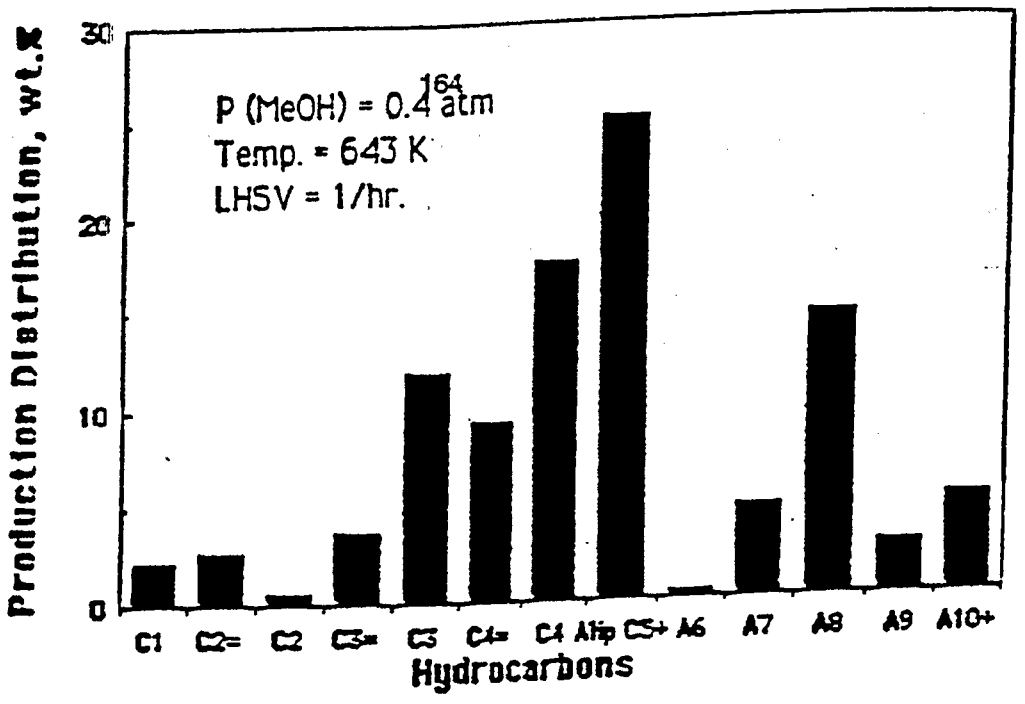

Figure 59. Product Distribution from Methanol Conversion
Zeolites ZSM-5/ZSM-48
Single Reactor Mode

It seems that ZSM-5 catalyst is the key to the aromatization reaction. The influence of pressure and temperature on methanol conversion over ZSM-5 was also investigated and the reaction index (RI) was used to describe the performance of the catalysts.

Pressure Effect

The pressure effect on methanol conversion over ZSM-5 is presented in Figure 60. Decreasing the pressure tends to decouple the formation of aliphatics. Increasing pressure results in an increase in the degree of aromatic substitution. Although not favored by thermodynamics, their formation can be attributed to the zeolite shape selectivity.

Temperature Effect

The effect of temperature on the methanol conversion is shown in Figure 61. The yields of xylenes show a maximum at a temperature of 643 K, at atmospheric pressure. It is worth noting that an increase in secondary alkylation occurred at higher temperature. Increasing temperature also results in an increase in the yield of aliphatics.

Reaction Index

In the simplified methanol conversion scheme, the light olefins react reversibly to heavier olefins, which convert further to aromatics and paraffins. The extent of reaction is monitored by a "reaction index," which is the propane/propene ratio. In the simplified scheme A->B->C, reaction index is proportional to the C/B ratio.[16] The reaction index for methanol conversion over ZSM-5 at 0.4 atm methanol partial pressure is presented in Figure 62. The reaction index decreased with increasing time on-stream. In other words, the aromatization reaction may be

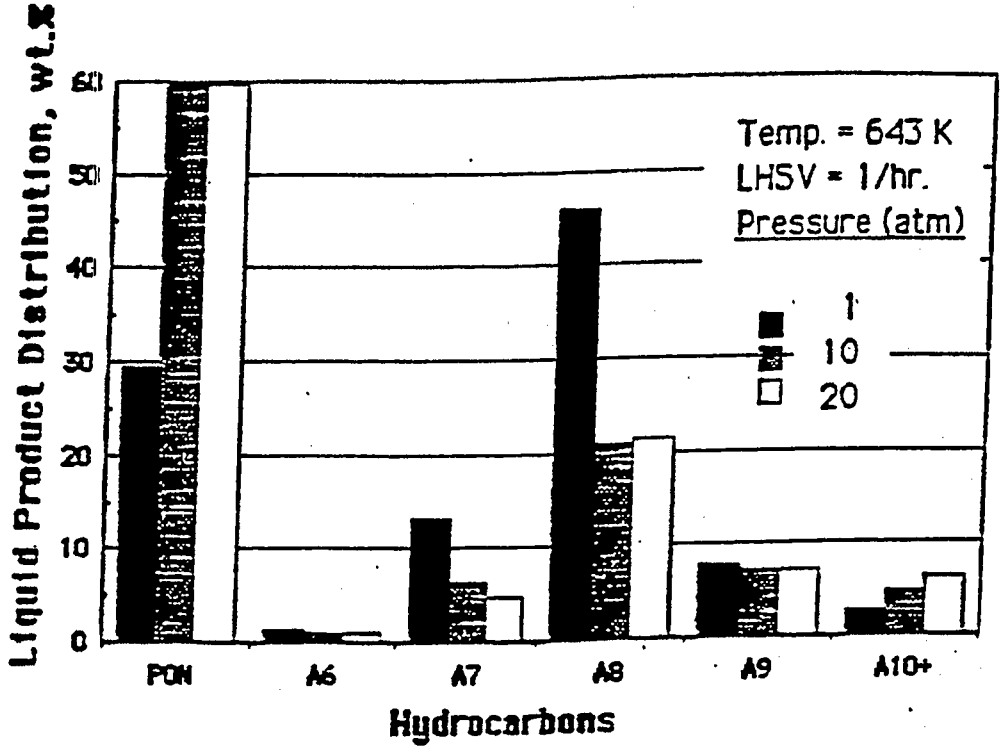

Figure 60. Product Distribution from Methanol Conversion
Effect of Reaction Pressure
Zeolite ZSM-5

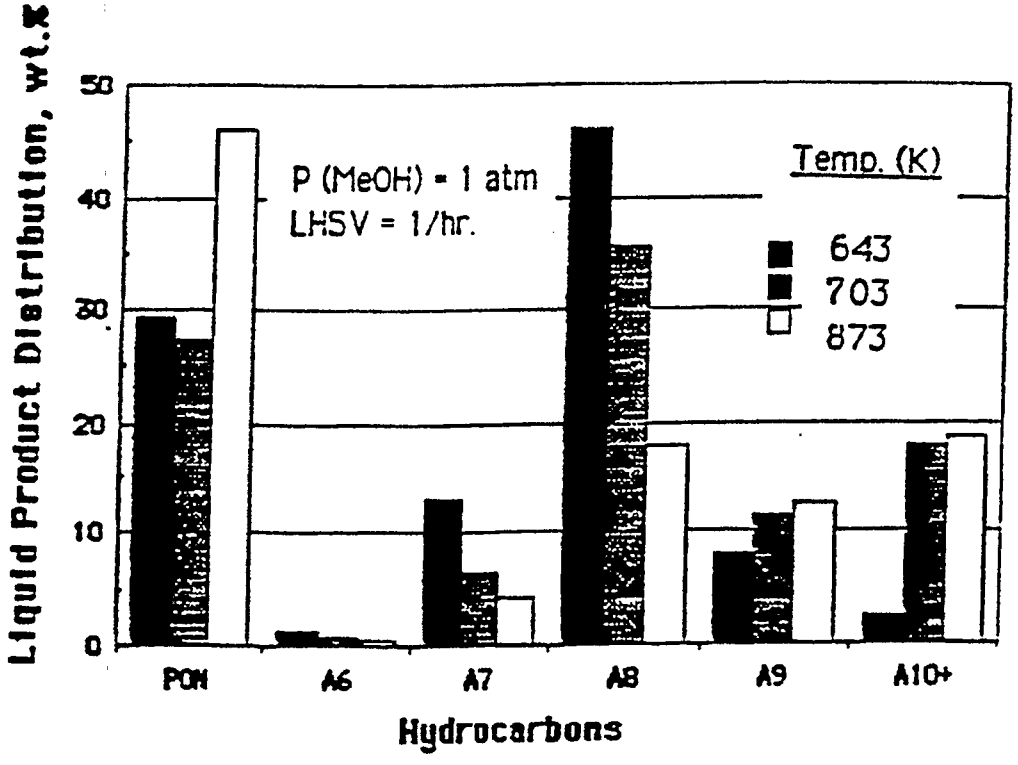

Figure 61. Product Distribution from Methanol Conversion
Effect of Reaction Temperature
Zeolite ZSM-5

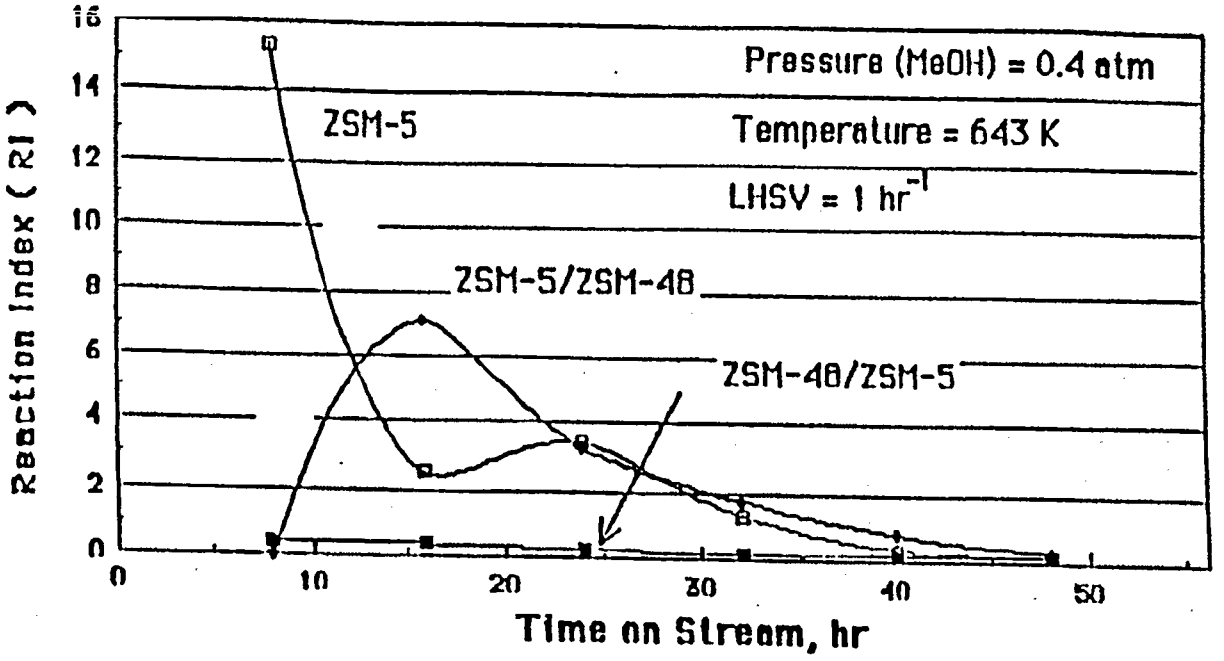

Figure 62. Reaction Index from Methanol Conversion

(a) ZSM-5
(b) ZSM-5/ZSM-48
(c) ZSM-48/ZSM-5

inhibited for an aged ZSM-5 catalyst, which has been deactivated by the formation of coke or by the partially destruction of the zeolite structure by steaming. The reaction index for methanol conversion over ZSM-5/ZSM-48 and ZSM-48/ZSM-5 is also shown in Figure 62. The various combinations and sequences of ZSM-5 and ZSM-48 in a single reactor for methanol conversion do not favor the formation of high molecular weight hydrocarbons. It may be due to high concentration of steam fed to the second bed of catalyst in the lower section of the reactor. Furthermore, it was believed that high molecular weight hydrocarbons could be produced from methanol over ZSM-48 and ZSM-5 at elevated reaction pressures in a dual reactor system.[19]

In the first stage, methanol was reacted over a ZSM-48 catalyst that had a high selectivity for olefins. The product from the first reactor was passed through a gas-liquid separator where the light aliphatics were separated from water and liquid phase hydrocarbons. The light olefins were compressed to the inlet pressure of the second reactor where the olefins can react to form aromatics over ZSM-5. Alternatively, the light olefins can be condensed, pressurized and pumped into the second stage reactor.

Dual-Reactor Study

A schematic of the dual-reactor catalyst testing system is presented in Figure 19. The apparatus consisted of a reactor containing ZSM-48 in which olefins were produced, followed by the aromatics-forming reactor containing ZSM-5. The pressure of the second reactor could be increased to ~ 7 atm by a compressor. It should be noted that higher pressures (> 7 atm) in the second reactor could not be obtained due to the liquefaction of light gases in the compressor at pressures > 7 atmospheres. Furthermore, a minimum inlet pressure of five atmospheres was

necessary for operating the compressor. Thus it may not be suitable for compressing olefins such as butenes to or above its critical pressure point (Pc = 40 atm). It was not possible to develop a cryogenic pumping system to transfer the olefin produced over ZSM-48 from the outlet pressure of the first reactor to 100 atm. The operating conditions for these exploratory dual reactor fixed-bed process studies were as follows:

	First Reactor	Second Reactor
Catalyst	ZSM-48	ZSM-5
Temperature, K	643	573
Pressure, atm	5	7
LHSV, 1/hr	6	-

About 7 wt. percent of high boiling point (> B.P. of naphthalene) hydrocarbons was obtained from the conversion of methanol in this system (see Figure 63). High yields of trimethyl-benzenes and low yields of paraffins, olefins, and naphthene (PON) indicate that a high degree of aromatization occurred. The major products of the olefin reaction at 773 K were xylenes (see Figure 64).

The yields of higher molecular weight hydrocarbons were low since the maximum attainable pressure in the second stage (ZSM-5 reactor) was about seven atmospheres and high hydrocarbons could be obtained only at elevated pressures such as 100 atm. The olefins produced in the first stage would condense in the compressor when compressed to a pressure higher than seven atmospheres. The condensed olefins can be collected cryogenically and pump with a liquid feed pump to pressurize to about 100 atm in the second stage.

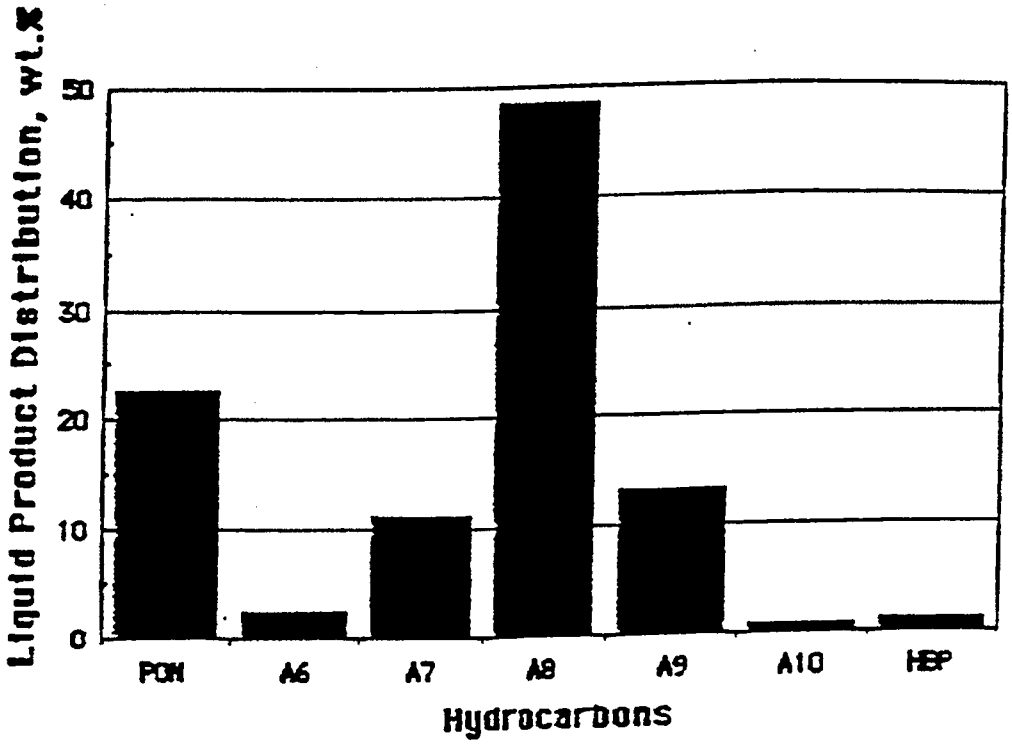

Reactor I	Reactor II
ZSM-48	ZSM-5
T = 643 K	T = 573 K
P = 5 ATM	P = 7 ATM

Figure 63. Product Distribution from Methanol Conversion over Zeolites ZSM-48 and ZSM-5 Dual Reactor Mode

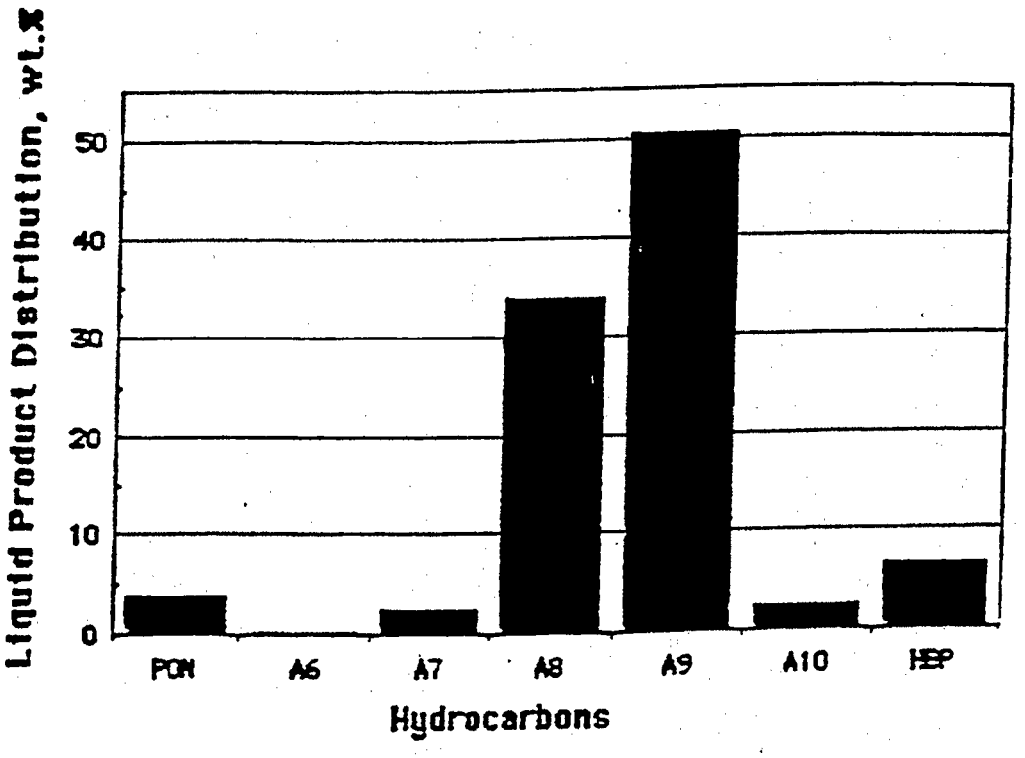

Reactor I	Reactor II
ZSM-48	ZSM-5
T = 643 K	T = 773 K
P = 5 ATM	P = 7 ATM

Figure 64. Product Distribution from Methanol Conversion over Zeolites ZSM-48 and ZSM-5 Dual Reactor Mode

The difficulties experienced in transferring low molecular weight olefins (C_2-C_4) from low pressures (1 to 5 atmospheres) to high pressures (100 atmospheres) have slowed the demonstration of the dual reactor concept for the production of dicyclic aromatic hydrocarbons in the aviation turbine fuel boiling range. However, we believe that at 100 atmospheres the yield of these species could be substantial. The dual reactor study has been placed on inactive status until an appropriate method can be developed to operate the ZSM-48 reactor at low pressures and the ZSM-5 reactor at high pressures in series.

Section V: SELECTIVE HYDROGENATION OF AROMATIC HYDROCARBONS

Research Personnel: Lei-Yea Cheng
Graduate Student

Nabin K. Nag
Assistant Research Professor

Kien-Ru Chen
Postdoctoral Fellow

Francis V. Hanson
Associate Professor

Supported transition metals possess good activity for the catalytic hydrogenation of aromatic hydrocarbons.[233] Under the framework of this project, it was intended to synthesize various one- and two-ring aromatic hydrocarbons via methanol ZSM-5 route and then hydrogenate these aromatic species to fully-saturated naphthenic compounds that are reported to be the major components of high-density jet fuels.[234] The present section is devoted to the efforts toward preparation, characterization, and testing of some supported metal catalysts; however, it should be recognized that this component of the research program was discontinued upon instruction from the Technical Project Officer.

Supported Metal Catalyst Preparation

The incipient wetness or "dry impregnation" method was used to prepare γ-Al_2O_3-supported Ni, Ru, and Pd catalysts.[235] The basic concept involves saturating an appropriate support with that volume of impregnating solution corresponding exactly to the total pore volume of the support and containing the stoichiometric amount of the metal cation to be impregnated. The γ-Al_2O_3 support was purchased from Akzo Chemie, Holland, and its reported specific surface area and pore volume were 209 m^2g^{-1} and 0.6 cm^3g^{-1}, respectively. The support was calcined to 500°C overnight before

impregnation. The preparation procedure for a typical nickel catalyst is described in the subsequent discussion. The alumina sample was received in the form of extrudates which were crushed and sieved (35-48 mesh size) to get particles of the size 300-425 m. This material was calcined overnight at 500°C; 4.125 g of $Ni(NO_3)_2.6H_2O$ was dissolved in 50 cm^3 water, and 10.584 g of calcined alumina were impregnated with 6.35 cm^3 of this solution by dropwise addition and constant stirring. The impregnated sample was dried at 393 K for 16 hours followed by calcination at 773 K for 16 hours. After reduction, the final catalyst composition was: 1 wt percent Ni on alumina (designated as 1 percent Ni/Al_2O_3).

The following catalysts were prepared using the incipient wetness technique:

a. 0.1 percent Ni/Al_2O_3

b. 1.0 percent Ni/Al_2O_3

c. 2.0 percent Ni/Al_2O_3

d. 2.5 percent Ru/Al_2O_3

e. 2.5 percent Pd/Al_2O_3

$Ru(NO)(NO_3)_3$ and $Pd(NO_3)_2xH_2O$ (both from Alfa Products) were used as sources for ruthenium and palladium respectively. This series of catalysts, and others to be prepared in the course of this research program were intended to be fully characterized and tested for hydrogenation reactions.

Catalyst Characterization by Hydrogen Chemisorption

Measurement of Sites

The concept of the active sites in heterogeneous catalysis was formulated first by Taylor in 1925 when he suggested that catalyst surfaces might contain some sites particularly active for chemisorption and catalysis.[236] He also pointed out: "...the amount of surface which is catalytically

active is determined by the reaction catalyzed. There will be all extremes between the case in which all the atoms in the surface are active and that in which relatively few are so active." This non-uniformity of the catalytic surface has been confirmed by chemisorption studies in which the heat of adsorption (i.e., heat of formation of adsorption complexes[237] has been shown to vary significantly with surface coverage). Surface heterogeneity has also been confirmed in kinetic studies in which small concentrations of a selective poison significantly suppress catalytic activity. Catalyst poisons are known to affect both catalytic activity and chemisorption capacity; however, the reduction in catalytic activity is more severe than the reduction in chemisorption capacity. Thus, not all sites on which chemisorption occurs act as catalytic sites.

Chemisorption has long been used to characterize catalytically active materials.[238] The number of sites available for chemisorption is determined from the amount of adsorptive required to saturate the surface. The method assumes that a simple relationship exists between the number of molecules or atoms adsorbed at saturation and the number of surface atoms. The catalytic activity of supported metal catalysts, expressed as the turnover number, is related to the total number of surface metal atoms as determined from the selective chemisorption of hydrogen[239-245] or from the titration of preadsorbed oxygen with hydrogen.[256-250] If the reaction occurs on a fraction of the surface metal atoms, the turnover number based on the total number of surface metal atoms will define the lower limit of the turnover number for the reaction under investigation. When comparing the activities of a series of catalysts having the same active component (i.e., metal), the relative activities will be insensitive to the site concentration on which the turnover numbers are calculated. Thus, both the true site density (usually unknown) and the limiting site density (determined by selective chemisorption) provide a viable means of comparing catalyst performance for a chosen reaction.

Constant Volume Adsorption Apparatus

A constant adsorption apparatus was constructed to determine adsorption isotherms for the supported metal catalysts used in the aromatics synthesis, aromatic hydrogenation, and hydrodewaxing studies sponsored by the United States Air Force. The isotherms were obtained by expanding an adsorbate from a calibrated doser volume into an adsorption cell which contained the sample. The amount of the gas adsorbed was calculated from the known doser and cell volumes and the pressures and ambient temperatures before and after expansion of the adsorbate. A schematic of the apparatus is presented in Figure 65. Since this apparatus has not been described previously, it will be discussed in considerable detail.

Adsorption System

The adsorption system is depicted in the section of Figure 65 enclosed by the large dashed rectangle. The pressure was measured with a precision pressure gauge (A), model 145 servo-nulling read-out unit, manufactured by Texas Instruments, Inc., Houston, Texas. The pressure sensing device was a Type 5, fused quartz Bourdon capsule. The Bourdon tube was in the form of a spiral, to which a reflecting platinum mirror was attached (see Figure 66). An optical transducer was mounted on a gear that traveled concentrically around the capsule. The deflection of the pressurized Bourdon tube was found by rotating the gear until the light reflected from the tube mirror fell with equal intensity on a pair of matched photocells. The deflection of the tube was then read on the digital counter and the pressure was determined from the counter reading by means of a calibration table. The Type 5 Bourdon capsule had a resolution of 0.001° (corresponding to a minimum measurable deflection of 0.008 Torr). The apparatus was superior to conventional volumetric systems because of the high precision of the gauge, the absence of hysteresis, and the elimination of the need for mercury in the system. The reference side of the

A - Texas Instruments Precision Pressure Gage; B - adsorption cell; C - mechanical vacuum pump; D - oil diffusion pump; E,F - high vacuum cold traps; G - thermocouple vacuum gauge; H - ionization vacuum gauge; I - vacuum manifold; J - gas handling manifold; K - calibrated bulb; L - hydrogen reduction rotameter; M - palladium thimble hydrogen diffuser; N - 13X molecular sieve trap; P - 5 liter gas storage bulbs; R - reference port on fused quartz Bourdon capsule; S - measuring port on capsule; T - cold finger; U - cold trap; V,X,Y,Z - sliding doors on Plexiglas enclosure. All stopcocks are of the high vacuum type and the numbers identify the stopcocks discussed in the text.

Figure 65

Constant Volume Adsorption Apparatus

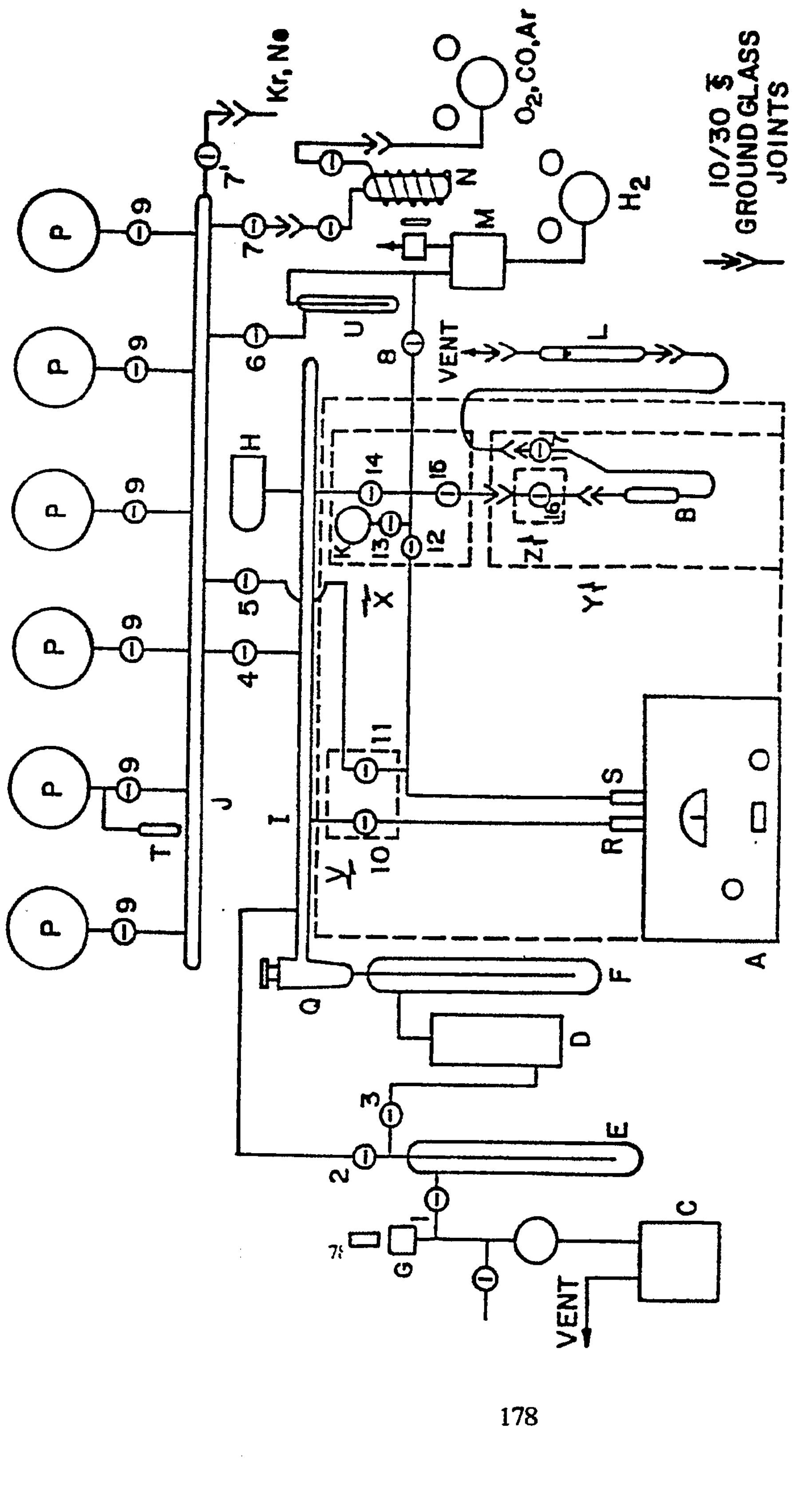
Kr, Ne
O_2, CO, Ar
H_2
10/30 ₮ GROUND GLASS JOINTS
VENT
VENT
P
T
J
I
U
H
K
X
Y
Z
N
M
L
B
A
R
S
F
Q
D
E
C
G

A - fused quartz Bourdon capsule; B - quartz spiral; C - platinum reflecting mirror; D - calibrated bulb (V_B = 49.055 cm^3); E - adsorption cell; V_{CD} - calibrated doser volume; V_{SC} - connecting stopcock volume; V_C - cell volume. The numbers identify the stopcocks discussed in the text. $V_D(=V_{CD}+V_{SC})$ - doser volume for isotherm determination.

Figure 66

Constant Volume Adsorption Apparatus
Detail of Doser System

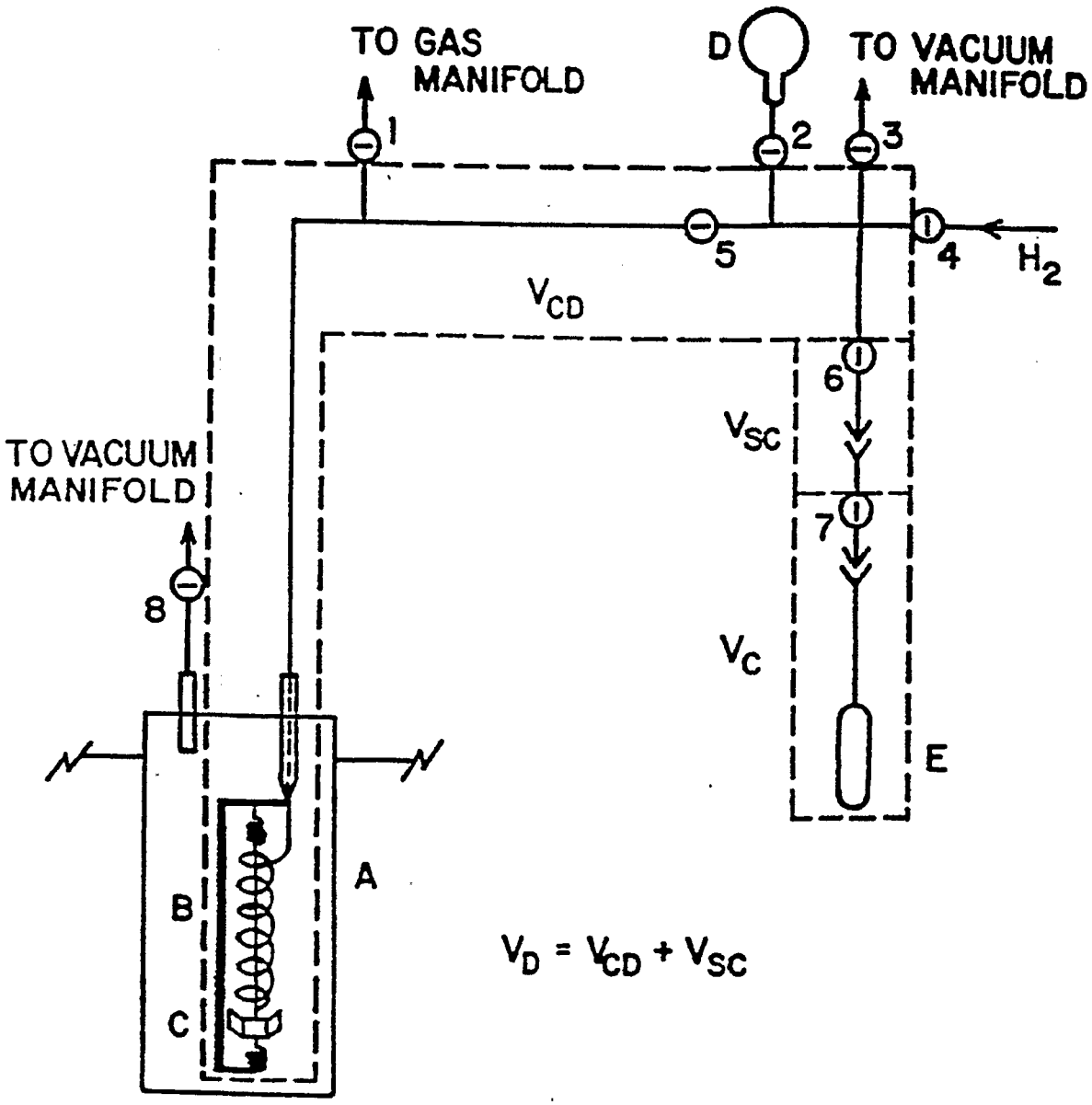
TO GAS MANIFOLD
D
TO VACUUM MANIFOLD
1
2
3
5
4
H_2
V_{CD}
6
V_{SC}
TO VACUUM MANIFOLD
7
8
V_C
E
A
B
C

$$V_D = V_{CD} + V_{SC}$$

capsule was connected to the vacuum manifold via stopcock (10) and the measuring side was connected to the doser volume by a graded glass seal.

The doser system was constructed from borosilicate glass capillary tubing to minimize the dead volume. All stopcocks were of the high vacuum type and were lubricated with Apiezon "N" grease. The doser volume was connected to the vacuum manifold via a four mm stopcock (14) and to the gas handling manifold via stopcocks (5) and (11). A calibrated bulb (K) was connected to the doser system via stopcock (3) for calibration of dead volumes in the adsorption system. The volume of the bulb was determined before it was glassblown onto the doser system. The bulb was filled with degassed distilled water and placed in a constant temperature bath. After thermal equilibrium was attained , the bulb was weighed on the Mettler Balance. The volume was calculated to 49.055 cm^3.

A detailed sketch of the flow adsorption cell (B) is presented in Figure 67. The catalyst chamber was made from eight mm OD borosilicate glass tubing and was 60 mm long. The inlet line was made from six mm OD borosilicate glass tubing 170 mm long and terminated in a 10/30 ground glass joint (inner). The exhaust line was made from Pyrex capillary tubing and contained a two mm capillary stopcock (17). The exhaust line was connected to the vent line by a 10/30 ground glass joint (inner). The cell was connected to the doser volume via a two mm capillary stopcock (16) that had 10/30 ground glass joints (outer) on both ends. The joint that joined the cell to the connecting stopcock (16) was sealed with Apiezon black wax and the joint that connected the assembled cell to the doser system was sealed with Apiezon "T" grease.

The entire adsorption system was enclosed in a borosilicate glass box (740 mm x 990 mm) to stabilize the ambient temperature during the course of an isotherm. The front of the box was equipped with three sliding doors (V, X, Z) which permitted access to the stopcocks in the doser

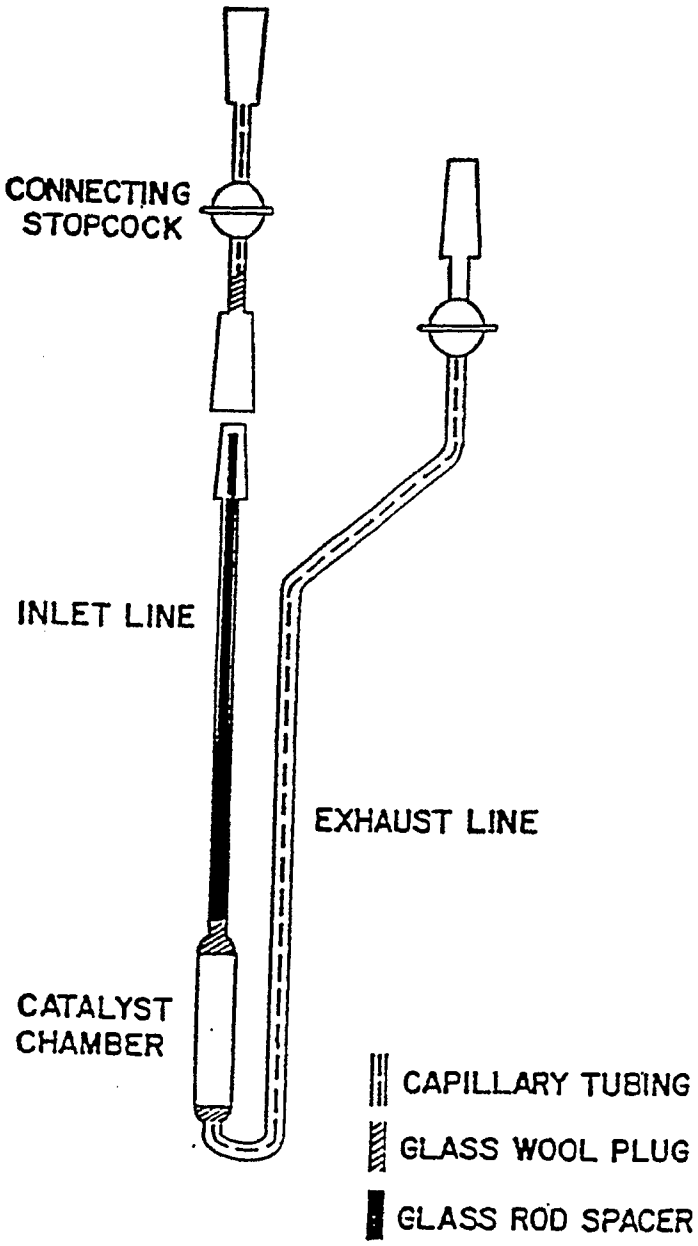

Figure 67. Adsorption Cell

system. The large door (Y) was used when the adsorption cell was changed or when the furnace and constant temperature bath were placed around the cell or were removed. The doors are indicated by the dashed lines in Figure 65 and the arrows indicate the direction each door moved. The box was assembled with machine screws and the front panel could be removed easily for minor repairs or modifications to the doser system or gauge.

VACUUM SYSTEM AND HANDLING APPARATUS

Vacuum System

The vacuum system consisted of a C. V. C. 112 liter per second oil diffusion pump (D), model PMCS-2C, backed by an 0.33 liter per second Precision Scientific mechanical vacuum pump (C), model 25. Dow Corning 704 silicone oil was used in the diffusion pump. The diffusion pump was connected to the vacuum manifold (I) by a 15 mm high vacuum stopcock (Q) which was mounted on top of a 55/50 vacuum cold trap (F). The mechanical pump was isolated from the vacuum manifold by a 40/50 vacuum cold trap to prevent contamination of the adsorbent when the system was rough pumped in the early stages of each evacuation. Both traps were immersed in liquid nitrogen at all times. A C.V.C. thermocouple vacuum gauge (G) was mounted on the mechanical pump side of the trap to monitor the mechanical pump vacuum.

The vacuum manifold was constructed of 25 mm OD borosilicate glass tubing (1050 mm long). The manifold vacuum was measured by a Veeco ionization gauge, model RG 75N, and was read on a C.V.C. ionization gauge controller, type GIC-110A. The ultimate dynamic vacuum of the manifold and adsorption cell was less than 10^{-6} Torr.

Gas Handling and Purification System

The gas handling manifold (J) was also constructed of 25 mm OD borosilicate glass tubing (1200 mm long) and was connected to the vacuum manifold by a 6 mm stopcock (4). Six five-liter gas storage bulbs (P) were connected to this manifold by 4 mm stopcocks (9). One of the bulbs was equipped with a cold-finger (T) for purification of hydrocarbon adsorptives and other condensible gases by repeated freeze-pump-thaw cycles.

All adsorptives, with the exception of hydrogen, were loaded into the gas storage bulbs via stopcocks (7) and (7'). High purity hydrogen (99.93 percent) was used as an adsorptive and was further purified by diffusion through a Milton Roy Company palladium thimble hydrogen purifier (M), model CH-A. The hydrogen also passed through a cold trap (U) at liquid nitrogen temperature before being stored in one of the five-liter bulbs. Matheson research grade oxygen (99.99 percent) was passed through a 13X molecular sieve trap (N) at a dry ice-acetone temperature before being stored in one of the five-liter bulbs, as was the Matheson C.P. grade carbon monoxide (99.5 percent). Matheson research grade neon (99.995 percent) and krypton (99.995 percent) were used without further purification for dead volume determinations. The molecular sieve traps were activated by evacuation at 600 K to a pressure of 5×10^{-4} Torr. A different trap was reserved for purification of each adsorptive.

Operating Procedures

Catalyst Loading

An acid-washed glass wool plug was inserted into the catalyst chamber to serve as a catalyst support grid. The catalyst was weighed without drying and was then loaded into the cell via the inlet line. A second acid-washed glass wool plug was placed on top of the catalyst and a glass rod

was placed in the inlet line to reduce the cell dead volume. The cell was sealed to the connecting stopcock with Apiezon black wax and the assembled adsorption cell was attached to the doser system.

Catalyst Pretreatment

The evacuation was begun by setting stopcocks (Q) and (3) to bypass the diffusion pump and by opening (2) to the vacuum manifold. Stopcock (12) was closed and (14) was opened to the doser system. Stopcock (15) was opened and the connecting stopcock volume was evacuated. When the thermocouple vacuum gauge (G) registered a pressure of 30-40 x 10^{-3} Torr, stopcock (2) was closed and the evacuation with the diffusion pump was begun. The furnace was placed around the cell (B) and the temperature programmer-controller was started after a one-hour evacuation at room temperature. The sample was evacuated at 423 K for two hours and then cooled to room temperature under evacuation.

The reduction was carried out in the following manner. Stopcock (16) was closed and (12) was opened to the vacuum manifold via stopcock (14). After evacuation of the Bourdon tube, stopcocks (12) and (14) were closed and (8) was opened to admit hydrogen to the doser system. The hydrogen was then slowly admitted to the Bourdon tube by opening stopcock (12). The flare on the hydrogen diffuser (M) was lit, the diffuser heater was turned on, and the hydrogen pressure in the doser system and the cell was allowed to increase. When the pressure was greater than the atmospheric pressure (95° on digital counter), stopcock (17) was opened to the vent line and the flow rate was measured on the rotameter (L). All catalysts were reduced at a space velocity of 0.5-3.0 volumes of hydrogen per unit volume of catalyst per second. After the hydrogen flow was established, stopcock (12) was closed and the hydrogen was evacuated from the measuring side

of the capsule (S) via stopcocks (5) and (11). The furnace was placed around the cell and the temperature programmer-controller was started. All catalysts were heated to the reduction temperature over a period of eight to ten hours and were reduced for four hours. After the reduction, the furnace was removed and the catalyst was cooled to room temperature in flowing hydrogen. Stopcock (17) was closed and the hydrogen diffuser was immediately shut down to prevent overpressuring the cell. Stopcocks (4), (5), (8), and (11) were closed and (14) was opened to the vacuum manifold to evacuate the hydrogen from the cell. Stopcock (12) was opened the doser volume and the adsorption cell were evacuated to a manifold vacuum of less than 10^{-5} Torr. During this evacuation the gauge was zeroed with stopcock (10) open to the vacuum manifold. The furnace was placed around the cell and the catalyst was heated to the final evacuation temperature (723 K) with the programmer-controller system. Usually the catalyst was evacuated for 1-1/2 to 2 hours at this temperature. The furnace was removed and the catalyst was quickly cooled to room temperature under evacuation. The constant temperature bath was then placed around the cell and its temperature was adjusted to the desired isotherm temperature. Stopcock (16) was closed to isolate the cell from the doser volume and (14) was closed to isolate the dosing system from the vacuum manifold. The gas to be adsorbed was transferred from its storage bulb to the gas manifold and from there to the dosing system via stopcocks (5) and (11).

Adsorption Isotherm Procedure

The calculation of the adsorption isotherm required a knowledge of the dead volume of the adsorption cell with the constant temperature bath placed around the cell. Neon was used to determine the dead volumes because helium was shown to diffuse through the quartz spiral into the evacuated reference side of the capsule. The cell and the doser system were evacuated and

stopcocks (14), (15), and (16) were closed. The calibrated doser volume (see Figure 65) was filled with neon to a pressure of 600-750 Torr via stopcock (11). The pressure and ambient temperature were recorded after stopcock (11) had been closed. The neon was then expanded into the connecting stopcock volume via stopcock (15). The pressure and temperature were again recorded. Finally, the neon was expanded into the cell by opening stopcock (16). AFter the final pressure and temperature were recorded, the neon was evacuated and the procedure was repeated. The dead volume was usually determined three to six times for each catalyst loading. The pressure and ambient temperature were recorded at 120-second intervals over 600 seconds, and the ratio P (degrees)/T (K) was computed for each point. The system was assumed to be equilibrated when the ratios for two successive points agreed to within five in the fifth significant figure.

Stopcocks (4) and (14) were opened to the vacuum manifold and the neon was evacuated from the doser system, the adsorption cell, and the gas handling manifold. Stopcocks (5) and (11) were also opened the evacuate the neon from the transfer line. The system was evacuated to less than 10^{-5} Torr and stopcocks (4), (11), (14), and (16) were then closed. After the adsorptive was expanded from its gas storage bulb into the gas handling manifold and the transfer line, stopcock (5) was closed. The adsorptive was then admitted to the doser system via stopcock (11) very slowly to avoid excessive vibrations of the Bourdon tube. The initial pressure in the doser system was usually three to four times the final desired pressure after the initial expansion into the cell. Stopcock (11) was closed and the pressure and ambient temperature were recorded. The adsorptive was expanded into the cell via stopcock (16). After the system equilibrated, the pressure and temperature were recorded, and stopcock (16) was closed. This first point was equilibrated for 3600 seconds and the ratio P (degrees)/T (K) was calculated every 300 seconds. The pressure in the doser system was increased by adding adsorptive from the gas handling manifold via stopcock

(11). The pressure and the temperature were recorded and the adsorptive was expanded into the cell. The system was equilibrated for 720 seconds and the pressure and temperature were read. This sequence of steps was repeated five or six times to complete the isotherm.

When carbon monoxide was used as the adsorptive, stopcock (12) was closed after the final point of the isotherm was take, and the cell was evacuated for 120 seconds via stopcock (14). Stopcocks (14) and (16) were closed and a second isotherm was obtained to determine the amount of physically adsorbed carbon monoxide.

The procedure for the hydrogen-titration isotherms varied from isotherm to isotherm in the surface reconstruction studies. For the case of the high temperature (673 K) reduction isotherm, the cell was cooled to room temperature in flowing hydrogen following the reduction. The hydrogen diffuser was shut down and the hydrogen was evacuated as described in the preceding section. Oxygen was transferred from its storage bulb to the doser volume via stopcocks (5) and (11). Stopcock (11) was closed and the oxygen was expanded into the cell to a pressure of 500-600 Torr by opening stopcock (16). The stopcock was closed and the oxygen was evacuated from the system. After 3600 seconds, the oxygen was evacuated from the cell at room temperature for 3600 seconds. The hydrogen-titration isotherm was then obtained in the manner described above.

Adsorption Isotherm Calculation Procedure

The adsorption isotherm calculation outlined below was based on the procedure for the determination of adsorption isotherms that was discussed previously. The volumes and stopcocks mentioned in the subsequent discussion refer to Figure 66. The volumes were defined as follows: the cell volume, V_C, was the volume of the adsorption cell and included the bore of stopcock (7); the connecting stopcock volume, V_{SC}, was the volume between stopcocks (6) and (7) and included

the bore of stopcock (6); the calibrated doser volume, V_{cd}, was the volume enclosed by stopcocks (1), (2), (3), (4), and (6), and included the volume of the quartz Bourdon spiral (B); and the doser volume, V_D, was the sum of V_{CD} and V_{SC}. It was necessary to use neon for the calibration because it was shown that helium diffused through the quartz spiral into the evacuated reference side of the capsule (A).

Doser Volume Calibration

The standard bulb (D) was calibrated in the following manner before it was attached to the doser volume. The bulb plus stopcock was weighted, evacuated, and filled with degassed, distilled water. AFter the bulb filled with water and had been equilibrated for 16 hours, it was removed from the constant temperature bath and weighed a second time. The volume was calculated from the mass and the specific gravity of water at the bath temperature. This procedure was repeated five times and the volume of the bulb (V_{CB}=49.055 cm^3) was determined from the average of the measurements.

The calibrated bulb and the doser volume to be calibrated, V_{CD}, were filled with neon and initial pressure, P_1, and the ambient temperature, T_1, were recorded. Stopcock (2) was closed and the dose volume was evacuated via stopcock (3) to 10^{-5} torr. Stopcock (3) was closed, (2) was opened, and the neon was expanded from the bulb into the doser volume. The final pressure, P_2, and the ambient temperature, T_2, were recorded after equilibration. The neon was assumed to behave as an ideal gas; thus

$$\frac{P_1 V_{CB}}{T_1} = \frac{P_2 V_{CB}}{T_2} + \frac{P_2 V_{CD}}{T_2} \quad . \qquad (5\text{-}1)$$

This equation was rearranged to express the calibrated doser volume as

$$V_{CD} = \left(\frac{P_1}{T_1} - \frac{P_2}{T_2}\right)\left(\frac{T_2}{P_2}\right) V_{CB} \qquad (5\text{-}2)$$

The values of P_1/T_1 and P_2/T_2 were determined in 25 sets of measurements, of which ten were discarded on the basis of the 4d and 2.5d rules. The range of initial pressures was 150 to 450 torr and the corresponding range of final pressures was 130 to 400 Torr. There was no systematic variation in the value of V_{CD} as a function of the initial pressure, P_1. The calibrated doser volume was 6.2890 cm^3 with a standard deviation of 0.018 and a 95 percent confidence level that the volume was between 6.279 and 6.299 cm^3.

Calculation of the Cell Volume

The volumes of the connecting stopcock, V_{SC}, and the adsorption cell, V_C, were determined by filling the calibrated doser volume, V_{CD}, with neon and expanding the neon sequentially into the connecting stopcock and the cell which had been previously evacuated. The cell volume was determined the cell at the ambient temperature or with the cell immersed in the thermostated bath at the isotherm temperature. The equations were derived for the case with the cell immersed in the bath.

If

$$V_1 = V_{CD}$$

$$V_2 = V_{CD} + V_{SC}$$

$$V_3 = V_{CD} + V_C = V_2 + V_C$$

and P_1, P_2, and P_3 were equilibrium pressures of the neon in the volumes V_1, V_2, and V_3, respectively, measured at the ambient temperatures T_1, T_2, and T_3 in the Plexiglas enclosure, then, from the ideal gas law,

$$\frac{P_1V_1}{T_1} = \frac{P_2V_2}{T_2} = \frac{P_3V_2}{T_3} + \frac{P_3V_C}{T_C} \quad . \tag{5-3}$$

The connecting stopcock was calculated from the first two terms of Equation (5-3); that is,

$$\frac{P_1V_{CD}}{T_1} = \frac{P_2(V_{CD} + V_{SC})}{T_2} \tag{5-4}$$

which gave

$$V_D = V_{SC} + V_{CD}. \tag{5-5}$$

The doser volume was then calculated from

$$V_D = V_{SC} + V_{CD}.$$

The cell volume was calculated from the second two terms of the Equation (5-3); that is,

$$\frac{P_2V_D}{T_2} = \frac{P_3V_D}{T_3} + \frac{P_3V_C}{T_C}$$

which was rearranged to give

$$V_C = \left(\frac{P_2}{T_2} - \frac{P_3}{T_3}\right)\left(\frac{T_C}{P_3}\right) V_D \quad . \tag{5-6}$$

If the cell was at the ambient temperature, the expression for the cell volume was

$$V_C = \left(\frac{P_2}{T_2} - \frac{P_3}{T_3}\right)\left(\frac{T_3}{P_3}\right) V_D \ . \qquad (5\text{-}7)$$

Adsorption Isotherm Calculation

Adsorption isotherms were determined in the following manner. The adsorption cell and the doser volume were evacuated to less than 10^{-5} Torr and stopcock (7) was closed. The doser volume was filled with adsorptive to pressure P_1 (1) at the ambient temperature TR_1 (1). Stopcock (7) was opened and the adsorptive was admitted to the cell. The equilibrated pressure P_2 (1) at the ambient temperature T_2 (1) was recorded after one hour.

A material balance on the doser volume and the adsorption cell gave

$$n_{D,1}(1) = n_{D,2}(1) + n_{C,2}(1) + n_{a,2}(1) \qquad (5\text{-}8)$$

where $n_{D,1}(1)$ was the moles of adsorptive in the doser volume at the initial conditions for the first isotherm point; $n_{D,2}(1)$ was the moles of adsorptive in the doser volume at the final conditions for the first isotherm point; $n_{C,2}(1)$ was the moles of adsorptive in the gas phase in the cell at the final conditions for the first isotherm point, and $n_{a,2}(1)$ was the moles of adsorbate at the final conditions for the first isotherm point. The amount adsorbed, assuming the adsorptive obeyed the ideal gas law, was given by

$$n_{a,2}(1) = \frac{P_1(1)\ V_D}{R\ T_1(1)} - \frac{P_2(1)\ V_D}{R\ T_2(1)} - \frac{P_2(1)\ V_C}{R\ T_C} \qquad (5\text{-}9)$$

or

$$n_{a,2}(1) = \left(\frac{P_1(1)}{T_1(1)} - \frac{P_2(1)}{T_2(1)}\right)\frac{V_D}{R} - P_2(1)\ \frac{V_C}{R\ T_C} \ . \qquad (5\text{-}10)$$

The amount adsorbed was expressed as

$$n_{a,2}(1) = \frac{P_S V_a(1)}{R\,T_S} \qquad (5\text{-}11)$$

where P_S was 760 Torr, T_S was 273.16 K, and $V_a(1)$ was the volume of adsorbate at the standard temperature and pressure. Substituting Equation (5-11) into (5-10), an expression was obtained for the amount of adsorbate for the first isotherm point in PV units, that is

$$P_S V_a(1) = \left\{ \left(\frac{P_1(1)}{T_1(1)} - \frac{P_2(1)}{T_2(1)} \right) V_D - P_2(1)\,\frac{V_C}{R\,T_C} \right\} T_S \,. \qquad (5\text{-}12)$$

The cell was isolated from the doser volume after equilibrium of the first isotherm point by closing stopcock (7). Adsorptive was added to the doser volume and the initial pressure for the second isotherm point, $P_1(2)$ at $T_1(2)$, was recorded. Stopcock (6) was opened, the adsorptive was expanded into the cell and the equilibrated pressure $P_2(2)$ and $T_2(2)$ was recorded. A second material balance gave

$$n_{D,1}(2) + n_{C,2}(1) + n_{a,2}(1) = n_{D,2}(2) + n_{C,2}(2) + n_{a,2}(1,2) \qquad (5\text{-}13)$$

where $n_{D,1}(2)$ was the moles of adsorptive in the doser volume at the initial conditions for the second isotherm point, $n_{D,2}(2)$ was the moles of adsorptive in the doser volume at the final conditions for the second isotherm point, $n_{C,2}(2)$ was the moles of adsorptive in the gas phase in the cell at the final conditions for the second isotherm point, and $n_{a,2}(1,2)$ was the total moles of adsorbate at the final conditions for the second isotherm point. The total moles of adsorbate, the sum of the moles adsorbed after each expansion into the cell, was given by

$$n_{a,2}(1,2) = n_{a,2}(1) + n_{a,2}(2) \qquad (5\text{-}14)$$

where $n_{a,2}(2)$ was the moles of adsorptive that adsorbed at the final conditions for the second isotherm point as a result of the second dose. Equation (5-14) was substituted into (5-13) and the amount adsorbed, $n_{a,2}(2)$, was given by

$$n_{a,2}(2) = \frac{P_1(1)}{R\,T_1(2)} + \frac{P_2(1)\,V_C}{R\,T_C} - \frac{P_2(2)\,V_D}{R\,T_2(2)} - \frac{P_2(2)\,V_C}{R\,T_C} \qquad (5\text{-}15)$$

or in terms of volume adsorbed,

$$P_S V_a(2) = \{ \left(\frac{P_1(2)}{T_1(2)} - \frac{P_2(2)}{T_2(2)}\right) V_D = \left(P_2(2) - P_2(1)\right) \frac{V_C}{T_C} \} T_S. \qquad (5\text{-}16)$$

The procedure was repeated for the third isotherm point. The initial pressure, $P_1(3)$ at $T_1^*(3)$, was recorded, and the adsorptive was expanded into the cell, after which the equilibrated pressure $P_2(3)$ at $T_2(3)$ was recorded. The material balance gave

$$n_{D,1}(3) + n_{C,2}(2) + n_{a,2}(1,2) = n_{D,2}(3) + n_{C,2}(3) + n_{a,2}(1,2,3) \qquad (5\text{-}17)$$

where $n_{D,1}(3)$ was the moles of adsorptive in the doser volume at the initial conditions for the third isotherm point, $n_{d,2}(3)$ was the moles of adsorptive in the doser volume at the final conditions for the third isotherm point, $n_{C,2}(3)$ was the moles of adsorptive in the gas phase in the cell at the final conditions for the third isotherm point and $n_{a,2}(1, 2, 3)$ was the total moles of adsorbate at the final conditions for the third isotherm point. The total moles of adsorbate after the third dose was

$$n_{a,2}(1,2,3) = n_{a,2}(1) + n_{a,2}(2) + n_{a,2}(3) \qquad (5\text{-}18)$$

where $n_{a,2}(3)$ was the amount of adsorptive that was adsorbed as a result of the third expansion of adsorptive into the cell. The amount adsorbed was given by

$$P_S V_a(3) = \{ \left(\frac{P_1(n)}{T_1(n)} - \frac{P_2(n)}{T_2(n)}\right) V_D - (P_2(n) - P_2(n-1)) \frac{V_C}{T_C} \} T_S \qquad (5\text{-}19)$$

The expression for the nth isotherm point was obtained after inspection of Equations (5-12), (5-16), and (5-19); that is,

$$P_S V_a(n) = \{ \left(\frac{P_1(n)}{T_1(n)} - \frac{P_2(n)}{T_2(n)}\right) V_D - (P_2(n) - P_2(n-1)) \frac{V_C}{T_C} \} T_S \qquad (5\text{-}20)$$

where $V_a(n)$ was the amount of adsorptive that adsorbed at the final pressure $P_2(n)$ as a result of the nth expansion of adsorptive into the cell and $P_2(n-1)$ was zero when $n=1$. The amount of adsorptive that was adsorbed per gram of catalyst was a result of the nth expansion was given by

$$V_a(n) = \frac{P_S\ V_a(n)}{(760\ \text{Torr})\ (\text{mass catalyst, g})} \qquad (5\text{-}21)$$

or, in μmol per gram of catalyst,

$$n_a(n) = \frac{V_a(n)}{0.22414\ \text{cm}^3\ \mu\text{mol}^{-1}} \qquad (5\text{-}22)$$

The total amount of adsorbate at the equilibrium pressure $P_2(n)$ for the nth isotherm point was

$$n_a\ (\mu\text{mol g}^{-1}) = \sum_{n=1}^{n} n_a(i). \qquad (5\text{-}23)$$

The value of n_a (μmol g^{-1}) for each $P_2(n)$ was plotted versus $P_2(n)$. The best straight line through the n isotherm points was extrapolated to zero pressure, and this intercept was taken as the amount of adsorptive taken up by the supported metal.

A series of typical isotherms are presented in Figures 68 and 69 for hydrogen, oxygen, and carbon monoxide chemisorption on an 0.53 weight percent platinum on silica hydrogenation catalyst.

A second platinum hydrogenation catalyst 0.56 percent Pt/Al_2O_3 (obtained from a different source) was used for additional testing of the apparatus. The catalyst was reduced in-situ in flowing of hydrogen at 450°C for four hours prior to chemisorption experiments which were conducted at room temperature (25°C). The reduced catalyst was evacuated (down to 10^{-5} torr) at 50 percent above the temperature of reduction for 1-1/2 hours in order to remove any residual hydrogen before hydrogen chemisorption. A double isotherm method was used to ascertain the hydrogen uptake values (Figure 70). The first isotherm represented both chemisorbed and physisorbed hydrogen. After this, the sample was evacuated at room temperature to remove the physisorbed fraction of hydrogen and then the second isotherm, representing only physisorbed hydrogen, was generated. As shown in Figure 70, the isotherms were essentially parallel. The amount of chemisorbed hydrogen was obtained by taking the difference in the hydrogen uptake values corresponding to the two isotherms at zero pressure. In this particular case, the amount of hydrogen chemisorbed was found to be 4.019 μmol/g^{-1} catalyst. This gave a dispersion of 20.3 percent, which was considered reasonable.

A computer program (listed in Appendix D) was written and used to analyze the chemisorption data. A representative output of this program is included in Appendix D.

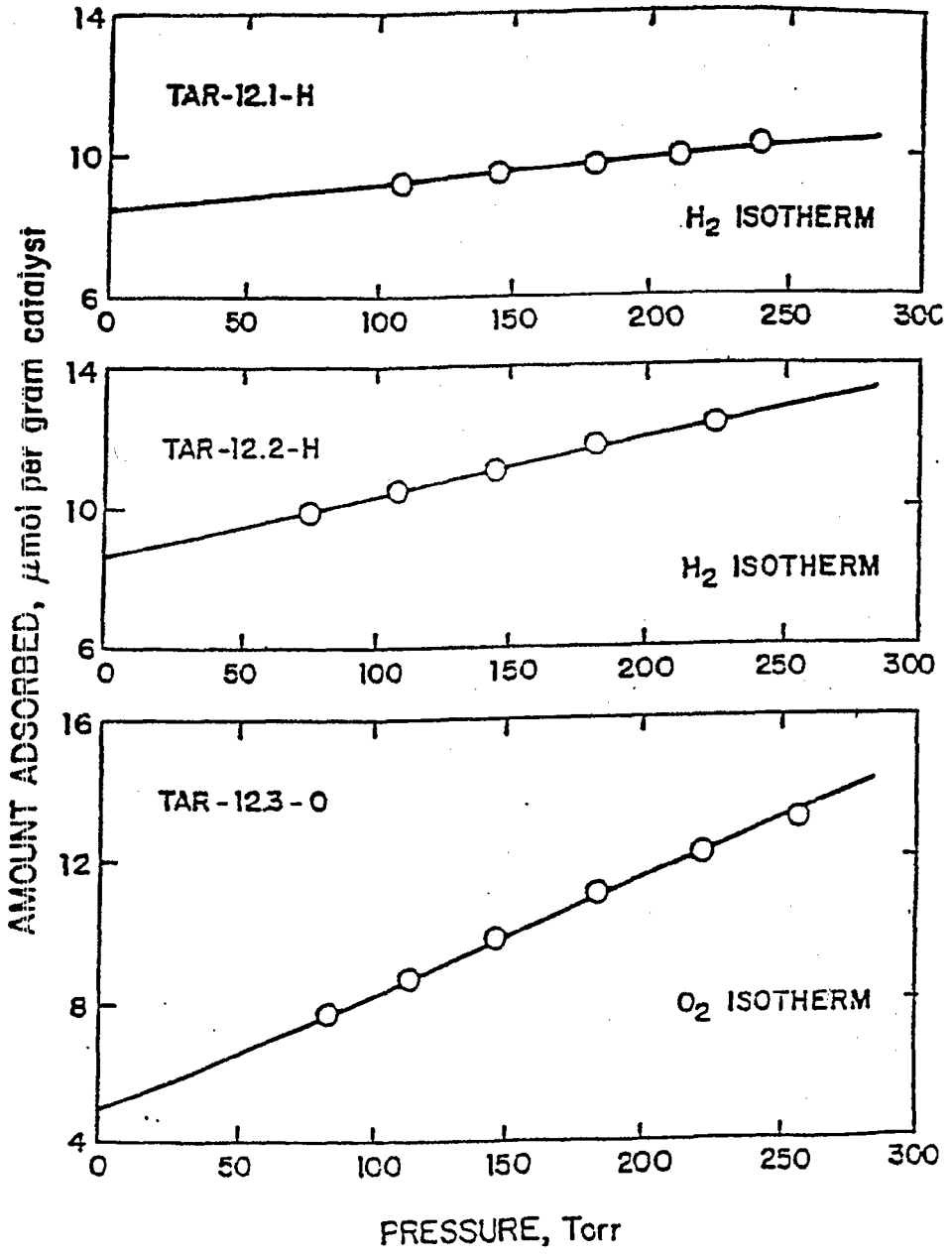

Figure 68. Hydrogen and Oxygen Adsorption Isotherms
0.53% Pt/SiO_2 Catalyst

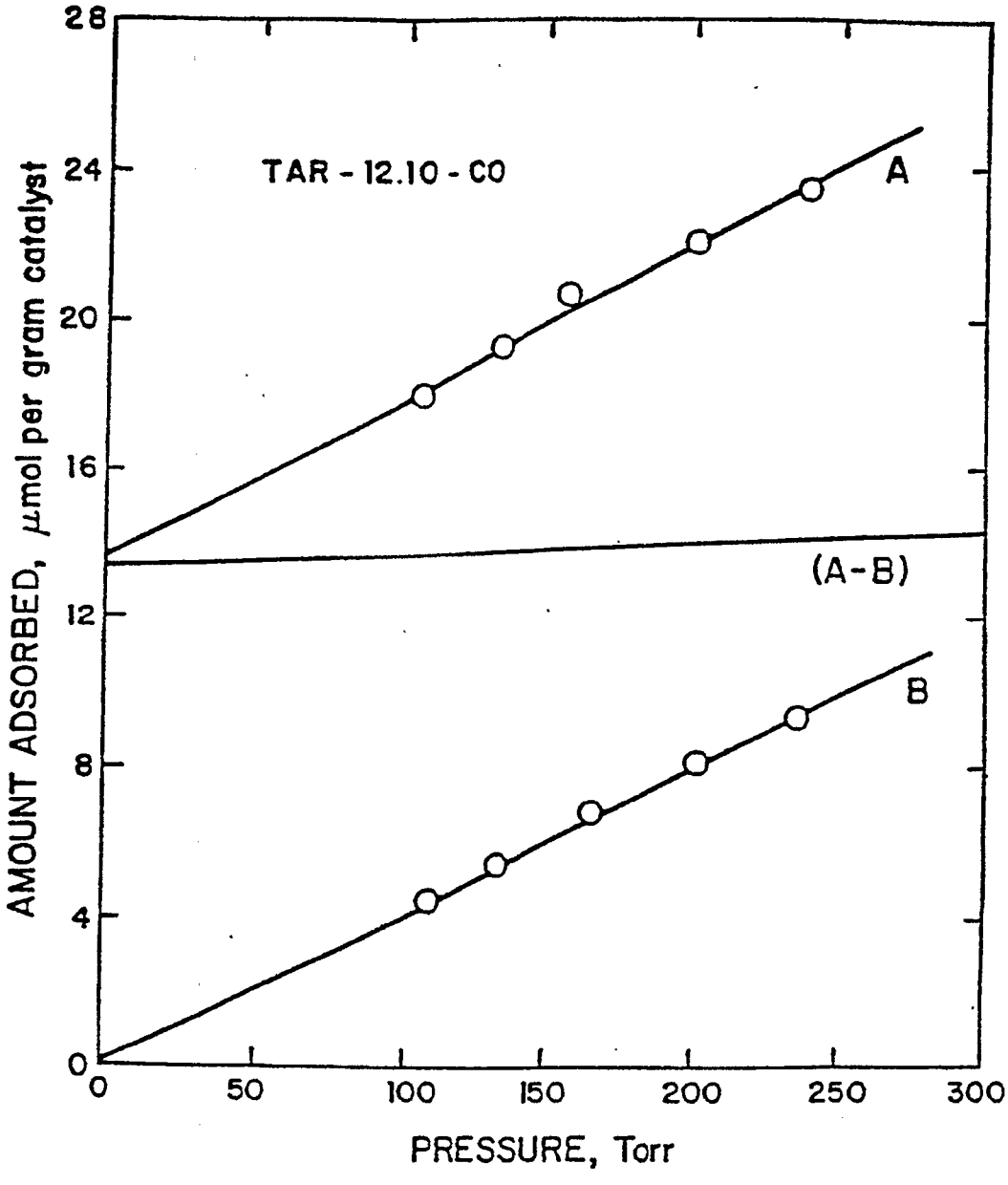

Figure 69. Carbon Monoxide Adsorption Isotherm
0.53 Pt/SiO_2 Catalyst

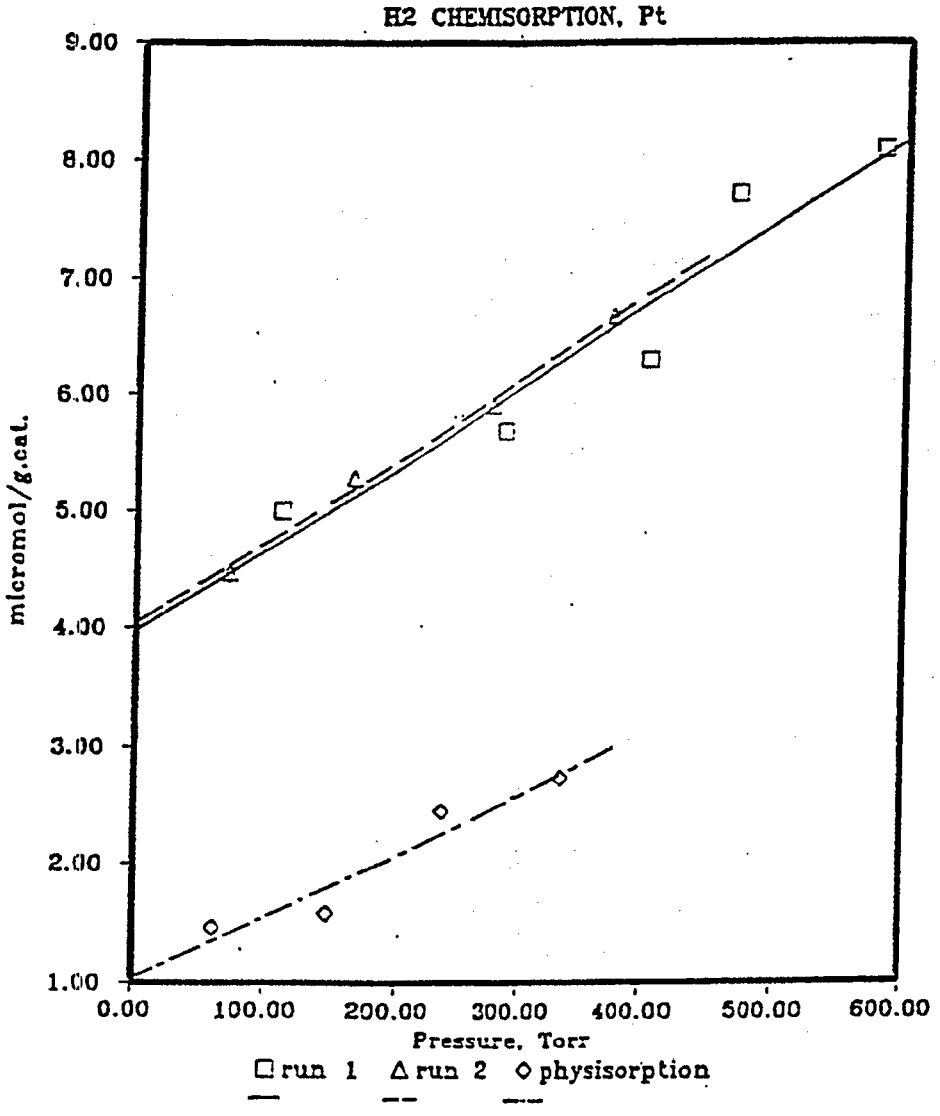

Figure 70. Hydrogen Chemisorption Isotherm for Pt/Al_2O_3

Table 29

Chemisorption Data for Pt/SiO_2 Catalyst

TAR-12

Catalyst:	0.53 percent Pt/SiO_2
Catalyst loading:	2.0078 g (wet) 54.55 μmol total Pt
Cell temperature:	293 K
Cell volume:	10.4403 cm^3
Doser volume:	6.8593 cm^3

TAR-12.1-II (Hydrogen Isotherm)

P_1 (Torr)	T_1 (K)	P_2 (Torr)	T_2 (K)	n_a (μmol g^{-1})
326.6	300.7	107.8	300.8	9.20
209.0	300.8	146.6	300.8	9.53
232.6	300.9	179.8	300.9	9.75
260.4	300.8	210.8	300.8	9.93
284.4	300.7	239.0	300.7	10.19

---

catalyst pretreatment:	evacuation, 423 K, 2 h reduction, 673 K, 4 h evacuation, 723 K, 1-1/2 h
intercept:	8.54 μmol g^{-1} H_2 uptake

Table 29 (con't)

Chemisorption Data for Pt/SiO_2 Catalyst

TAR-12.2-H (Hydrogen Isotherm)

P_1 (Torr)	T_1 (K)	P_2 (Torr)	T_2 (K)	n_a ($\mu mol\ g^{-1}$)
244.6	301.5	74.2	301.7	9.90
162.4	301.8	107.6	301.8	10.46
205.7	301.8	144.5	301.8	11.06
243.7	301.6	181.8	301.5	11.71
293.1	301.5	223.9	301.3	12.27

---

catalyst pretreatment: evacuation, 573 K, 1-1/2 h
intercept: 8.67 $\mu mol\ g^{-1}$ H_2 uptake

TAR-12.3-O (Oxygen Isotherm)

P_1 (Torr)	T_1 (K)	P_2 (Torr)	T_2 (K)	n_a ($\mu mol\ g^{-1}$)
253.8	300.3	82.7	300.6	7.70
166.4	300.7	113.4	300.8	8.64
205.7	300.9	146.9	300.9	9.79
245.6	301.0	182.8	300.9	11.03
284.6	300.9	220.1	300.9	12.13
318.4	300.8	256.3	300.8	13.14

---

catalyst pretreatment: evacuation, 723 K, 2 h
intercept: 5.0 $\mu mol\ g^{-1}$ O_2 uptake

Table 29 (concluded)

Chemisorption Data for Pt/SiO_2 Catalyst

TAR-12.10-CO (Carbon Monoxide Isotherm)

P_1 (Torr)	T_1 (K)	P_2 (Torr)	T_2 (K)	n_a (μmol g^{-1})
363.4	296.7	104.8	296.7	18.00
183.0	297.0	132.9	298.2	19.24
223.4	298.5	165.3	298.7	20.72
265.3	298.8	201.5	299.0	22.16
303.8	299.1	238.7	299.3	23.51

catalyst pretreatment: reduction, 673 K, 4 h
evacuation, 723 K, 1-1/2 h

P_1 (Torr)	T_1 (K)	P_2 (Torr)	T_2 (K)	n_a (μmol g^{-1})
298.9	299.5	107.5	299.8	4.48
182.8	299.9	134.7	300.0	5.53
223.7	300.2	166.7	300.2	6.84
265.4	300.3	202.5	300.4	8.16
295.9	300.5	236.4	300.5	9.34

catalyst pretreatment: evacuation, 293 K, 120 s
intercept: 13.45 μmol g^{-1} net CO uptake

Hydrogenation of Toluene

A high-pressure flow reactor was used to make an exploratory hydrogenation reaction run with toluene as feed and 2 percent Ni/Al_2O_3 as catalyst. The reactor system was available and was used for these preliminary experiments. The experimental conditions were as follows:

Catalyst:	2 percent Ni/Al_2O_3 (6.5 cm^3)
Temperature:	300°C
Pressure:	370 Psig
Toluene LHSV:	15.2 cm^3/hr cm^3 cat.
Hydrogen GHSV:	0.21 cm^3/hr cm^3 cat.
Reaction Time:	4 h.

The catalyst was secured between two layers of inert 'Denstone' and separated by two stainless steel mesh cloths. A thermocouple was placed through a thermowell so that the tip of it was exactly at the center of the catalyst bed. The calcined catalyst was reduced in-situ in flowing hydrogen (at 1 atm and at 37 cm^3/min) for four hours at 450°C. After reduction, the reactor was cooled down to 300°C and the toluene flow was started. A sample was taken after 4 hours of run and analyzed. The conversion was found to be about 10 percent and the products were mainly methyl cyclohexane. A GC column (10 percent OV-17 on chromwax, 12') was purchased and tested for analysis. This is capable of analyzing aromatic hydrocarbons and naphthenes and naphthenoaromatics containing up to at least 14 carbon atoms.

Hydrogenation of Naphthalene

A series of experiments was conducted with a variety of metals supported upon alumina. The metals included ruthenium, rhodium, palladium, and rhenium. At high temperatures (>275°C),

the predominant reaction pathway was cracking, whereas at low temperatures (<230°C), the cracking reactions were suppressed and the hydrogenation pathway was dominant. The preliminary results are summarized in Table 30. The reported data were obtained at a hydrogen partial pressure of 2300 psig with a 0.5 wt percent naphthalene in normal heptane feedstock. The duration of each run was 2.5 hours. The catalysts were reduced in-situ in flowing hydrogen (40 cm^3 min^{-1}) at 500°C for six hours. As indicated previously, this work was deemphasized and placed on inactive status at the direction of the Technical Project Officer.

Table 30

Hydrogenation of Naphthalene over Various Catalysts

Run #	Catalyst	Temp, °C	percent Conversion	percent Selectivity		
				Tetralin	Decalins	Cracking
1.	2.5 percent Ru/Al_2O_3	300	100	0	11.0	89.0
2.	2.5 percent Ru/Al_2O_3	225	100	0	97.0	3.0
3.	2.5 percent Ru/Al_2O_3	125	100	0	100.0	0.0
4.*	2.5 percent Ru/Al_2O_3	300	90	--	10.0	90.0
5.	2.5 percent Rh/Al_2O_3	300	100	trace	95.0	4.9
6.	2.5 percent Pd/Al_2O_3	300	100	trace	99.0	--
7.	5.0 percent Re/Al_2O_3	300	82	29.5	65.5	5.0

*This run was made with decalin as feed.

Section VI: SELECTIVE CATALYTIC CRACKING OF NORMAL PARAFFINS IN KEROSENE BOILING RANGE FEEDSTOCKS OVER ZSM-5

Research Personnel: Daniel C. Longstaff
Graduate Student

Francis V. Hanson
Associate Professor

Introduction

The research activities reported in this section were primarily concerned with producing higher density aviation turbine fuel from waxy naphthenic crudes. The method proposed to produce a high density fuel was to expand the boiling range of the fuel by increasing the end-point of the kerosene fraction of a naphthenic crude. The expansion of the boiling range will result in a higher density kerosene; however, it will also have an undesirably high freeze point. Dewaxing will reduce the freeze point of the kerosene so it can meet aviation turbine fuel specifications while having a higher density.

Normally jet fuels are not subjected to any catalytic treatment other than perhaps a mild catalytic hydrogenation to reduce the sulfur content when the sulfur content exceeds specifications or a mild catalytic oxidation to oxidize mercaptan sulfur so it can be removed more easily by a caustic wash. Catalytic dewaxing would represent a new processing step in the production of aviation turbine fuels and would increase the cost of producing jet fuels. However, it would also broaden the range of acceptable crudes for the production of standard and high density aviation turbine fuels to include the use of certain waxy naphthenic crudes.

A secondary effect would be the stabilization of crude availability for aviation turbine fuel manufacture, particularly during an oil shortage or in wartime.

Experimental Apparatus

Commercial catalytic dewaxing of lubricating oils is carried out in a fixed bed reactor system. A fixed bed reactor system was modified for this investigation.

The modifications included the following:

1. a liquid feed reservoir and pump were added to the apparatus;
2. the gas feed system was modified to handle a single gas; and
3. a reactor by-pass line was added to facilitate operation of the system.

Description of the Components of the System

A schematic of the apparatus is presented in Figure 71. The reactor system consisted of four main components:

1. the gas feed system;
2. the liquid feed system;
3. the reactor; and
4. the product collection system.

Gas Feed System

The gas feed system was designed to regulate and monitor the flow of the diluent gas to the reactor. The pressure of the gas exiting the reactor was controlled by a Mity Mite Inc. back pressure control valve (BPCV) which was rated to 2000 psig. The BPCV was pressurized to the desired operating pressure with nitrogen. The gas flow rate to the reactor was controlled by a Union Carbide Mass Flowmeter Model FM-12C.

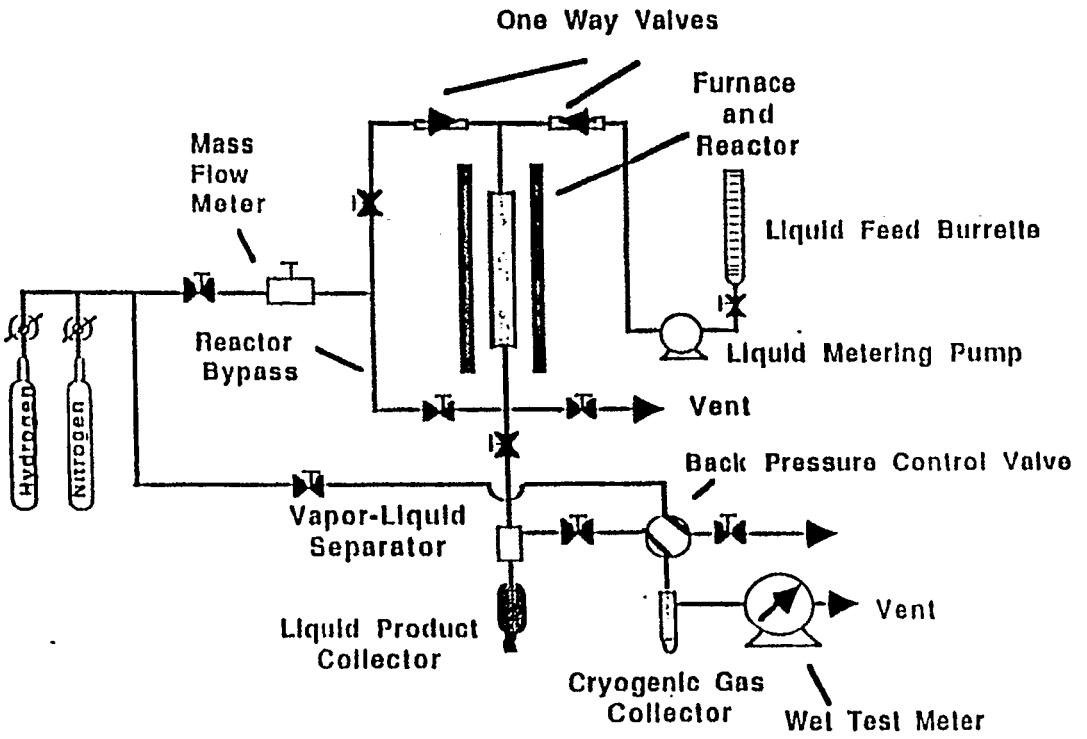

Figure 71. Diagram of Catalytic Dewaxing Reactor System

The system was protected from overpressuring by a Swagelok, Inc., model SS-4R3A-C, pressure relief valve which could be set to open at pressures between 750 and 1500 psig. The pressure relief valve was usually set to open at 970 psig which was 30 psig below the maximum pressure rating of the liquid feed pump.

A bypass line made it possible to flush the product collection system without passing the gas through the reactor. The gases used in the gas feed system were hydrogen and nitrogen. Hydrogen was used as the diluent in most experiments and nitrogen was used to flush the reactor or to pressurize the BPCV.

Liquid Feed System

The liquid feed system was designed to control and monitor the flow of liquid into the reactor. The main component of the system was a Milton Roy model DB-1-60R metering liquid feed pump. The volume pumped could be controlled by adjusting a dial on the pump which controlled the stroke length of the pump piston. The minimum steady state pump rate was such that a weight hourly space velocity (WHSV) of 1-3 g of feed/(g of catalyst)(h) could be maintained over a two gram sample of catalyst. The maximum operating pressure of the pump was 1000 psig. In order to avoid the possibility of damaging the pump by overpressurizing, a pressure relief valve was connected to the liquid feed line. The Swagelok Inc. model SS-4R3A-C pressure relief valve could be set to open between 750 and 1500 psig. During normal operation the valve was set to open at 970 psig.

A valve was connected to the liquid feed line so that the pump could be primed prior to operating at elevated pressures. The liquid feed passed into the gas-liquid mixing zone through a one way valve to prevent the flow of gas into the liquid feed system.

Reactor

The reactor consisted of a 1/2 inch inside diameter stainless steel tube encased in a cylindrical copper block which acted as a heat sink to evenly distribute the heat from the furnace. The intent was to prevent large localized heat variations in the reactor due to hot or cold spots in the electrical furnace. A 1/8 inch OD thermowell was located on the axis through the reactor tube to monitor the temperature profiles in the catalyst bed.

The reactor tube had a flange threaded onto each end of it. These flanges could be connected to matching flanges through which feed or products could flow. The reactor was sealed by stainless steel o-rings.

Product Collection System

The effluent stream from the reactor passed into a vapor-liquid separator which also served as a liquid collector. The non-condensible vapor stream was vented through the BPCV.

The cryogenic gas collector consisted of a vaporizer test tube that was packed with shredded cellulose submerged in a liquid nitrogen bath to condense all the condensibles into a vessel which could be weighed to determine the mass of material collected.[251] This method usually provided a mass balance of 100 ± 0.5-2 percent.

The composition of the gases condensed were determined by gas chromatography. The volume of the gas that passed through the cryogenic gas collector was determined with a wet test meter.

Operating Procedure

The acquisition of meaningful data required that the following be observed:

1. the reaction conditions must remain constant, that is the temperature, pressure, catalyst activity and liquid and gas feed rates should not change during the time period when a material balance is made; and
2. a complete mass balance must be obtained on the hydrocarbon feed.

The experimental operating procedures were developed to maintain the reaction conditions constant and to enable collection and measurement of the liquid and gas products of the reaction.

Catalyst Loading Procedure

The catalyst bed was located between two sections of inert packing. The inert packing serves to support the catalyst as well as providing a surface for heating the reactant mixture. The catalyst was loaded into the reactor according to the following procedure. The top flange was secured to the reactor. The thermowell was connected to the top flange and positioned along the axis of the reactor. The reactor was clamped upside down in a vise. A plug of nitric acid washed glass wool was inserted in the reactor without pushing it through the top flange. Alundum that had been soaked in hot nitric acid, rinsed with deionized water and dried was then poured into the reactor to within 1/2 inch of the point along the entered thermowell where the catalyst bed was to be placed. Distances in the thermowell were gauged by means of a rod that was slid into the reactor to determine the depth of the alundum bed. After the alundum was packed to the appropriate depth a second wad of nitric acid washed glass wool was placed in the reactor and a sample of catalyst was placed on top of the plug of glass wool.

The catalyst was then held in place by a third plug of acid washed glass wool. The glass wool plug was then followed by enough acid washed alundum to fill up the reactor to within 1/2 inch of the top. A fourth and final plug of glass wool was then placed in the reactor to keep particles of alundum from falling out of the reactor.

After the reactor was completely packed the bottom flange was bolted onto the reactor and it was pressure tested with nitrogen. A mixture of silicon carbide and dodecane would be used to polish the o-rings so that they would form a proper seal with the reactor.

The pressure test was done with the reactor in the vise. This facilitated any necessary adjustments. The orientation of the o-rings with respect to the reactor tube was changed if a particular configuration had a tendency to leak. When it was determined that the reactor did not leak it was connected to the reactor system and the standard catalyst pretreatment procedures were followed.

Mass Balance Procedure

Experiments must be conducted so as to obtain complete material balances so that definitive conclusions concerning catalyst activity and selectivity can be drawn. In most cases catalytic runs with complete mass balances were only attempted once a day due to the effort required.

The reactor was always left at reaction temperature to save time and to avoid possible effects on the catalyst resulting from heating and cooling cycles. Prior to making a material balance the feed and diluent gas were passed over the catalyst for a period of time ranging from an hour to several hours to ensure that the catalyst and the system were operating at steady state. The gas flow rate was determined with a wet test meter. The liquid feed pump set point was set so that the correct liquid hourly space velocity was established. The rate of liquid feed was determined by measuring the amount of liquid removed from the liquid feed buret during a given period of time.

During the equilibrated stage of the experiment the liquid accumulated in the vapor-liquid separator was occasionally removed from the separator by means of a valve at the bottom of the

separator. This was always done slowly to minimize the reduction of the pressure in the system. The cryogenic gas collector was not cooled during this period because it was much more difficult to empty than the vapor-liquid separator.

Prior to the start of the material balance a sample of gas leaving the vapor-liquid separator was taken to determine the methane to ethane ratio of the product gas. This was done because the vapor pressure of methane is high enough in the cryogenic liquid separator that most of it escapes to the vent. This does not significantly affect the mass balance because of the small amount of methane that is normally produced but it makes it impossible to accurately correlate data based on methane collected in the cryogenic liquid separator.

At the start of the material balance the vapor-liquid separator was carefully emptied without upsetting the system pressure, the volume of liquid in the buret was recorded, the reading on the wet test meter was set to zero and the timer was started. The cryogenic gas collector was filled with liquid nitrogen and kept filled for the duration of the material balance. During the course of the run the reactor temperature was recorded. A reactor temperature profile was sometimes recorded if it was thought that it might provide useful information about the nature of the reactions taking place in the catalyst bed.

When the material balance was completed the volume of liquid in the buret and the reading on the wet test meter were recorded. The time that had elapsed since the start of the material balance was also noted. The pump was shut off and the valve between the reactor and the vapor-liquid separator was shut off to prevent extra product being collected in addition to the product that was collected during the time period of the material balance. The valve in the reactor bypass was opened so that gas would continue to flow from the gas supply system to the product collecting system while keeping the reactor separated from the rest of the system.

The C_3 and C_4 species dissolved in the liquid product collected in the vapor-liquid separator were weathered into the cryogenic vapor collector. The test tube in the cryogenic vapor collector was removed and weighed to determine the mass of vapor collected.

The test tube from the cryogenic vapor collector was allowed to warm to room temperature and the vapors evolved were collected by water displacement. The gas that was collected in the water bottle was transferred to a gas sampling bottle and a sample was injected into a gas chromatograph to determine the relative amounts of the different hydrocarbons.

While the test tube from the cryogenic vapor trap was warming to room temperature the liquid from the vapor liquid separator was collected and weighed. A sample of the liquid was saved in a glass sample bottle which was then stored in a refrigerator. About 0.05 μl of the liquid was injected onto a 10 percent Phenylmethyl silicon 10 M X 530 μm column for gas chromatographic analysis.

The mass balance was determined by comparing the sum of the weight of the gas and liquid products with the weight of liquid feed.

Computer Analysis of Results

If the mass balance was good (100 ± 2 percent), the chromatographs of the gas and liquid products were analyzed for the amounts of different species. A computer program was written to compute the conversions to paraffins, olefins and naphthenes, and aromatics of different carbon numbers. The program is found in Appendix B along with a sample input and output.

Model Compound Studies

Catalyst Preparation

It is accepted that ZSM-5 catalysts exhibit the shape selective properties necessary to selectively crack normal paraffins and isoparaffins in a mixture of kerosene and higher boiling range naphthenes.[8-10,252,253] However, the optimum parameters that are required for catalyst synthesis, catalyst pretreatment and reaction conditions are not outlined in the literature. The objective of this research was to dewax an expanded boiling range distillate, to produce a high density aviation turbine fuel rather, than to produce a high octane naphtha. Therefore, it was decided to maximize catalyst activity at the expense of high octane cracked products.

Initially it was thought best to study the cracking of a model compound, n-hexadecane, because it is a normal paraffin of approximately the same boiling range as the distillates that were to be catalytically dewaxed. In addition there are several literature references to the cracking of n-hexadecane over HZSM-5[254] and Pt/HZSM-5.[255]

Unfortunately these reports lack details on how the catalysts were activated. It has been reported[16] that the active cracking sites in HZSM-5 are the strong acid tetrahedral aluminum sites which are not fully activated from the ammonium form of the catalyst except by calcination at temperatures above 623-773 K (350-500°C). Care was taken not to heat the catalyst to a temperature higher than that necessary to activate the strong acid sites to avoid the possibility of dehydroxylation of strong Brönsted sites to weaker Lewis base sites[256] and the consequent reduction of total cracking activity.

Ammonia TPD indicated that most of the strong acid sites are activated by heating above 773 K (500°C). Therefore it was decided to activate the ZSM-5 catalysts by heating in air to 783 K (510°C) in air at a programmed rate of 5 K/ min. The sample was held at 783 K (510°C) for

10 minutes followed by cooling to room temperature. The catalysts were then loaded in the reactor and heated to the reaction temperature.

Thermal Cracking

In order to establish that the reactor possessed no inherent catalytic cracking activity due to the wall surface or to the inert packing in the reactor a set of blank cracking runs were conducted. The reactor was packed with inert alumina and hexadecane was passed over the alumina at different temperatures to determine the conversion. Five runs were done at 50 K intervals from 573 to 773 K (300 to 500°C). No attempt was made to collect or analyze the gas product. The liquid product was analyzed by gas chromatography.

At 573 K, 623 K, and 673 K (300, 350 and 400°C) there was little or no conversion as evidenced by the lack of chemical species other than normal hexadecane in the liquid product. At 723 K (450°C) a series of equally sized peaks from C_{10} to C_{15} were obtained. These species were believed to have been alpha olefins resulting from the thermal cracking of normal hexadecane. A series of other peaks were also obtained. At 773 K (500°C) a higher yield of the same product slate was obtained. These experiments indicated that the reactor and the inert alumina packing possessed no inherent cracking activity at temperatures below 673 K (400°C). Above 673 K (400°C) the alumina packing may exhibit the ability to catalyze thermal cracking reactions. It was also concluded that at temperatures greater than 673-723 K (400-450°C) the apparent selectivity of the catalyst will reflect nonshape-selective thermal cracking reactions.

Hexadecane Cracking at 573 K (300°C)

A series of experiments were performed at 573 K (300°C) to determine if the cracking product boiling above C_4 could be maximized by the right choice of operating conditions. The

way to achieve this object is to minimize secondary cracking of the primary cracked products. The cracking experiments were performed over a range of WHSV at constant total pressure and temperature.

The temperature at which the cracking of n-hexadecane over ZSM-5 was studied was selected to minimize secondary cracking of the primary products of the reaction. However, low rates of secondary cracking are achieved at the expense of cracking activity. In commercial hydrodewaxing over ZSM-5[10] the initial temperature of reaction is 563 K (290°C) with fresh HZSM-5. As the catalyst deactivates the temperature is gradually raised to 643 K (370°C) over a period of several weeks. The reactor then operates at temperatures between 643 and the end of the cycle temperature, 703 K (430°C) At 703 K (430°C) the catalyst is regenerated.

It is also noted that a study of n-hexadecane cracking on ZSM-5 by Bezouhanova et al.[254] indicated that at a LHSV of 1 and a temperature of 643 K (370°C) the primary product obtained with HZSM-5 of varying Si/Al ratios were C_3's and C_4's and to a lesser extent aromatics. Therefore it was thought that by lowering the temperature of reaction that the yield of higher boiling products could be increased. A temperature of 573 K (300°C) was chosen to study the rate of formation of secondary and primary cracked products as a function of the space velocity.

A pressure of 200 psig was chosen for the experiments because it was thought that hydrogen pressure would reduce the rate of coke formation and maintain catalyst activity. In commercial dewaxing processes a pressure of 400-800 psig of hydrogen and hydrocarbon is used with HZSM-5[10] and 300-1500 psig with Pt-H-Mordenite.[11]

The hexadecane was diluted with hydrogen at 200 psia to prevent the condensation of hexadecane in the reactor due to the vapor pressure of hexadecane at 573 K (300°C) (≈19 psia).

The ammonium form of the catalyst was pressed into pellets at 90000 psig. The pellets were then crushed and sized between 14 and 35 mesh. Pellets smaller than 35 mesh were crushed into powder and repressed into new pellets. Pellets that were larger than 14 mesh were recrushed. This procedure was followed until all the zeolite was incorporated into granules between 14 and 35 mesh.

The zeolite was 93 percent crystalline and ammonia temperature programmed desorption measurements showed that it had 0.5 mmol/g of Brönsted acid sites. After calcination at 783 K (510°C) two grams of this sample was placed in the reactor according to the procedure described previously.

An initial experiment was conducted to determine how the catalyst activity and product selectivity changes during catalyst utilization.

Hydrogen flow at 200 psig was established over the catalyst and the flow of hexadecane was started. The temperature of the reactor was about 577 K (304°C) initially. The flow rate of hydrogen was 12 l(STP)/(g•cat)(h) and the WHSV of liquid normal hexadecane was 12.

In the first two or three minutes the temperature of the catalyst rose five or ten degrees centigrade and then dropped as an endothermic temperature profile was established.

Samples of liquid flowing between the catalytic reactor and the vapor liquid separator were collected and analyzed every several hours. The first drops of liquid product contained about 35 weight percent normal hexadecane. Liquid product after 45 min was about 50 weight percent normal hexadecane and after two hours the liquid product was about 65 weight percent normal hexadecane and it remained at that level for the duration of the run.

It was shown from this experiment that the ZSM-5 synthesized and utilized for hydrodewaxing required less than two hours to achieve a metastable activity. There is no doubt

from the literature[10] that there is a very slow decline in the total catalytic activity that occurs over weeks and even months. A time period ranging from an hour to several hours was employed for fresh catalyst attenuation in further experiments.

Cracking Reactions as a Function of Residence Time

A series of cracking experiments were done to study the effect of residence time with respect to the formation of different products. Only those experiments in which a mass balance of 100 ± 2.5 percent were considered acceptable.

The fraction of n-hexadecane feed converted and the yields of primary and secondary cracking products as a function of the space time are presented in Figure 72. The yields of each carbon number produced per one hundred moles of normal hexadecane converted for two different space times are presented in Figure 73.

The percentage of feed converted to primary cracked products and to secondary cracking products was determined by the fact that the moles of feed consumed is equal to the moles of primary cracking reactions and to one half the moles of primary products. The difference between the total moles of cracked products and the moles of primary products is the moles of secondary cracking products.

It is also assumed that the average molecular weight of primary cracked products is equal to one half of the molecular weight of the feed and that the average molecular weight of the secondary cracked products is equal to one fourth of the molecular weight of the feed. These relationships were used in the derivation of the mass balance equation to express that the weight percent of feed converted, the weight percent converted to primary cracked products and to secondary cracked products. The data obtained from these experiments was processed and is presented in Figures 72 and 73.

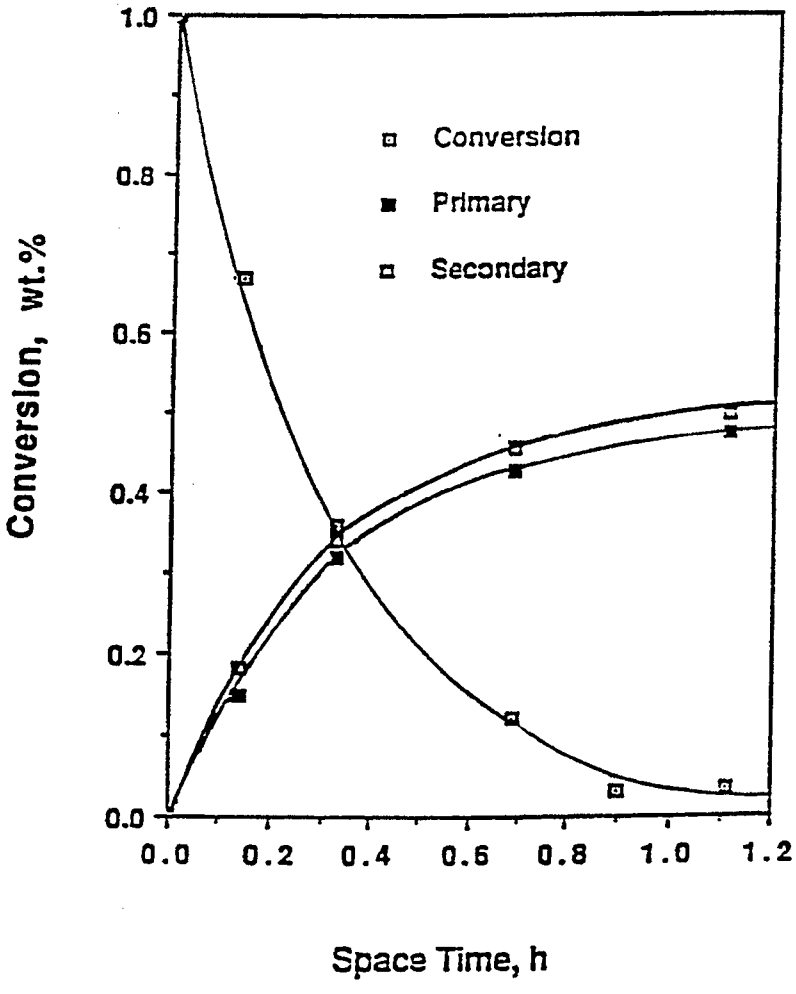

Figure 72. Conversion of n-Hexadecane to Primary and Secondary Cracked Products

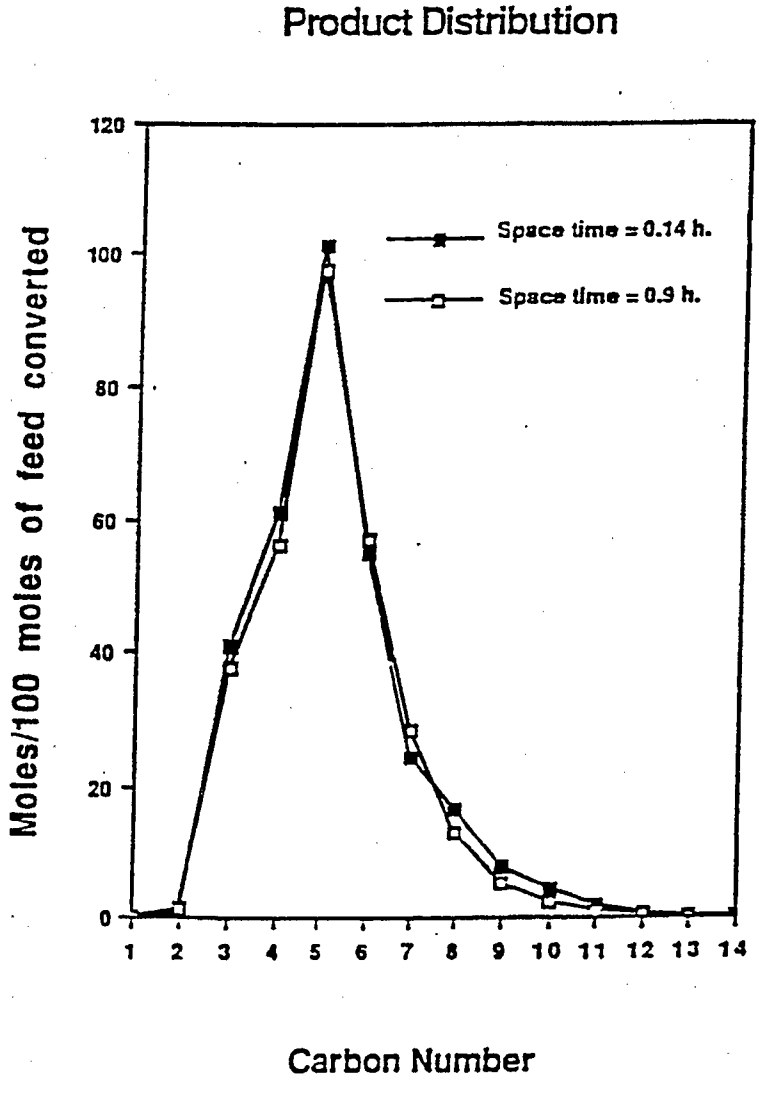

Figure 73. Carbon Number Yield as a Function of Space Time for the Cracking of Normal Hexadecane at 575 K and 200 psia

The conversion of feed, the yield of primary and secondary cracked products as a function of $WHSV^{-1}$ are presented in Figure 72. The secondary cracked products appear to form in parallel with the primary cracked products in Figure 72. This indicates that the lag time between the formation of primary cracked products and the formation of secondary cracked products is very short.

The carbon number yields per 100 moles of feed converted is presented in Figure 73 for two different space times. As in Figure 72, the distribution of product carbon numbers is not a function of space time (or conversion of the feed) indicating that the formation of secondary products from primary cracked products is rapid. It was originally theorized that at lower space times (lower conversions) the products would have significantly more gasoline range boiling material than at longer space times and higher conversions. However at the two space times for which data is presented in Figure 73 there is very little variation in the carbon number yields even though there is a large difference in the two space times.

When the mechanism of cracking is considered it is apparent why the formation of secondary cracked products occurs so rapidly in parallel with the formation of primary cracked products. The rate determining step for the formation of secondary cracked products is the same as the rate determining step for the formation of primary cracked products. The rate determining step for the formation of primary products from hexadecane, as in other catalytic cracking reactions, is the abstraction of a hydride ion to form a carbonium ion.[11] The carbonium formed rapidly cracks and to a smaller carbonium ion and an olefin. The carbonium ion formed in the primary cracking reaction can rapidly crack to form secondary products.

Plots of the weight fraction of the feed converted to paraffins, olefins and naphthenes, and aromatics as a function of space time is presented in Figure 74. Aromatics and paraffins are

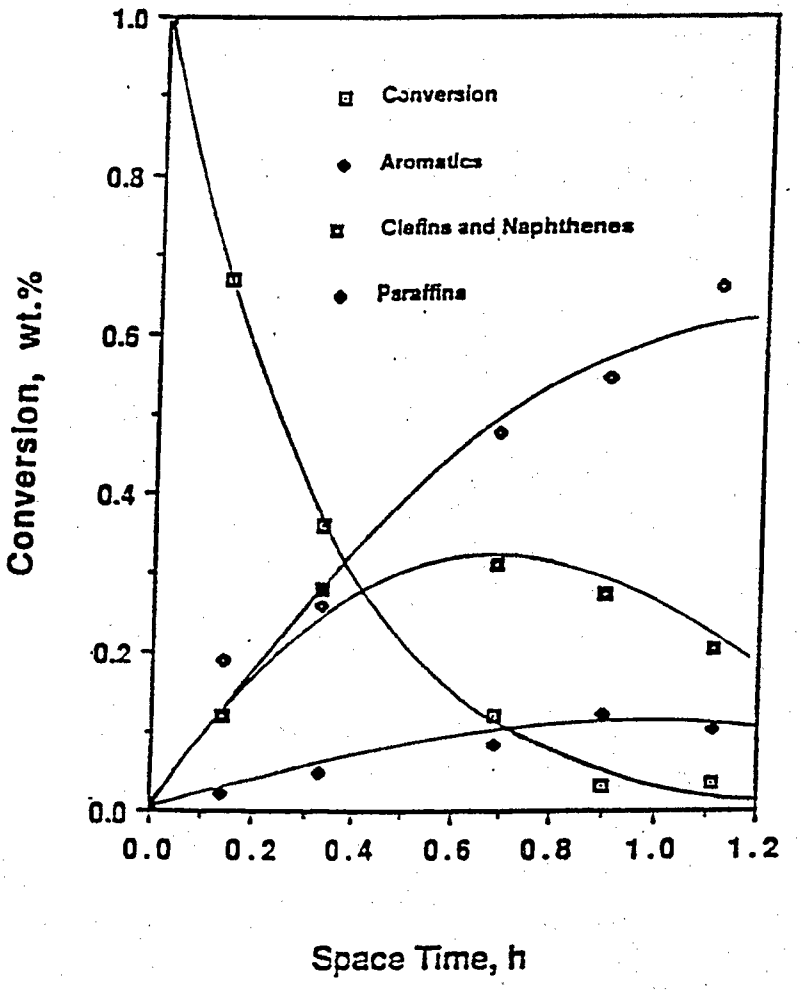

Figure 74. Product Distribution as a Function of Space Time for the Cracking of Normal Hexadecane at 575 K and 200 psia

secondary products formed from olefins (primary products) by hydrogen transfer reactions. There is no lag time in their formation indicating that the secondary reactions of olefins to form aromatics and paraffins occurs more rapidly than the formation of olefins.

These sets of experiments indicated that the ratio of primary to secondary cracked products cannot be varied by varying the retention time of the feed. This is because secondary cracked products are formed so quickly from primary cracked products that the formation of secondary cracked products appears to take place in parallel with the formation of primary cracked products.

It is recognized that the selectivity of the catalyst for the formation of primary products can be adjusted by altering the conditions of catalyst synthesis and pretreatment. However, the objective of this research was not to maximize naphtha production so further investigations concentrated on kerosene freeze point reduction by dewaxing.

Distillate Fuel Studies

Freeze Point Reductions of Kerosene and Diesel Fuels

Samples of kerosene and diesel fuel were obtained from the Flying J Oil Refinery in Salt Lake City. Both were distillate cuts from a blend of Wyoming Sweet and Altamont crudes.

The kerosene cut had an initial boiling point of 411 K (138°C) and an end point of 603 K (330°C) The diesel had an initial boiling point of 456 K (183°C) and an end point of 673 K (400°C). The initial boiling points and endpoints were based on boiling points at normal atmospheric pressure. From the GC analysis it was estimated that the kerosene had an average molecular weight of 182 g/mol.

The kerosene as received had a freeze point of 253 K (-20°C). The diesel had a freeze point of 280.45 K ± 0.1 K (7.3°C ± 0.1°C) and a cloud point between 278.15 and 278.95 K (5. and 5.8°C)

A sample of kerosene was cracked over HZSM-5 at a WHSV of 12, a hydrogen/ hydrocarbon ratio of 13.5, a temperature at 643 K (370°C) and a total pressure of 200 psia. The reaction was run discontinuously for three days. This was done to collect enough liquid product to have sufficient sample for the determination of the freeze point after distillation of the naphtha fraction. No mass balance was attempted. At the conditions of the experiment 30 percent of the total kerosene feed was converted to cracked products.

The liquid products collected in this run were distilled to 446 K (173°C) to remove the cracked products from the unconverted kerosene boiling range feed. The freeze point of the product boiling above 446 K (173°C) was less than 213 K (-60°C) The density of the kerosene had increased from 0.791 to 0.822 at ambient temperature.

A sample of kerosene was cracked at a WHSV of 11.1, a hydrogen/hydrocarbon ratio of 13.9, a temperature of 642.5 K (369.5°C), and a pressure of 200 psia. A mass balance of 101.1 percent was obtained in this experiment. The purpose of this run was to determine the products obtained from cracking of kerosene on HZSM-5 under approximately the same conditions for which the kerosene based jet fuel was obtained. A plot of the product carbon number yield per 100 moles of converted feed as a function of feed and conditions is presented in Figure 75. These results can be compared to Figure 73 which was obtained for the cracking of normal hexadecane at 575 K (302°C). A list of the different products produced from cracking normal hexadecane at 575 K (302°C) on HZSM-5 and from cracking kerosene on at 643 K (370°C) on HZSM-5 is presented in Table 31. The products per one hundred moles of kerosene cracked were adjusted to the same value as the products per one hundred moles of hexadecane cracked. This was necessary because of the lower molecular weight of the kerosene. The factor by which they were multiplied was the molecular weight of normal hexadecane (226 g./mol.) divided by the average molecular weight of the kerosene (182 g./mol.)

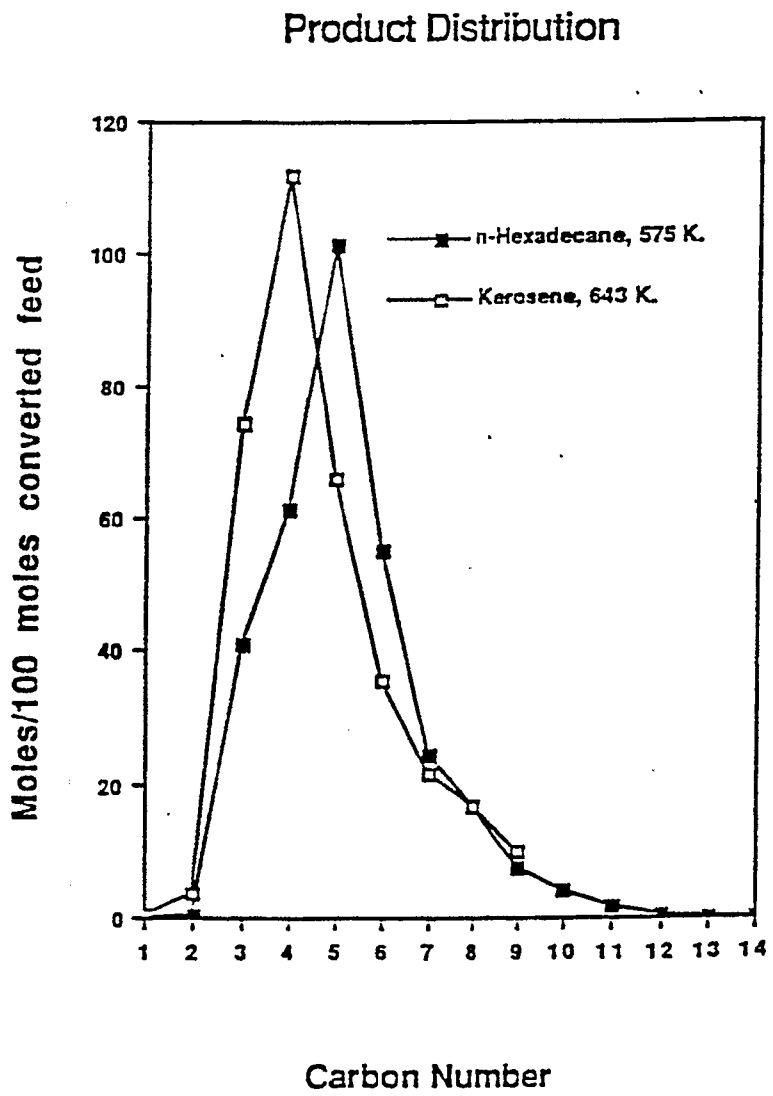

Figure 75. Carbon Number Yield for the Cracking of Kerosene and for the Cracking of n-Hexadecane

Table 31

Product Distribution from the Cracking of Normal Hexadecane and Kerosene over HZSM-5

	Feedstock	
	Normal Hexadecane	**Altamont & Wyoming Sweet Kerosene**
Temperature, K	**575**	**643**
Reactor Pressure, psia	**200**	**200**
C_1	-	0.5
C_2=	1.0	3.2
C_2	0.1	0.6
C_3=	-	31.4
C_3	37.5	42.7
i-C_4	13.5	19.3
n-C_4	21.7	47.1
C_4=	21.2	45.5
i-C_5	19.3	11.6
n-C_5	54.4	19.4
C_5=	23.8	34.6
C_6	39.4	12.2
C_6=*	9.3	20.3
Benzene	6.4	3.2
C_7	14.8	7.4
C_7=*	4.2	10.9
Toluene	5.5	3.4
C_8	7.6	4.3
C_8=*	4.5	6.6
C_8 aromatics	4.3	5.5
C_9	2.0	3.1
C_9=*	0.9	2.6
C_9 aromatics	4.4	4.4
+C_{10}	6.6	-
Total Moles/100 Moles Cracked (adjusted)	302.4	340.3

* olefins and naphthenes

At 643 K (370°C) C_4 is the most abundant product when converting kerosene and that at 573 K (300°C) C_5 is the most abundant product when converting n-hexadecane (Figure 75). The difference is due to temperature rather than to the difference in the molecular weight of the feed. This is confirmed by Corma and co-workers[257] who found that C_3 is the major product for cracking normal heptane on HZSM-5 at 723 K (450°C) and by Bezouhanova et al.[254] who cracked normal hexadecane on HZSM-5 at 643 K (370°C). They found that at low Si/Al ratios that C_3 was the major product and at higher Si/Al ratios that C_4 was the major product.

On acid catalysts paraffins are cracked by a β-scission mechanism. Traditionally propylene and butenes are thought to be the main product of β-scission.[258] This is true for cracking operated at high temperatures but at low temperatures butenes and pentenes are the major products from cracking over HZSM-5. This is probably because carbonium ions are more stable on the fourth or fifth carbon at lower temperatures than on the third and fourth carbons. Because of the predominance of carbonium ions located at higher carbon atoms there is a resulting increase in the formation of C_4 and C_5.

A sample of diesel fuel was passed over HZSM-5 at a WHSV of 12.5-13 with a hydrogen flow of 15-18 l(STP)/(g•cat)(h) at 643 K (370°C) and a total pressure of 200 psia. The reaction was run continuously for two days. The runtime was extended to two days to produce a reasonable amount of kerosene after distilling out the naphtha. No mass balance was attempted but the conditions of the run were such that 30 percent of the feed was converted.

The total liquid product was distilled to 485 K (212°C) to remove the gasoline product from the unconverted diesel feed. The freeze point of the remaining uncracked diesel was reduced from 280.3 K (7.3°C) to less than 208 K (-65°C) The specific gravity had been increased from 0.81 to 0.835. Even though the diesel had an initially higher freezing point than the kerosene, after

dewaxing both samples had essentially no freezing point whatsoever. Since the unconverted portion of the cracked kerosene and distillate cuts consisted principally of naphthenic molecules there was a vast number of different species and different isomers. Consequently, it is difficult for crystals to form because of the low possibility that molecules of the same species or of the same shape can agglomerate to form crystals. Instead of forming orderly crystal structures unlike molecules bond together by van der Waals' forces and the viscosity of the mixture increases. The result of molecules being held by van der Waals' forces without crystals being formed is the formation of a gel that probably does not form crystals even if cooled to cryogenic temperatures.

This does not mean that the low temperature properties of such a mixture would be suitable for use in aviation turbines simply because the fuel does not freeze. Rather, the low temperature viscosity properties of the fuel become more crucial than it's freeze point in aviation turbine fuel applications.

These two experiments showed three things:

1. the freeze point of a waxy naphthenic kerosene and diesel could be reduced to meet jet fuel specifications for freeze points;
2. the freeze point of catalytically dewaxed jet fuels may be replaced by the viscosity of the fuel in setting the low temperature limit in aviation turbine fuel applications; and;
3. the density of a waxy naphthenic distillate is increased by catalytic dewaxing.

Dewaxing of Kerosene and Diesel to Maximize Density

The possibility of increasing the density of the kerosene or diesel cuts by catalytic dewaxing was investigated. The dewaxing of these two samples had not completely removed the paraffins. Since paraffin and isoparaffin molecules reduce the overall density of a distillate, a sample of

kerosene and diesel were submitted to shape selective cracking under such conditions that all or nearly all the paraffins were selectively removed by cracking. These experiments were conducted so that the catalyst operated in a hydrocracking mode induced by hydrogen partial pressures over 900 psia which caused an increase in catalyst activity and selectivity.

The kerosene was cracked at a WHSV of 11, a temperature of 643 K (370°C) and a hydrogen partial pressure of 900 psia. The hydrogen/hydrocarbon pressure ratio was 40. It was kept high to keep the kerosene partial pressure low enough so it would vaporize completely in the reactor. The conditions of the experiment were such that 60 percent of the feed was converted to lighter products.

The liquid product was distilled to 471 K (194°C) to match the initial boiling point of the United States Air Force (USAF) high density JP-8 grade jet fuel. The kerosene feed had a final boiling point of 603 K (330°C) which surpassed the final boiling point of JP-8 grade jet fuel by 30 K. It was assumed that the final boiling point of the kerosene did not change during dewaxing.

The undistilled kerosene was filtered with activated charcoal to remove a light lemon color that developed during distillation. The specific gravity of the liquid was 0.83 at ambient temperature and represented a specific gravity increase of 0.04 above that of the unreacted kerosene and almost 0.01 above the density of the kerosene cracked at less severe conditions.

A sample of diesel was hydrocracked under the same conditions hydrocracking conditions. It was distilled up to 475 K (212°C). The specific gravity of the diesel boiling product was 0.855 and represented a specific gravity increase of 0.045 over the unreacted kerosene and a specific gravity increase of 0.025 over the diesel cracked under less severe conditions.

These two experiments show that the density of a jet fuel can be increased at the expense of the total yield of the product.

There is no doubt that mild hydrodewaxing can increase the yield of jet fuel from the original feed at the expense of the density and still meet the freeze point specifications.

Conclusions

It is possible to reduce the freeze point of jet fuel boiling distillates by shape selective cracking of paraffins in the presence of naphthenes on HZSM-5 catalyst. The freeze point reduction is due to the reactant selectivity of HZSM-5 which allows paraffins and isoparaffins to diffuse to active cracking sites while it restricts the diffusion of bulkier naphthenes into the pore structure. The standard reaction conditions were 643 K (370°C) and 200 psia total hydrogen plus hydrocarbon pressure. The feed rate of hydrogen was such that the hydrocarbon feed to the reactor was in the vapor phase.

The catalytic reactor was operated to crack kerosene and diesel boiling range cuts in the presence of HZSM-5 cracking catalyst. Due to the restricted size of the pores of HZSM-5 catalyst, paraffins were selectively cracked in the presence of bulkier naphthenes. After the distillation of the naphtha formed from the cracking of the paraffins, the resulting distillate had a greatly reduced freeze point. Densities were also increased by several percent due to the selective removal of the less dense paraffins and isoparaffins from the feedstocks.

Under more severe hydrocracking conditions it was possible to produce a kerosene boiling range distillate with very low freeze point and a density of 0.83, which was well within the density requirements (0.775-0.84)[3] for the military high density JP-8 fuel. The high density of the fuel was a result of two factors:

1. the high naphthene content of the dewaxed kerosene; and
2. the expanded boiling range of the kerosene (a 30 K higher endpoint than JP-8 grade jet fuel).

Under the same conditions a diesel boiling distillate (485-673 K [212-400°C]) with a very low freeze point and a density of 0.855 could be obtained which surpassed the density range for JP-8 grade jet fuel.

High density jet fuels can be produced by dewaxing expanded boiling range kerosene. The density obtained is a function of the endpoint of the fuel. The dewaxed diesel had a higher endpoint than the dewaxed kerosene and as a consequence, a higher density.

Normally the freeze point sets the low temperature limits of potential jet fuels. If jet fuels can be economically dewaxed to remove paraffins the freeze point of jet fuels will be less of a factor for determining what kinds of feedstocks can be used for jet fuels. The low temperature viscosity will become a more important factor in determining what distillate cuts will be suitable for the production of jet fuels.

Cracking of kerosene and normal hexadecane over HZSM-5 occurs by β-scission. At 573 K (300°C) the activity of the catalyst is low enough so that C_5 is the most abundant product. At 643 K (370°C) C_4 is the main product. It is anticipated that at temperatures over 673-723 K (400-450°C) that C_3 would be the main product. Higher temperatures result in smaller fragments from β-scission cracking.

Secondary cracking and aromatization reactions appear to be occurring parallel to primary cracking reactions. This is because the rate determining step for primary cracking, secondary cracking and aromatization reactions is the same, the abstraction of an hydride from a paraffin to form a carbonium ion which can crack and recrack, or crack and abstract an hydride from a naphthene or another feed molecule. At conversions higher than maybe a few percent the product yield is not a function of conversion and residence time, it is a function of other variables like the temperature, the Si/Al ratio and the method of catalyst pretreatment.

Section VII: DESIGN AND CONSTRUCTION OF A BET SURFACE AREA APPARATUS

Research Personnel: Daniel C. Longstaff
Graduate Student

Kien-Ru Chen
Postdoctoral Fellow

Francis V. Hanson
Associate Professor

Introduction

Catalytic activity is related to the number of active sites that are distributed over the surface of the catalyst. It is generally assumed that the number of catalytic sites per unit mass of catalyst will increase as the surface area of the catalyst increases. During catalyst pretreatment or use changes in the catalyst may occur that could result in an increase or decrease in the total catalyst surface area. If the pretreatment of a porous oxide catalyst includes a calcination procedure caution must be exhibited to insure that the calcination temperature does not induce collapse of the pore structure of the catalyst. When the calcination temperature is too high the collapse of the pore structure will cause a significant reduction in the surface area of the catalyst with a loss of active sites and a concomitant loss of activity. Sintering of the metal crystallites in supported metal catalysts during calcination or reduction will also be accompanied by a significant loss in catalytic activity.

The surface area of porous catalysts can also be affected by chemical processes which take place during the course of the reaction such as the deposition of carbonaceous residues. For example, in zeolite cracking catalysts such as ZSM-5 there are two types of catalyst deactivation due to coke deposition. Coke or organic residue may deposit either (1) directly on the catalytically active site, or (2) at the pore mouths of the catalyst (pore mouth plugging).

If the zeolite catalyst deactivation occurs via mechanism 1, large losses in catalyst activity would be accompanied by small losses in catalyst surface area. In the case of mechanism 2, large losses in catalyst activity are accompanied by large losses in accessible catalyst surface area. Thus a knowledge of the surface area of fresh, equilibrated, and deactivated catalysts is necessary for the complete evaluation of catalyst performance.

In addition to surface area changes the adsorption and desorption of an adsorptive such as nitrogen can provide important information regarding the pore structure of a catalyst.

The most widely applied technique for the determination of the surface areas and pore sizes for porous materials is the BET method.[259] Thus, a BET surface area measurement system was designed and fabricated for use in the determination of surface areas of laboratory prepared samples of the ZSM-family of zeolites.

Procedure for Surface Area Measurement

Surface areas of porous adsorbents and catalysts are calculated by determining the amount of an adsorptive that forms a monolayer on the surface of the adsorbent. The amount of an adsorptive that is required to form a monolayer on a catalyst can be determined by either of two methods:[260]

1. the volumetric method, and
2. the gravimetric method.

The volumetric method consists of determining the pressure of a quantity of the adsorptive in the presence of the solid. The amount adsorbed is calculated by taking a mass balance over the system. An adsorption isotherm is determined by measuring the amount adsorbed for a series of different pressures at a specified temperature.

In the gravimetric method the amount of gas adsorbed on the solid is directly measured by weighing the sample on a microbalance. The weight of the clean catalyst is determined in a vacuum. The weight of the catalyst is then determined after it has come to equilibrium with the adsorptive at a known pressure and temperature. The volumetric method was used in this investigation and a volumetric adsorption apparatus was designed and constructed.

Monolayer coverage cannot be directly determined for physisorption because multiple layers of adsorptive molecules are formed on the catalyst surface. However, the BET equation[259] may be used to calculate the volume of a gas adsorbed at the temperature and pressure required to form a monolayer on a catalyst surface. The BET equation is based on the concept that the second and higher monolayers of physisorbed adsorptive are a liquid phase, while the first monolayer exists as a physisorbed phase on the bare surface. The BET equation, which is derived in Appendix A, provides a relationship between the volume of gas adsorbed on a surface and the pressure at which it is adsorbed. The monolayer volume, v_m, appears in the equation and can be calculated if the volumes adsorbed at different pressures and a single temperature are known.

Experimental Apparatus

The BET system constructed for this investigation consisted of four parts:

1. an adsorption system for the determination of adsorption and desorption isotherms;
2. a vacuum system to properly evacuate all parts of the system prior to the determination of the isotherms;
3. a gas supply system to properly store and handle gases used in the system without contamination; and
4. a catalyst pretreatment system to prepare the catalyst samples.

A schematic of the BET system is presented in Figure 76. All the major components are labelled. The BET system was constructed so that dynamic pressures of 10^{-6} torr could be attained. Consequently, the BET system was constructed with Pyrex glass tubing and high vacuum Pyrex glass joints lubricated with high vacuum grease. The system's small volume in relation to the capacity of the diffusion and mechanical vacuum pumps minimized the system evacuation time.

Adsorption System

The adsorption and gas handling system is the dashed rectangle labelled I in Figure 77. A more detailed diagram of the adsorption system and the gas supply system is shown in Figure 78. The adsorption system consists of:

1. a calibrated doser manifold of known volume, V_D, to introduce the adsorptive into the sample cells;
2. two sample cells to hold the catalyst sample cells during the determination of adsorption/desorption isotherms;
3. a pressure gauge to determine pressure in the doser volume and in the sample cell during adsorption experiments; and
4. a calibration bulb of known volume to determine the dead volume and to supplement the dosing volume when needed.

The pressure gauge was an MKS Baratron Type 222B Absolute Pressure Gauge. It consisted of a capacitor positioned between the system and a volume evacuated to 10^{-7} torr. The capacitor was connected to an electronic signal conditioner which converts electronic frequencies to voltage outputs, and sends a signal to an MKS Brand 200/400 Series PDR-D-1 Power Supply and Digital Readout. The Baratron gauge operates as a result of the deflection of a metal diaphragm which serves as one side of the capacitor. When the pressure causes the diaphragm to

1. Storage bottle
2. Supply manifold
3. Capillary manifold
4. Calibration bulb of known volume
5. Sample cells
6. Baritron pressure gauge
7. Main manifold
8. Sample pretreatment connection
9. Penning high vacuum gauge
10 Diffusion pump cold trap
11. Diffusion pump
12. Diffusion pump bypass
13. Mechanical pump cold trap
14. Mechanical pump

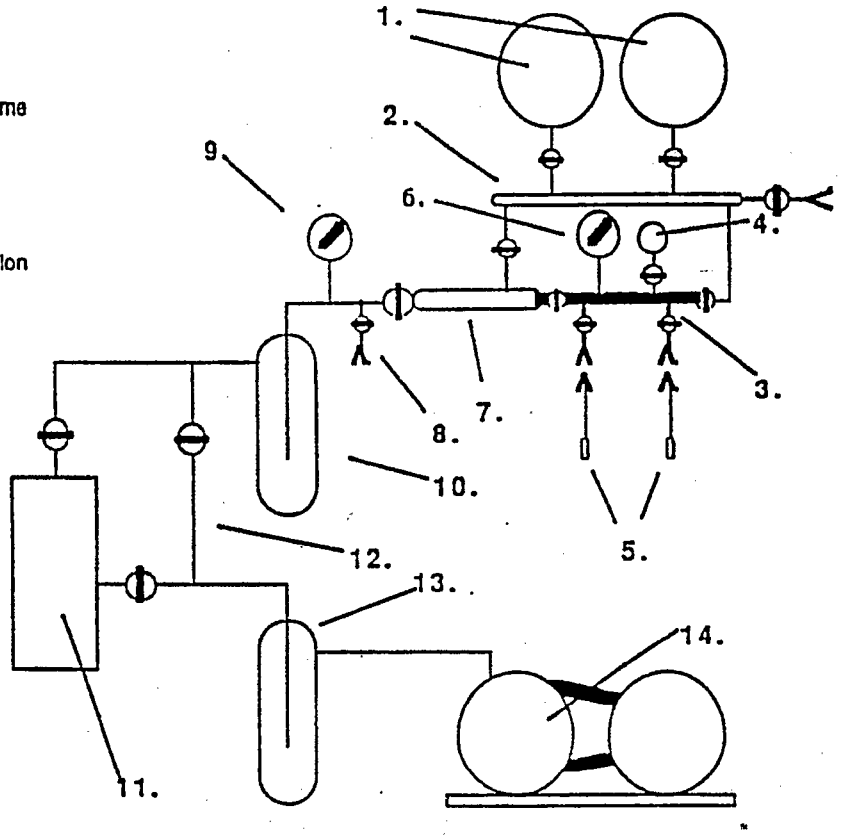

Figure 76. Schematic of the BET System

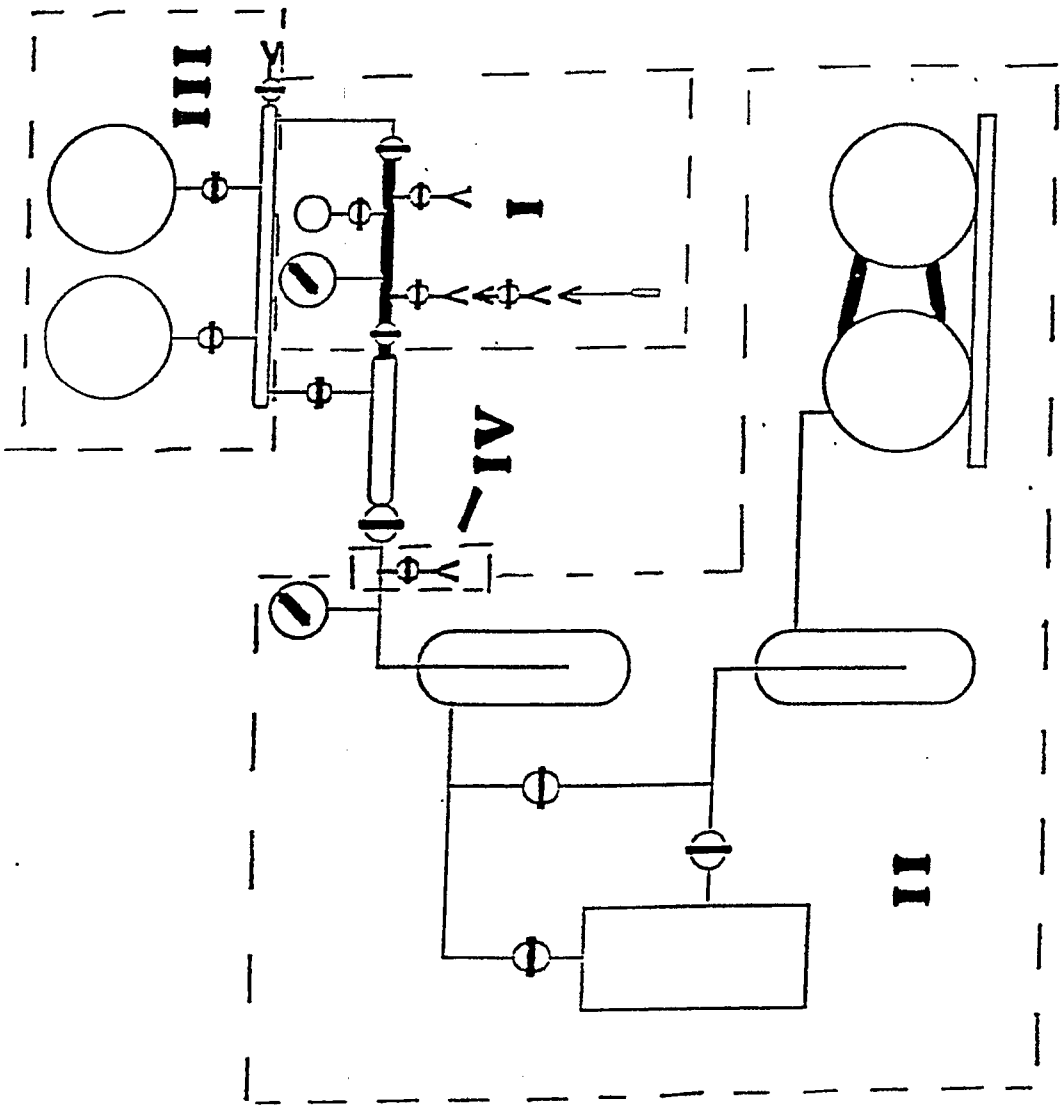

Figure 77. Components of the BET System

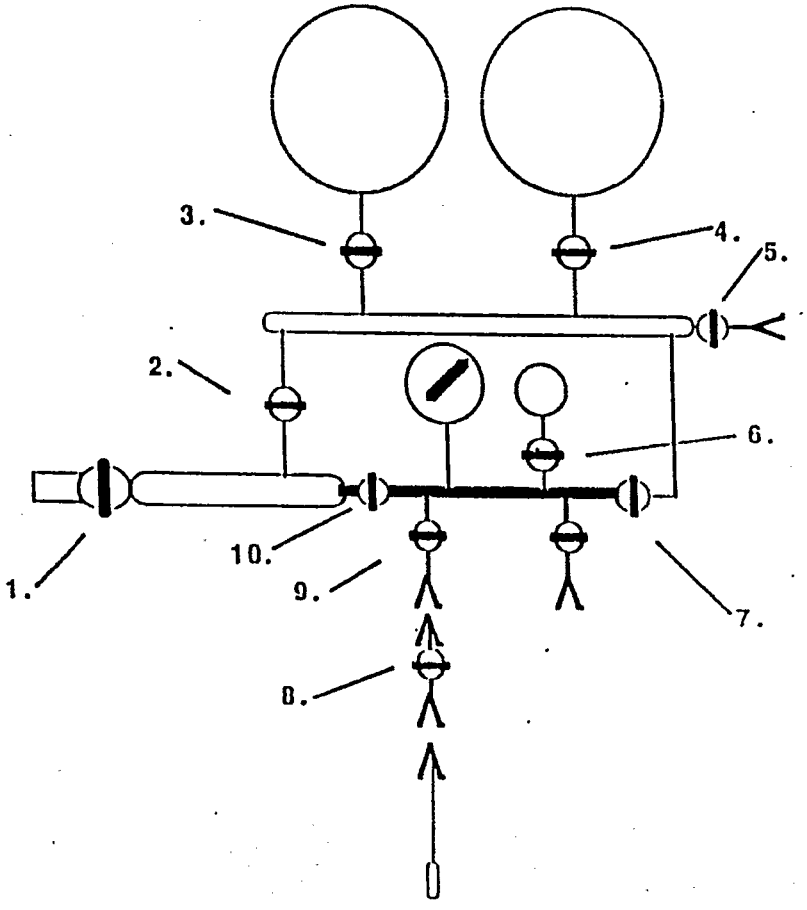

Figure 78. Adsorption and Gas Handling System

deflect, the capacitance of the capacitor changes. This change in the capacitance is measured electronically, recorded, and displayed. The Baratron pressure gauge was connected to the capillary manifold by a 1/2 inch Cajon Ultratorr union. The doser system had a suitable connection which allowed the Baratron gauge to be mounted in a vertical position to prevent contamination of the diaphragm.

The doser system was constructed from two mm inside diameter Pyrex tubing to minimize its volume. The volume of the doser system was determined by calibration with a calibration bulb of known volume. The volume of the calibration bulb was determined prior to the construction of the gas adsorption system. A glass bulb was blown and connected to a two mm stopcock which allowed the bulb to be sealed. The bulb was evacuated with a vacuum pump, then weighed on a laboratory balance capable of reading to 10^{-5} g. The bulb was filled with degassed distilled water. The bulb and the water were allowed to come to thermal equilibrium in a calorimeter. The temperature of the water was determined and the stopcock was shut. The exterior of the bulb was dried and the bulb and water were weighed. The volume of the bulb was calculated from the density and weight of the water. This procedure was repeated nine times and the volume of the bulb was determined to be 51.26 cm^3 ± 0.011 cm^3.

In order to connect the sample cells to the doser volume, the doser volume was outfitted with two connections which consisted of a two mm stopcock and a 10/30 female connection.

The cells consisted of two parts, the actual cell itself which consisted of an oblong bulb. The oblong bulb contained a thermowell for temperature measurement. This bulb was connected to a 12/30 ground glass male joint by a 10 inch long neck. This allowed the cell to be fairly well submerged in a liquid nitrogen bath. The other portion consisted of a two mm stopcock with a 12/30 ground glass female joint to which the cell was connected, and a 10/30 ground glass male

joint which allowed the stopcock and cell to be connected to the doser manifold. This arrangement permitted the transfer of the catalyst sample from the sample pretreatment connector to the doser volume connector without exposing the catalyst sample to the atmosphere.

Vacuum System

The vacuum system is indicated by the dashed box labelled II in Figure 77. The vacuum system permitted the evacuation of the adsorption cell pressure to less than 10^{-4} torr without the back migration of oil vapors into the system. It consisted of a CVC PMCS-4B diffusion pump backed by a GCA Precision Scientific D25 mechanical vacuum pump. Dow-Corning 704 diffusion pump fluid was used in the diffusion pump.

The adsorption system was isolated from the vacuum pumps by liquid nitrogen cold traps to prevent back streaming of the pump oils. These cold traps were kept filled with liquid nitrogen in normal operation. One cold trap was placed between the dosing and gas storage manifolds and the vacuum system, and the other was between the mechanical pump and the diffusion pump. The pumps could be isolated from one another and from the system by three 25 mm glass stopcocks.

The system vacuum was monitored with a CVC brand GPH-320C Penning Vacuum Gauge mounted between the vacuum system and the supply manifold. The gauge was capable of measuring pressures in the range 10^{-7} to 0.25 torr.

Gas Storage System

The gas storage system is indicated by the dashed box labelled III in Figure 77. Nitrogen was most frequently used as an adsorptive in determining isotherms. $Neon^{261}$ was used for determining cell dead volumes because at ambient temperature it does not physisorb on catalysts or adsorbents and it does not diffuse through glass like helium. The gas storage system consisted

of a gas supply manifold connected to two 5000 cm^3 glass bulbs by high vacuum stopcocks. One bulb was used to store nitrogen. The other was used to store neon. Gas was added to the supply manifold and storage bulbs through a four mm stopcock connected to a 12/30 female joint. The supply manifold was constructed of 25 mm i.d. Pyrex tubing. The supply manifold was connected to the vacuum manifold and to the doser volume by means of a four mm stopcocks.

Catalyst Pretreatment System

The catalyst pretreatment system is indicated by the dashed box labelled IV in Figure 77. It was connected to the cell by Pyrex tubing which was placed below the diffusion pump bypass on the BET system. The cell was heated with a 1200 watt Autoclave Engineer's brand furnace controlled by a Variac.

Adsorption/Desorption Isotherm Procedure

Determination of Sample Cell Dead Volume

In the volumetric method for determining BET isotherms and hysteresis curves, it is necessary to know the total cell dead volume and the cell volume at the isotherm temperature. This made it necessary to determine the total cell dead volume, V_C, and the cryogenic cell volume, V_{CC}, prior to putting the catalyst into the cell. Before initiating the BET isotherm the cell volume is again measured with the catalyst in the cell. The reduction in the total volume is assumed to be totally due to the volume of catalyst in the cell and is subtracted from the cryogenic cell volume that was originally measured when the cell was empty.

The procedure for determining the cell volumes consisted of the following steps. An acid washed glass wool plug was placed in the top of the cell and the cell and stopcock assembly were connected to the doser volume. The cell system was evacuated to less than 10^{-4} torr. Stopcock

(8) (Figure 78) was shut to separate the doser volume from the cell. Neon was admitted to the doser volume and the pressure indicated on the Baratron gauge was recorded. Stopcock (8) was then opened and the neon allowed to enter the cell. This procedure was repeated several times to insure reproducibility. The cell volume was then calculated from Equation (7-1), which assumes that the temperature of the doser manifold and the empty cell are equal.

$$V_C = V_D \left(\frac{P_1 - P_2}{P_2 - P_o}\right) \tag{7-1}$$

where

P_o is the original pressure in the cell, torr;

P_1 is the original pressure in the doser volume, torr;

P_2 is the pressure in the cell and doser volume after the stopcock is opened, torr;

V_D is the doser manifold volume, torr; and

V_C is the total dead cell volume, cm^3.

After the cell dead volume had been determined, the cell was immersed in liquid nitrogen up to a specific level. The above procedure was repeated to determine the cryogenic cell volume. The cryogenic cell volume was calculated from Equation (7-2):

$$V'_{CC} = (V_C+V_D) \frac{T_C}{(T_H-T_C)} \frac{(P_2 - P_o)}{(P_1 - P_2)} \tag{7-2}$$

where:

V'_{CC} is the cell volume at the cryogenic temperature, cm^3;

T_C is the temperature of the liquid nitrogen bath, K; and

T_H is the ambient temperature, K.

The cell volume at ambient temperature is calculated from Equation (7-3).

$$V_{CH} = V_C - V'_{CC} \tag{7-3}$$

where:

VCH is the cell volume at ambient temperature, cm^3.

Once the total cell volume and the cell volume at cryogenic temperature were determined, the cell and stopcock were removed from the doser volume. The glass wool plug was removed from the cell and saved. A weighed amount of catalyst was placed into the cell and the glass wool plug was reinserted into the cell.

The sample was then ready for degassing. The purpose of degassing is to remove any adsorbed species from the catalyst surface. Water is usually the main adsorptive that needs to be removed. The temperature and total time of degassing were a function of the catalyst. For ZSM-5, holding the sample of ZSM-5 at 623 K (350°C) for several hours under the diffusion pump vacuum was more than sufficient. ZSM-5 is a hydrophobic material and almost all the water is desorbed below 523 K (250°C).[262] A 10/30 female connector and stopcock were available on the BET vacuum system for degassing samples. The position of the degassing connector allowed samples to be degassed while the adsorption isotherms were being determined for other samples. Once the degassing was completed, the stopcock on the cell was shut to maintain the sample under vacuum. The stopcock and cell were transferred to the doser volume manifold to obtain the isotherm.

Prior to the determination of the adsorption isotherm, it was always necessary to redetermine the total cell dead volume with the sample in the cell. This was done with the dosing volume and the cell at ambient temperature. The procedure described above was used to

determine the dead volume of the catalyst-cell system. The difference in the cell volume before and after putting the sample in was assumed to be the volume of the sample, and this volume was subtracted from V'_{CC}, the volume of the empty cell at the isotherm temperature. This volume was denoted V_{CC} and represented the dead volume of the cell at the cryogenic temperature of liquid nitrogen. V_{CH}, the dead volume of the cell at ambient temperature, did not change even though the cell contained a sample, because the sample was positioned in the portion of the cell that was submerged in liquid nitrogen during the determination of the adsorption isotherm. The difference between the total cell volume and the volume at liquid nitrogen temperatures was denoted V_{CH} and appears in the mass balance.

An alternate and more efficient method requires helium to be used as the gas to determine the cell dead volume. The first step is to load the catalyst into the cell before determining the cell's dead volume, and then degas the sample. After degassing, the cell is connected to one of the sample ports on the dosing manifold, the system is evacuated, and the sample cell is submerged in liquid nitrogen to the level at which it is submerged during the determination of the BET surface area. The procedure is then followed for determining the cell's dead volume at ambient temperature, but helium is used instead of neon because it is expected that helium will not physisorb on the adsorbent. The volume is then calculated from Equation (5-23), and a revised form of the mass balance is used when the adsorption/desorption isotherm is calculated. The volume determined by this method will be several times larger than the actual dead volume because the helium will be concentrated in the portion of the cell held at cryogenic temperatures. This method was never used but it is recommended because of its simplicity as compared with the method outlined previously. One attempt was made to do this procedure with neon, but it was unsuccessful because neon will physisorb on zeolite at liquid nitrogen temperatures, even though

the temperature of liquid nitrogen is well above the critical temperature of neon (boiling point of nitrogen @ 650 torr = 76.1 K, critical temperature of neon = 44.4).[263]

Determination of the Isotherm

The actual adsorption isotherm was determined according to the following procedure. The gas supply manifold, the dosing volume and the cell were all evacuated to 10^{-7} torr. The cell was immersed in a liquid nitrogen bath to the same level at which the cryogenic cell volume had been determined. Then stopcocks (1), (2), (6), (7), (9), and (10) were shut to separate each part of the system from every other part. Stopcock (4) on the nitrogen storage bulb was opened to admit nitrogen into the storage manifold. Stopcock (7) between the supply manifold and the dosing volume was opened, and nitrogen was admitted to the dosing volume. The nitrogen initial pressure in the dosing volume was adjusted by withdrawing a small amount of the nitrogen into the calibration bulb until the pressure reached the desired level. The gas in the calibration bulb was then available for further use.

The appropriate initial doser volume pressure is critical in order to have the desired amount of adsorption on the catalyst. During the determination of the adsorption isotherms, the pressure in the doser volume must be greater than the pressure in the sample cell at each step. During the determination of the desorption isotherms, the pressure in the dosing manifold must be less than the pressure in the sample cell. The pressure in the doser volume was recorded as P_1. Stopcock (9) on the cell was opened, and nitrogen flowed into the cell and was adsorbed by the sample. The pressure in the doser volume-sample cell-catalyst system usually required up to 30 min for the pressure to equilibrate. The greater the amount of nitrogen adsorption, the longer it took for the system to come to equilibrium. After equilibrium was established, the pressure (P_2) was recorded. Stopcock (9) on the cell was shut and additional nitrogen was admitted to the doser volume. This

procedure was continued for as many isotherm points as was deemed necessary. If the surface area of ZSM-5 was being determined, data was taken up to a value of p/p_o of 0.15. If a complete adsorption/desorption isotherm was being determined, the procedure was continued until the pressure had reached the saturation pressure of nitrogen vapor at the temperature of the sample followed by reduction of the pressure to a few torr.

When the complete adsorption/desorption isotherm was determined, the adsorption portion of the isotherm was terminated after the pressure in the cell had reached the vapor pressure of nitrogen at the temperature of the catalyst in the cell. This pressure was usually a few torr above the ambient pressure. This was because the ambient pressure regulates the temperature of the boiling liquid nitrogen bath which was always slightly above the boiling temperature of pure nitrogen at the ambient pressure due to the presence of condensed oxygen in the liquid nitrogen bath. At the maximum pressure, care was taken to insure that the pressure in the cell had indeed attained equilibrium. If this caution is not observed, desorption will cause a deviation in the adsorption isotherm at pressures below the hysteresis pressure. Therefore the adsorption isotherm was usually stopped a few torr below the actual vapor pressure of nitrogen.

In determining the isotherm it was important to always maintain the level of liquid nitrogen in the bath around the cell at the same level at which the value of V'_{CC} was measured to reduce the possibility of measurement errors.

Whenever nitrogen was admitted to the doser volume prior to opening the stopcock on the cell it was useful to estimate the appropriate P_1 in the doser volume to give the desired value of P_2 in the cell and doser volume after the pressure had been allowed to equilibrate. A semiquantitative method for estimating P_1 was developed. The quantity β was defined according to Equation (7-3):

$$\beta = \frac{(P_1-P_2)}{(P_2-P_o)} \qquad (7\text{-}4)$$

The ratio of pressures also appears in Equation 3-1 and β is a function of position on the adsorption isotherm, and gradually changes as a function of p/p_o. It gave good predictions of the value of P_1 to give a desired value for P_2. The procedure was to determine β for the point corresponding to P_n on the adsorption isotherm and then use Equation (7-5) to calculate the desired P_1 for the point corresponding to P_{n+1}.

$$P'_1 = P'_2 + \beta(P'_2-P'_o) \qquad (7\text{-}5)$$

where:

P_1' is the predicted pressure of the doser volume, torr;

P_2' is the desired equilibrium pressure, torr; and

P_o' is the pressure in the sample cell, torr.

The pressure, P'_1, in the doser volume required to raise the pressure in the sample cell from P'_o to P'_2 after stopcock (9) was opened was calculated from Equation (7-5). This method can calculate values for P_1 such that there is a very even spacing between consecutive points on the adsorption/desorption isotherm.

Calculation of the Adsorption/Desorption Isotherm

After sufficient data points had been taken, the mass balance was used to calculate the amount of nitrogen gas adsorbed on the catalyst for each set of data points. The mass balance equation used to calculate the volume adsorbed can be derived from the gas law and is given by:

$$V_{ads} = V_{ads,o} + \frac{T_{STP}}{P_{STP}}\frac{V_D}{T_H}(P_1-P_2) - \frac{T_{STP}}{P_{STP}}\frac{V_{CH}}{T_H}(P_2-P_o) + \frac{V_{CC}}{T_C}(P_2-P_o) \qquad (7\text{-}6)$$

where:

V_{ads} is the volume of gas at STP adsorbed, cm^3;

$V_{ads,o}$ is the volume of gas at STP adsorbed at the previous data point, cm^3;

P_{STP} is the standard pressure, 760 torr; and

T_{STP} is the standard temperature, 273.15 K.

After the amount of gas adsorbed on the sample for each P_{n+1} was calculated the linear form of the BET equation[259] was used to calculate $V_{ads,m}$, the monolayer volume of the adsorptive at the standard temperature and pressure that is required. The linear form of the BET equation is given in Equation (7-7). Equation (7-7) is also referred to as the BET (A) equation.

$$\frac{p}{V_{ads}(p_o-p)} = \frac{1}{V_m c} + \frac{(c-1)}{V_m c}\left(\frac{p}{p_o}\right) \qquad (7\text{-}7)$$

where:

V_m is the monolayer volume, cm^3;

V_{ads} is the volumes (STP) which adsorbed at a pressure p, cm^3;

p is the equilibrium pressure, torr;

p_o is the vapor pressure of adsorptive at the sample temperature, torr; and

c is the 'c-value'.

If p/p_o is plotted versus $p/V_{ads}(p_o-p)$ a straight line of slope $(c-1)/V_m c$ and intercept of $1/V_m c$ should be obtained. The slope and intercept can be solved to give V_m and c. V_m would then be used in Equation (7-8) to calculate S, the surface area of the catalyst or adsorbent per unit mass.

$$S = \frac{V_m}{22,400} \frac{N_{av}}{m} A \qquad (7\text{-}8)$$

where:

S is the surface area of sample g/cm^3;

V_m is the monolayer volume, cm^3;

m is the mass of sample in cell, g;

N_{av} is Avogadro's Number; and

A is the area covered by a single molecule of adsorptive, m^2.

The area covered by a single molecule of adsorbed nitrogen is 16.2×10^{-20} $m.^2$.

The variable c is related to the heat of adsorption of the adsorptive on the sample by Equation (7-9).

$$c = A_o \exp\left(\frac{(E_1 - E_L)}{RT}\right) \qquad (7\text{-}9)$$

where:

E_1 is the heat of adsorption of the first monolayer, cal/mol;

E_L is the heat of adsorption of further layers, assumed to be equal to the latent heat of condensation, cal/mol;

R is the Universal gas constant, cal/mol/K;

T is the absolute temperature of sample, K; and

A_o is the pre-exponential factor.

The relationship between A_o and the pore size is discussed in a subsequent section.

Scope of the BET System

In addition to being used to determine surface areas of catalysts and adsorbents the BET system can be used to investigate the deactivation of catalysts. For example, if ZSM-5 is heated

to 973 K (700°C) followed by contact with water vapor at 923 K (650°C) there is a 75 percent reduction in the number of strong acid sites; however, the reduction in surface area was only 10 percent. Thus the combinations of heat and water vapor did not appear to collapse the significantly collapse the crystalline structure, however it did selectively destroy the strong acid sites.

The shape selectivity of ZSM-type zeolites becomes less effective as the crystallite size is reduced because of a corresponding increase in the external crystallite surface area and active sites on the external surface of the crystallite. These external sites are not shape selective relative to the sites located inside the zeolite micropores. Two techniques have been developed to determine the external surface area of ZSM-5 crystallites[264] by adsorption techniques. The first method consists of adsorbing propane or butane vapor in the pores of the sample and then cooling the sample cell in liquid nitrogen. An adsorption isotherm is determined and since the pores are filled with frozen propane or butane the only adsorption is on the external surface of the crystallite. The second method is more involved because it involves the rate of the adsorption of neopentane on ZSM-5. Because of the large size of neopentane molecules with respect to the pores of ZSM-5, neopentane adsorbs more slowly onto the interior surface of ZSM-5 crystallites than onto the external crystallite surface area. The amount of adsorptive adsorbed on the external crystallite surface can be determined from a plot of the amount of adsorptive adsorbed with respect to time raised to the 0.5 power.

Results

Computer Program

A computer program was developed to process the data produced from the BET system. It appears in Appendix G along with a sample input and output.

Adsorption/Desorption Isotherm for Alumina

After the BET system was completed a series of surface area measurements were made using alumina as the adsorbent to determine the reproducibility of the system and to develop a proper technique for the efficient and accurate determination of isotherms. These results are included to provide a contrast between the physisorption properties of a macroporous solid like alumina with the physisorption properties of a microporous solid such as ZSM-5 zeolite.

A sample of Ketjen alumina was provided by Dr. Nabin K. Nag. The Ketjen company reported a surface area of 210 m^2/g and a pore volume of 0.6 cm^3/g for the sample. The alumina was calcined and then put in the adsorption cell. The alumina was degassed at 573 K (200°C) at 0.5 Torr followed by evacuation at 623 K (350°C) until the pressure in the adsorption cell was less than 10^{-3} torr. The sample cell was then cooled to the ambient temperature and transferred to the doser volume (without exposing the alumina to the atmosphere or moisture). The doser manifold and the volume of the sample cell were determined using the calibration bulb attached to the doser manifold. The sample cell volume was determined by expanding the neon from the doser volume into the sample cell. The average volumes and the standard deviation of the volume were then determined from the pressure-temperature data.

Several BET adsorption isotherms were determined. The first two runs did not give satisfactory results, due to lack of operating experience which resulted in unevenly spaced data and due to inappropriate operating procedures. The third run was an attempt at generating an adsorption/desorption isotherm which failed due to an operating mistake. However, enough good data was obtained during run number three to obtain a BET surface area for the alumina sample. Run number four consisted of a complete adsorption/desorption isotherm. The BET surface area of the alumina obtained during run number four will be compared with the BET surface area obtained during run number three to show the reproducibility of the data. Figure 79 is a plot of

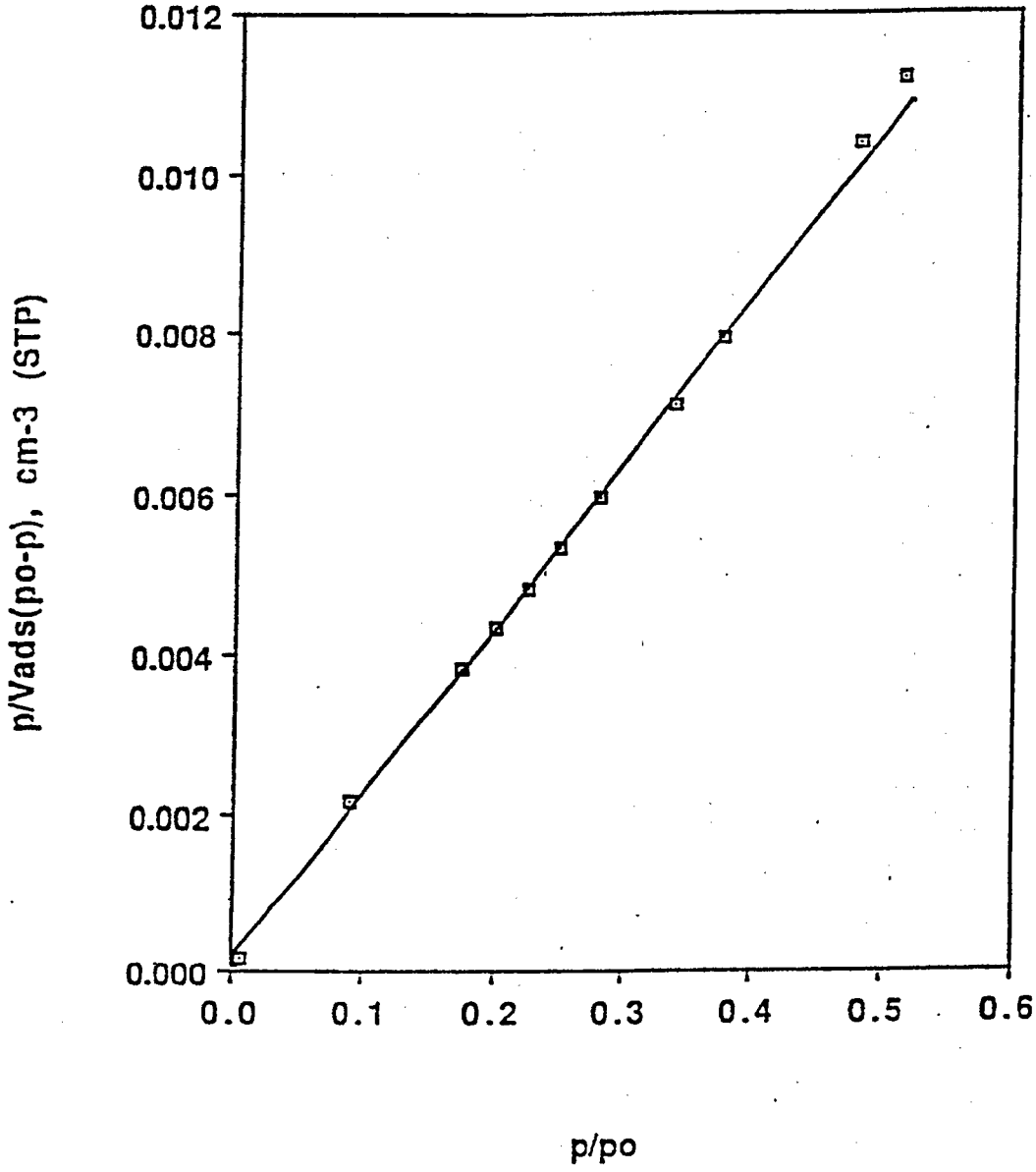

Figure 79. Plot of the BET (A) Equation for Alumina

p/po versus $p/V_{ads}(p_o-p)$. The plot is a straight line up to about $p/p_o = 0.35$ which is where the BET (A) equation starts to break down. The reduction in the amount of accuracy of adsorption at increased p/p_o is related to the filling of the smallest pores of the sample. In the derivation of the BET (A) equation it was assumed that adsorption of the sample took place on a flat surface such that an unlimited number of adsorbed layers could be formed. At low surface coverages this assumption is reasonable for most porous solids. However, as the pores fill up the adsorbed layers interfere with the adsorption of subsequent layers on opposite sides if the pores. The BET (B) equation relieves this assumption by introducing a quantity n, which is the number of monolayers that can be formed in the pores of an adsorbent. The use of the BET (B) equation on adsorbents of varying pore diameter has been reported to give a close fit of the adsorption isotherm up to a relative pressure of 0.6 to 0.7 for adsorbents with a range of pore sizes[259] and as high as a relative pressure of 0.93 for adsorbents of uniform pore size have given straight line fits up to p/po = 0.93.[259]

The adsorption/desorption isotherm for the Ketjen alumina sample is presented in Figure 80. The hysteresis loop obtained with the alumina is known as a type A hysteresis.[265] Type A hysteresis is defined as hysteresis where either the adsorption or desorption branches of the hysteresis loop are steep. The data was processed by the computer program that has been previously mentioned and the BET (A) equation was solved by the computer program to give the monolayer volume from which was obtained a surface area of 209 m^2/g and a value for (E1-EL) of 725 cal./mol. In determining the BET surface area it is important to use data points up to, but not surpassing the region (usually $p/p_o > 0.35$) where the BET (A) equation does not apply. The number of data points taken to determine the surface area was determined by calculating a least squares fit of the processed data points to the BET (A) equation up to several relative pressures

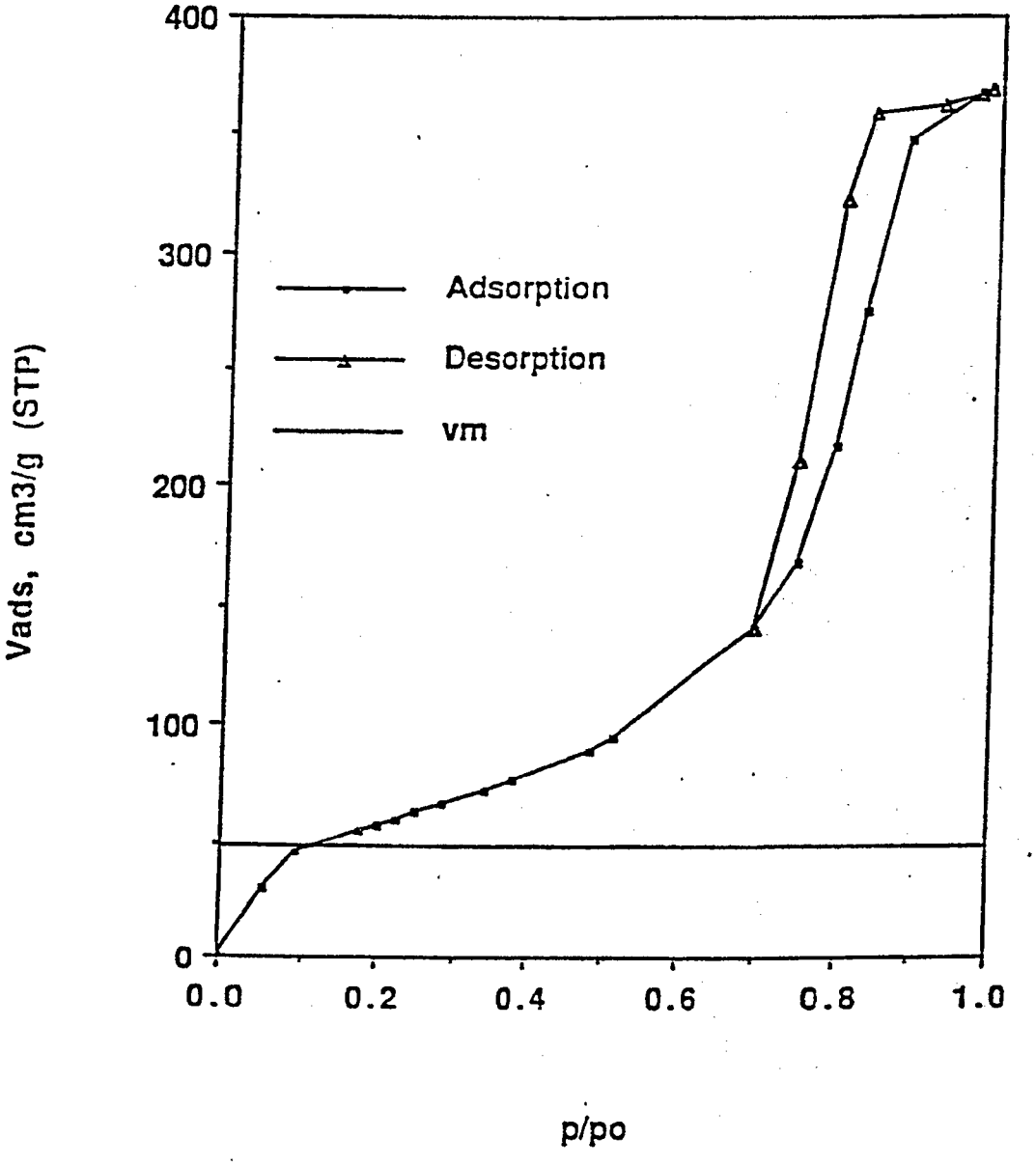

Figure 80. Adsorption/Desorption Isotherm for Alumina

and then taking the set of points that gave the best least squares fit of the data points processed according to the BET (A) equation to a straight line determined by least squares fitting. The BET surface area measured with the BET system during run number three was 209.2 m^2/g. The BET surface area of the same sample of alumina determined in run number four was 209.0 m^2/g. The small difference between these two values is just fortuitous and varied by several m^2/g depending on the number of data points used to determine the surface area.

These results correlated closely (within ~ 3 percent) with the surface area reported by Ketjen (210 m^2/g). The reproducibility of this technique was determined to be 99 percent.

Adsorption/Desorption Isotherm for ZSM-5

The adsorption/desorption isotherms were determined for several samples of ZSM-5. In particular two samples were carefully examined: A sample of commercially prepared ZSM-5 (ZSM-5M) donated by the Mobil Research and Development Corporation and the hydrogen form of ZSM-5 (HZSM-5-6) that was synthesized as part of this research project. Both of these samples were studied in the powder form.

It is believed that the Mobil sample was manufactured according to the Type B synthesis. Scanning electron micrographs of the HZSM-5M and the HZSM-5-6 samples are presented in Figure 81.

The hysteresis curve obtained with ZSM-5M was the first run in which the quantity ß, that was described in the previous section, was used. Its use resulted in very even spacing between consecutive points on the adsorption/desorption isotherm. During the collection of this set of data the calibration volume connected to the doser manifold was used to increase the dosing volume when the adsorption isotherm curve became quite steep as the intercrystalline voids filled with liquid nitrogen.

SEM Photomicrograph of ZSM-5M

SEM Photomicrograph of ZSM-5-6

Figure 81. SEM Photomicrographs of ZSM-5M and ZSM-5-6.

A plot of p/p_o versus $p/(V_{ads}(p_o-p)$ is presented in Figure 82 for the ZSM-5M sample. It is clear that the line starts to curve upward at a relatively low value of p/p_o, that is, 0.12.

The adsorption/desorption isotherm for ZSM-5M is presented in Figure 83 and exhibited a Type B hysteresis. Type B hysteresis is defined as hysteresis where the adsorption branch of the adsorption isotherm occurs at a relative pressure of unity and where the desorption branch occurs at relative moderate pressures.

A plot of p/p_o versus $p/V_{ads}(p_o-p)$ for HZSM-5-6 is presented in Figure 84. The data for ZSM-5M and HZSM-5-6 appear to be similar (Figures 82 and 83).

The adsorption/desorption isotherm for HZSM-5-6 is presented in Figure 85. ZSM-5-6 also displays Type B hysteresis.

The y-intercepts and the slopes of the lines in Figures 82 and 84 were determined and used to compute the monolayer volumes, v_m, and the c-values. The monolayer volumes were used to calculate the surface areas of the respective samples. The surface area of the ZSM-5M was 416 m^2/g and the surface area of ZSM-5-6 was 413 m^2/g. The agreement in the surface areas for the ZSM-5M and ZSM-5-6 indicate that the ZSM-5 preparation techniques employed in this study were capable of producing catalyst specimens similar to those prepared by commercial techniques.

Discussion

C-Values

The quantity (E_1-E_L), is the difference between the heat of adsorption of the first monolayer and the heat of adsorption of the first monolayer and the heat of adsorption of subsequent monolayers, may be calculated from the data. The BET (A) equation assumes that molecules in the second and higher monolayers have the same properties as molecules in the liquid phase, consequently the heat of adsorption of the second and higher monolayers should be

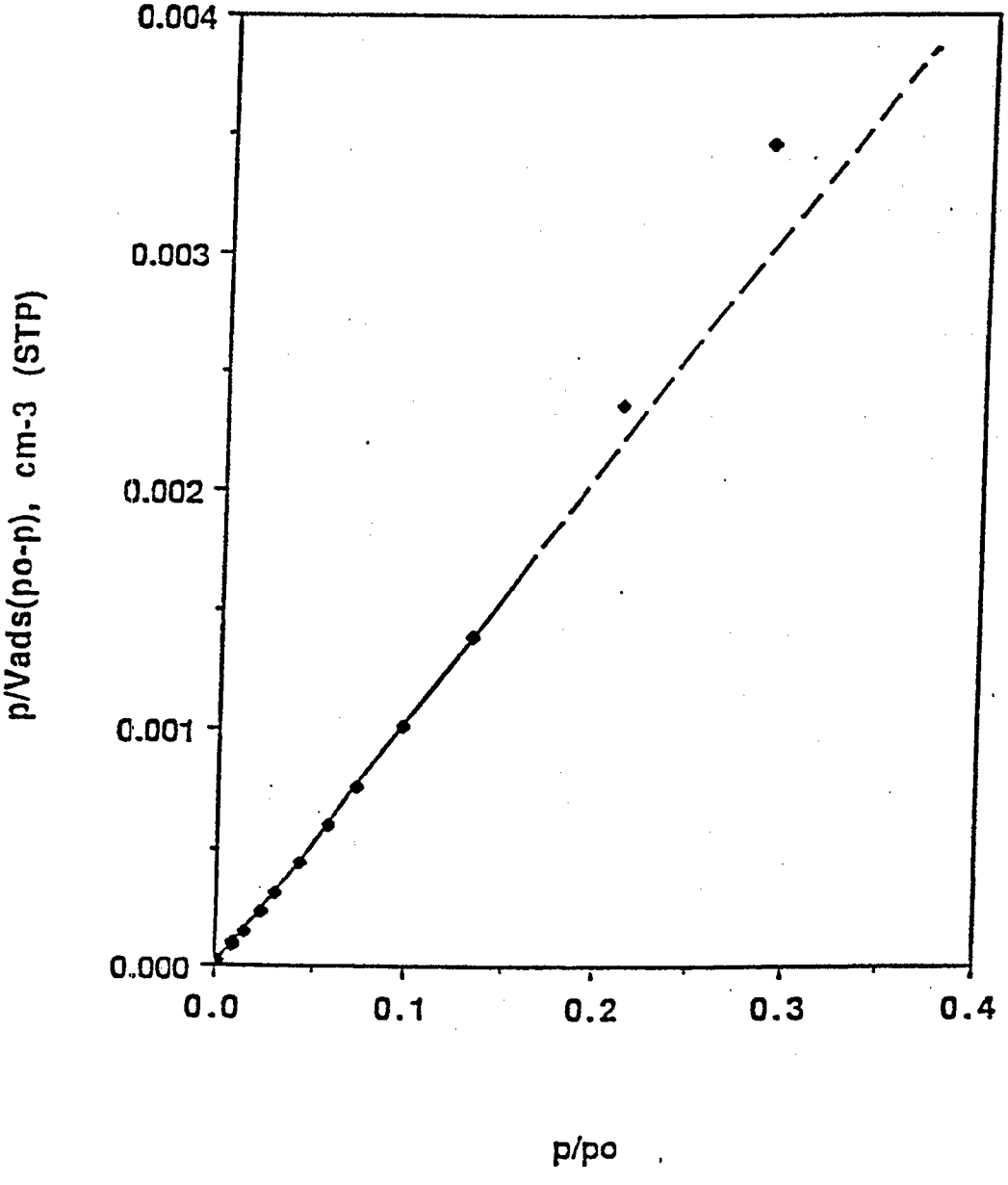

Figure 82. Plot of the BET (A) Equation for ZSM-5M

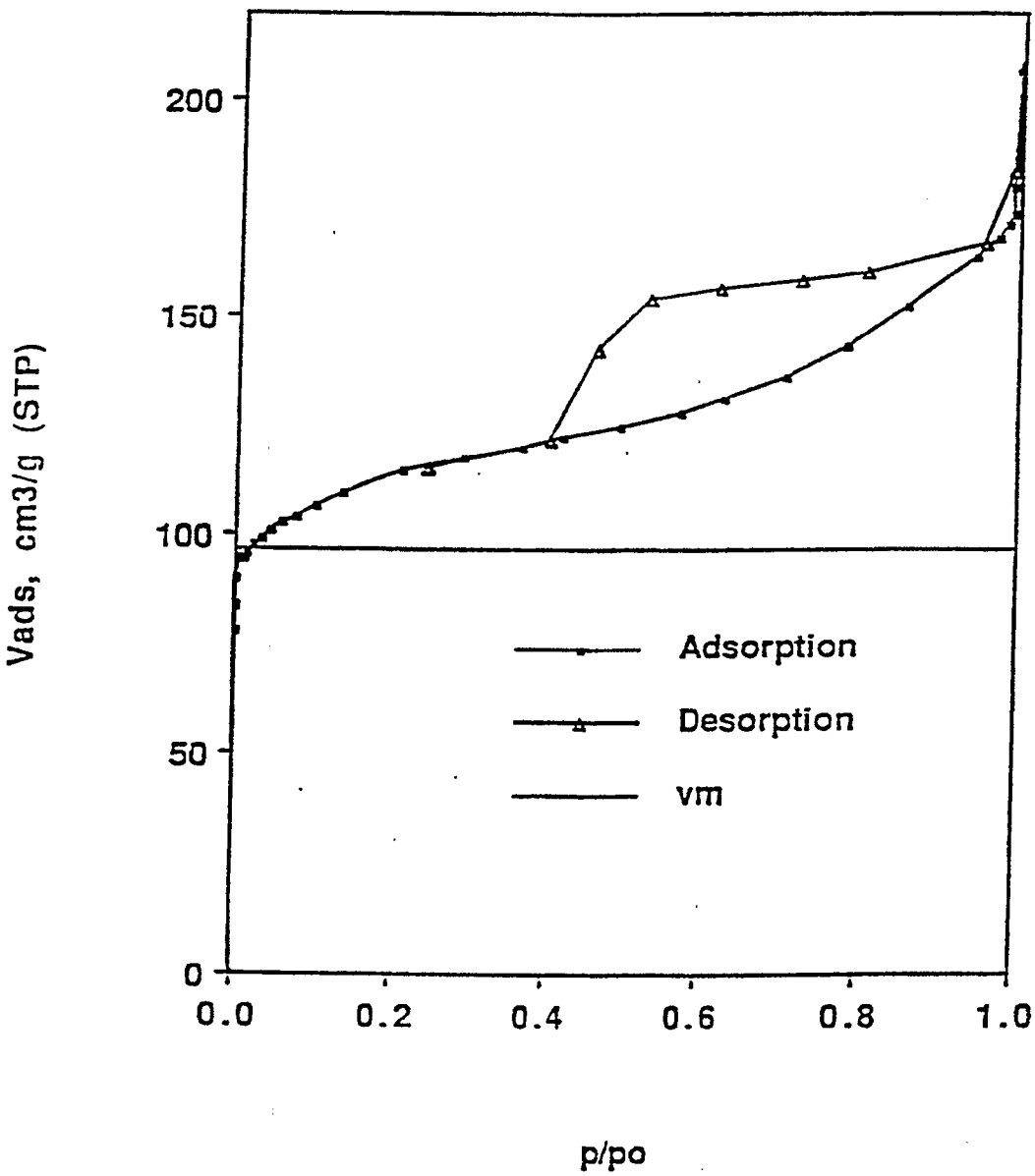

Figure 83. Adsorption/Desorption Isotherm for ZSM-5M

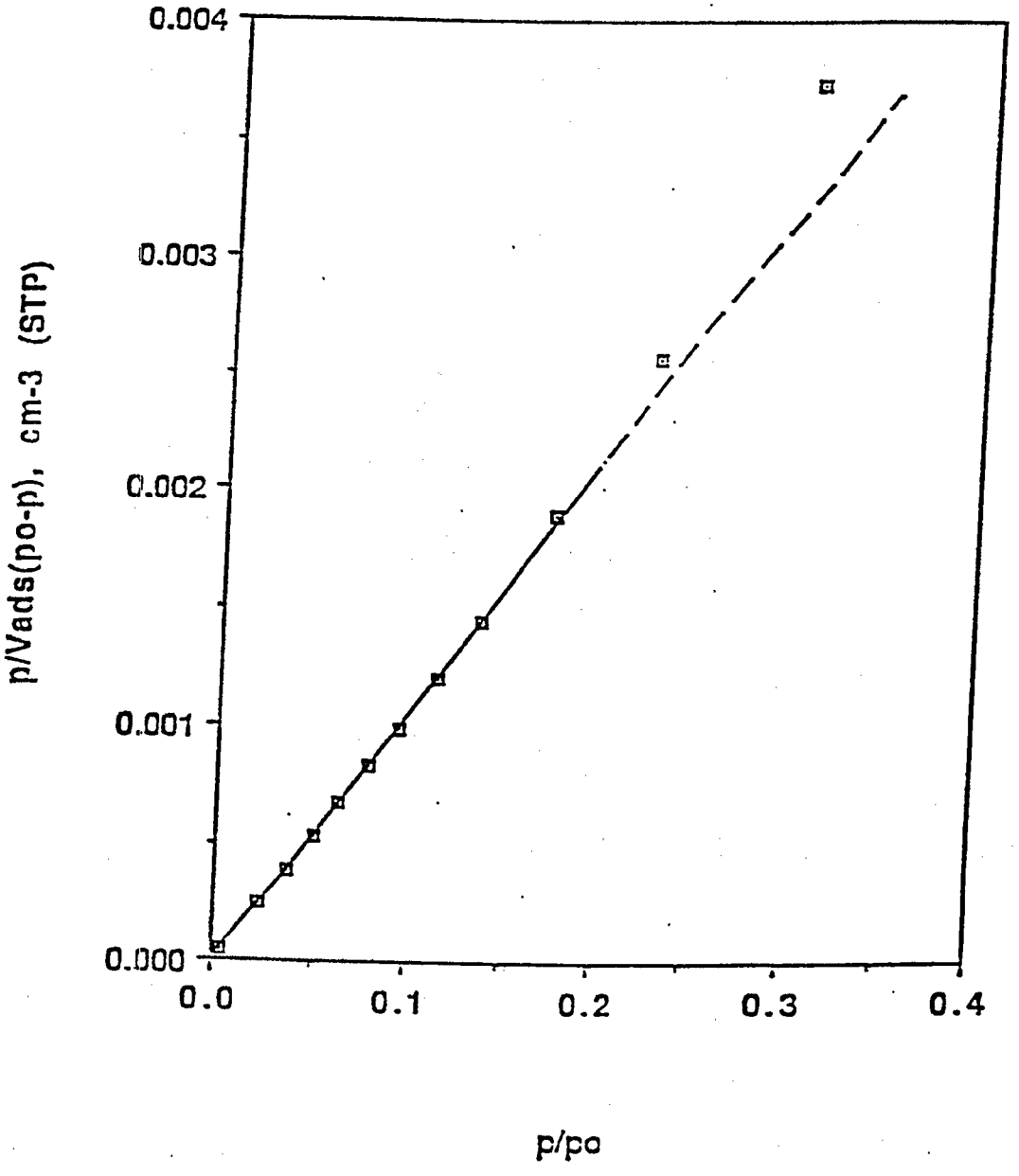

Figure 84. Plot of the BET (A) Equation for ZSM-5-6

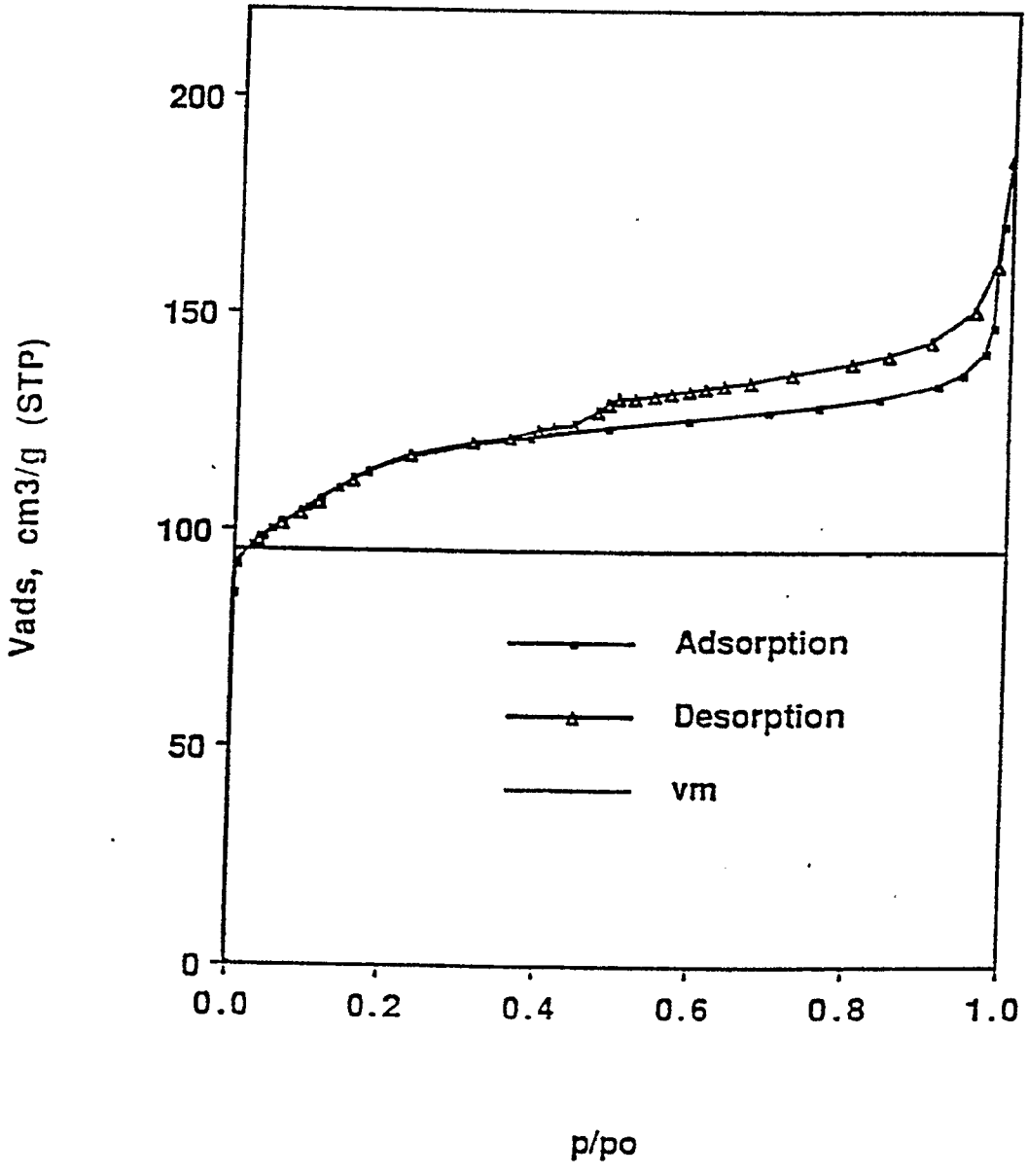

Figure 85. Adsorption/Desorption Isotherm for HZSM-5-6

equivalent to the latent heat of condensation of the adsorptive. Brunauer, Emmett and Teller[259] reported that (E_1-E_L) is fairly constant for the same gas on different adsorbents. They found that for nitrogen (E_1-E_L) is about 840 $\pm$ 50 cal/mol. They also pointed out that the value of the pre-exponential factor should be approximately unity. This is apparent from the nature of the pre-exponential factor, A_o, which is defined in Equation (7-10)

$$A_o = \left(\frac{a_1}{b_1}\right)\left(\frac{b_2}{a_2}\right) \qquad (7\text{-}10)$$

where:

a_1 is the frequency factor for condensation in the first monolayer;

a_2 is the frequency factor for condensation into the second monolayer;

b_1 is the frequency factor for desorption from the first monolayer; and

b_2 is the frequency factor for desorption from the second monolayer.

The similarity in the nature of these two sets of frequency factors indicates that the ratios should be unity.

The values of (E_1-E_L) were calculated for ZSM-5M and ZSM-5-6 based on the assumption that the A_o's were unity. (E_1-E_L) for physisorption on these two samples was 1400-1500 cal/mol. Thus the c-value obtained from the BET (A) equation is about 50 times greater than the c-value reported for nitrogen physisorption on silica gel by Brunauer et al.[259] Generally high c-values are characteristic of microporosity.[266]

The higher c-values may be a result of an increase in the pre-exponential factor rather than some unknown effect which causes a fifty percent increase in the heat of adsorption of the first monolayer. The pre-exponential factor contains the ratios of the adsorption frequency factors and the desorption frequency factors. These frequency factors are a function of the geometry of adsorptive molecules and of the geometry of the surface and the pore. In ZSM-5 the pore spaces

are very restricted and the opportunity for a desorbed nitrogen molecule to pass out of the pore without resorbing on the opposite side of the pore is greatly reduced. The frequency factor for desorption from the first monolayer, b_1, appears in the denominator of the expression for A_o, as a result of the greatly reduced value for b_1, there is a large increase in the term A_o for physisorption in ZSM-5.

Another effect of the small pore size is the deviation of the data from linearity in the plot of the BET (A) equation at low dimensionless pressures, p/p_o. In Figures 82 and 84, which were plots of data obtained for ZSM-5M and ZSM-5-6, respectively, the deviation from linearity starts at about $p/p_o = 0.10$. Usually the BET (A) equation applies past $p/p_o = 0.30$. The deviation at low values of p/p_o is related to the number of adsorbed layers that can form in the pores of the adsorbent. The smaller the pore diameter the fewer the adsorbed layers that can be accommodated in the pore and the lower the value p/p_o at which the deviation from linearity occurs.

Isotherm Modeling

The BET (B) equation relieves the assumption of the BET (A) equation that an infinite number of monolayers can be formed on the surface of the catalyst or adsorbent. It accomplishes this by introducing a quantity, n, which is the number of monolayers that can be formed in a pore. The BET (B) equation is applicable for an adsorbent or catalyst with a uniform pore size distribution. However, if an adsorbent has a range of pore sizes the BET (D) equation, which is a modified form of the BET (B) equation, can describe adsorption on such a material. The BET (B) and BET (D) equations are derived in Appendix F.

The BET (B) and/or the BET (D) equations are used by first determining the monolayer volume, v_m, and the heat of adsorption term, (E_1-E_L), for an adsorbent or catalyst. Then use v_m

and (E_1-E_L) in the BET (B) or the BET (D) equation for various values of n_i (where n_i is the number of monolayers that will form in a type i pore, different types of pores varying by pore diameter only). The combination of n_i's that give the best fit of the adsorption isotherm are taken to be the best description of the pore size distribution.

A modified form of the BET (D) equation was derived to account for the variation in 'c-values' that is observed in micropores. A Fortran language program, BETD, was written to model adsorption isotherms with an input value of v_m, $(E_1-E_L)_i$ and β_i.

The program BETD was used to model adsorption isotherms for a ZSM-5 type adsorbent, which is displayed in Figure 86, and a ZSM-48 type adsorbent, which is displayed in Figure 87. The combination of data used to generate Figure 86 does not represent a computer optimization to fit an adsorption isotherm of ZSM-5. This data results from estimates of noncrucial values and a rough optimization of the more crucial values. A ZSM-5 type adsorbent differs from a ZSM-48 type adsorbent in that ZSM-5 zeolite contains 5-6 Å pores and pore intersections while ZSM-48 zeolite contains 5-6 Å pores and no pore intersections.

The data used to obtain Figure 86, the adsorption isotherm for a ZSM-5 type adsorbent are v_m = 100 cm^3/g, with three types of pores, being characterized as follows:

Type (1) n_1 = 1.2; $(E_1-E_L)_1$ = 1500 cal./g; β_1 = 0.47; pores corresponding to the actual pores of ZSM-5;

Type (2) n_2 = 1.95; $(E_1-E_L)_2$ = 900 cal./g; β_2 = 0.50; pores corresponding to the pore intersections of ZSM-5; and

Type (3) n_3 = 30; $(E_1-E_L)_3$ = 800 cal./g; β_3 = 0.03; pores corresponding to intercrystalline mesopores of ZSM-5.

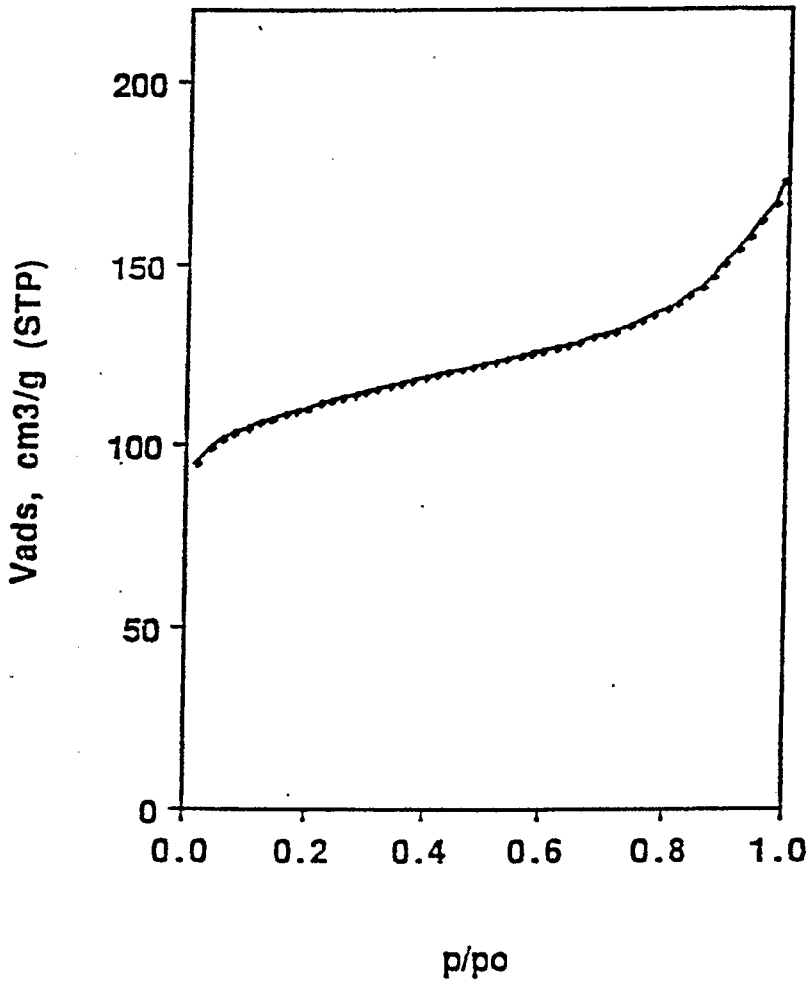

Figure 86. Adsorption Isotherm for a ZSM-5 Type Adsorbent

The variables defined here are the variables in the BET (D) equation. The number of monolayers formed in type i pores is n_i; $(E_1\text{-}E_L)_i$ is the heat of adsorption term for the 'c-value' for adsorption in pore type i; and β_i is the fraction of the surface area contained in type i pores. The quantity β_1 is approximately equal to β_2 which means to say that the surface area of pore intersections in ZSM-5 zeolite is approximately equal to the pore surface area in ZSM-5 zeolite. Consequently the selectivity and activity of reactions in ZSM-5 zeolite is as much a result of reactions in the pore intersections as in the pores themselves. Comparisons of Figure 86 with the adsorption isotherms of Figures 83 and 85 will show the relative similarity between the measured isotherms and the calculated isotherm.

An adsorption isotherm of a ZSM-48 type adsorbent is displayed in Figure 87. It differs from the adsorption isotherm for a ZSM-5 type adsorbent in that ZSM-48 has no pore intersections and ZSM-5 does. The data used to obtain Figure 87 are v_m = 100 cm^3/g, with two types of pores, being characterized as follows:

Type (1) n_1= 1.2; $(E_1\text{-}E_L)_1$ = 1500 cal/g; β_1 = 0.97, pores corresponding to the pores of ZSM-48; and

Type (2) n_2 = 30; $(E_1\text{-}E_L)_2$ = 800 cal/g; β_2 = 0.03, pores corresponding to the intercrystalline mesopores of ZSM-48.

The difference between the data used to obtain Figure 86 and the data used to obtain Figure 87 is simply that pore type 2 in the data used to obtain Figure 86 has been combined with pore Type 1.

The differences in Figure 86 and Figure 87 is because Figure 87 is the adsorption isotherm of a ZSM-48 type adsorbent which lacks pore intersections like a ZSM-5 type adsorbent. Consequently any differences arising between the selectivity and activity of reactions over ZSM-5

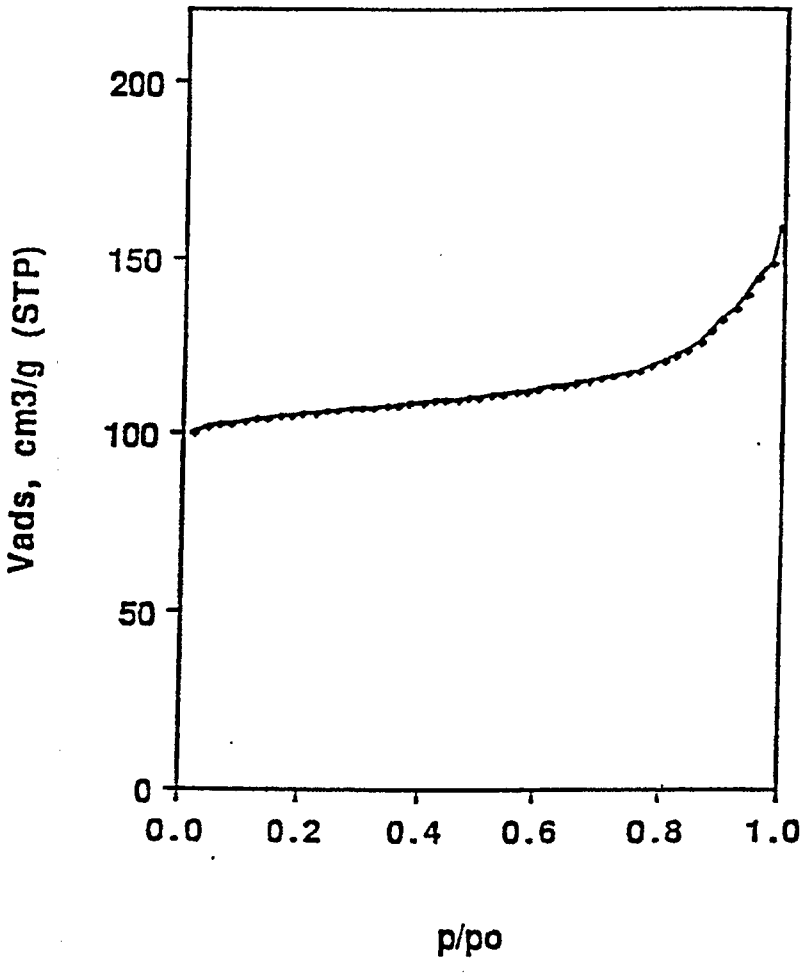

Figure 87. Adsorption Isotherm for a ZSM-48 Type Adsorbent

and over ZSM-48 results partly from the absence of pores in ZSM-48. This has been shown to be the case. The dehydration of methanol on ZSM-5 results in the production of olefins which oligomerize and transfer hydrogen to form aromatics and paraffins. However, the dehydration of methanol on ZSM-48 produces just olefins.[267] This is because ZSM-48 lacks pore intersections which are able to contain the bimolecular hydrogen transfer state necessary for the formation of aromatics.

The BET data outputs, temperature and adsorptive pressure, are sent directly to the computer and analyzed. The BET data acquisition scheme and the circuit design for interfacing the computer and the BET apparatus are presented in Figures 88 and 89, and the BET software algorithm is presented in Figure 90.

Hysteresis Loops

Breck[261] has reported that zeolites do not exhibit hysteresis loops. The reason is that hysteresis is only possible in pores where the radius of the pore is twice the diameter of the adsorbed molecules.[268] The pores of ZSM-5 have a diameter between 5.0 and 6.0 Å. A molecule of nitrogen has a diameter of 3.8 Å which is five or six times smaller than the minimum diameter for hysteresis in a pore of ZSM- 5. This is an apparent contradiction with the data that is presented in Figures 82 and 84 where a clear hysteresis loop for each sample of ZSM-5 is observed. The following observations were made regarding the adsorption desorption isotherms:

1. hysteresis loops were obtained for both samples of ZSM-5;
2. the hysteresis loop for the ZSM-5M differs somewhat from the hysteresis loop of ZSM-5-6, in that the difference between the adsorption and desorption branches of the hysteresis loop are more pronounced in ZSM-5M than in ZSM-5-6;

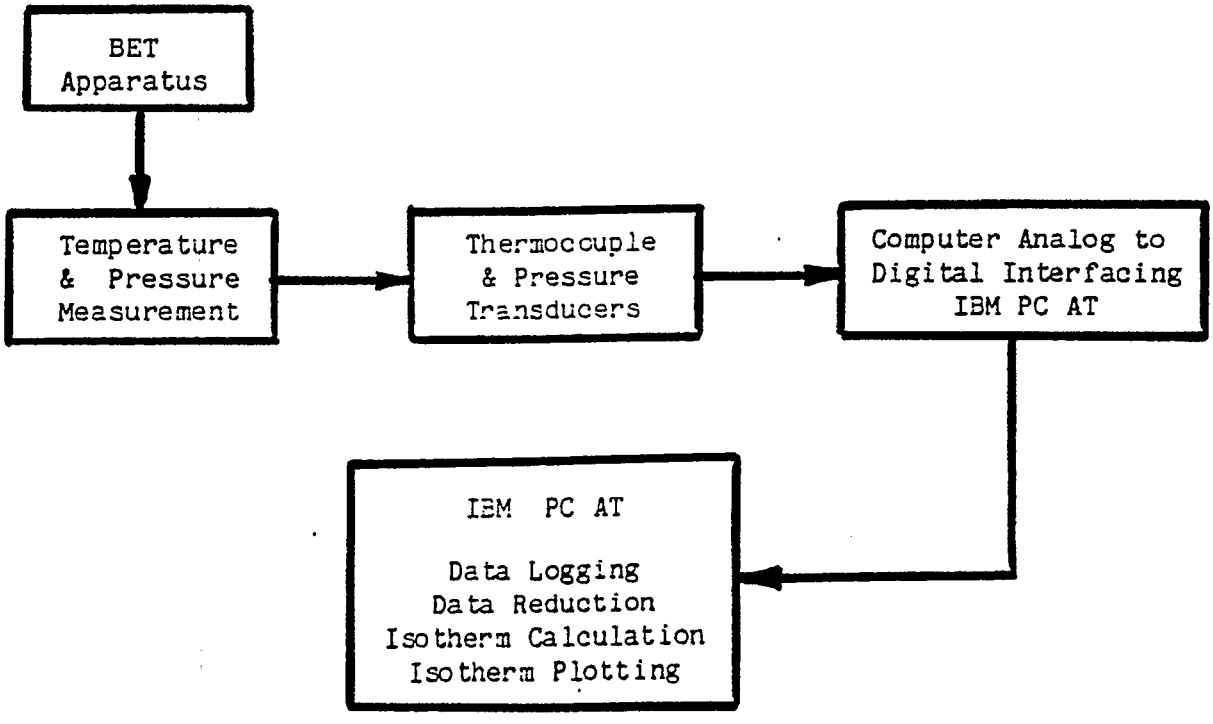

Figure 88. BET Apparatus Data Acquisition System

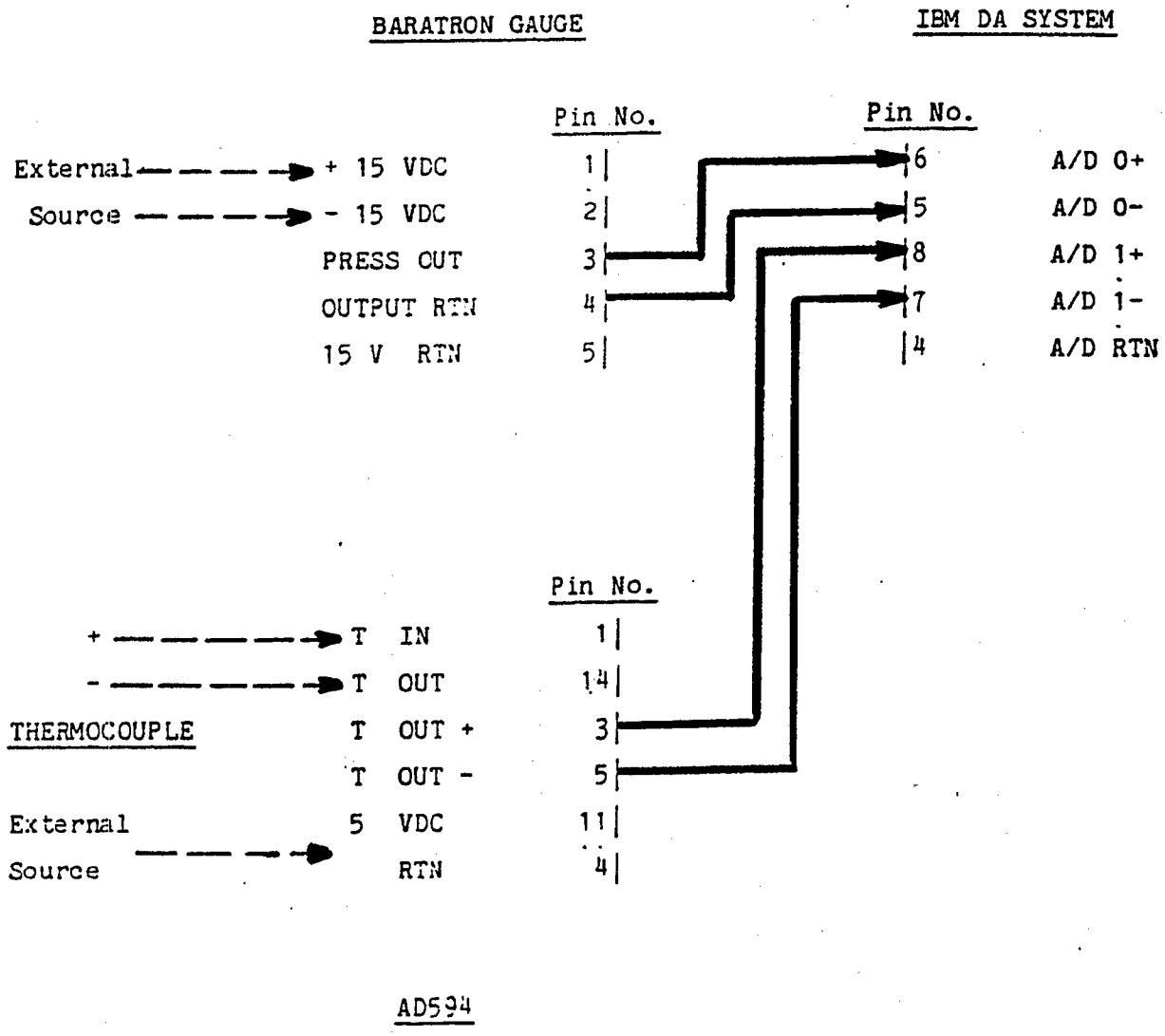

Figure 89. Circuit Design for Computer-BET Apparatus Interfacing

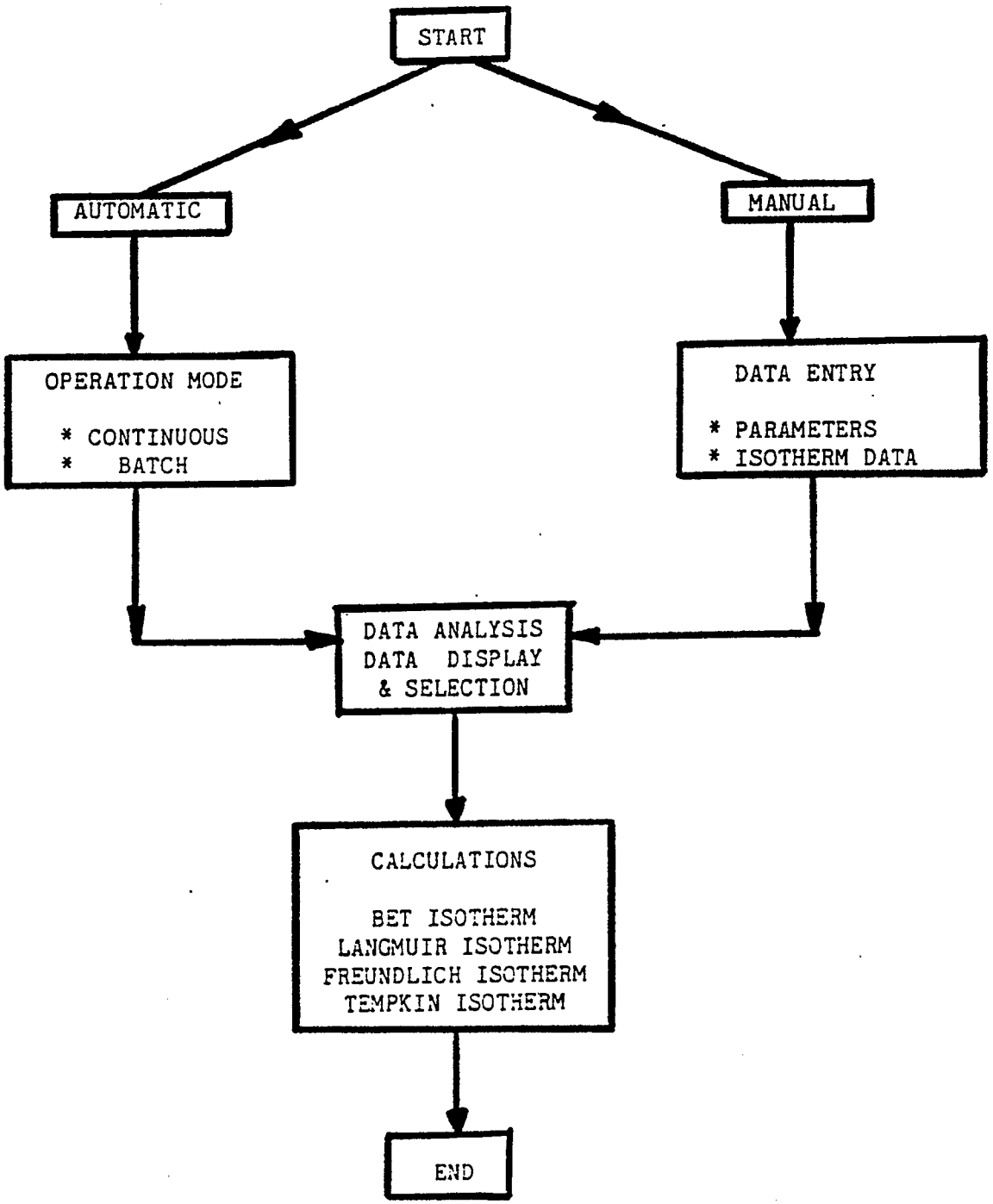

Figure 90. Schematic of BET Software Algorithm

3. the intercrystalline pore structure of the ZSM-5-6 differs from that of ZSM-5-6, in that the crystallites of ZSM-5M consist of smaller and more discreet crystallites than the crystallites of ZSM-5-6 which are larger and agglomerated together in 10 μm to 50 μm clusters; and

4. both hysteresis loops show hysteresis effects occurring in a broad size range of pores, from angstrom size pores up to micron size pores.

These four observations led to the conclusion that the hysteresis loops observed here on ZSM-5 are a result of hysteresis effects in intercrystalline mesopores and not in the intracrystalline micropores. It is expected that an adsorption/desorption isotherm of a single large crystal of ZSM-5 would not display hysteresis because of the lack of an intracrystalline pore structure.

Conclusions

In order to study the surface and pore properties of ZSM-5 a BET system was constructed and experiments, were developed for the reproducible determination of adsorption/desorption isotherms. ZSM-5 displayed two outstanding features:

1. higher c-values probably as a result of ZSM-5's microporosity; and

2. hysteresis loops which represent filling and emptying of intercrystalline pores.

Because of the differences in the hysteresis loops of different samples of ZSM-5 it should be possible to correlate different crystallite structures and arrangements with differences in hysteresis loops.